IN THE UNITED STATES PATENT AND TRADEMARK OFFICE

Applicants:	Kevin Jeffrey Barnham, et al.	**Examiner:**	D. Margaret M. Seaman
Serial No.:	10/521,902	**Art Unit:**	1625
Filed:	August 10, 2005	**Docket:**	18583

For: 8-HYDROXY QUINOLINE DERIVATIVES

Confirmation No.: 7111

Commissioner for Patents
P. O. Box 1450
Alexandria, VA 22313-1450

DECLARATION OF DR. KEVIN BARNHAM

I, Kevin Barnham, hereby declare as follows:

1. I am a consultant to Prana Biotechnology Ltd. ("Prana"), the assignee of the above-identified application. I hold the position of Principal Research Fellow at The University of Melbourne.

2. I hold a Bachelor of Science (Hons) in Chemistry and a Doctorate Degree in chemistry. A true and correct copy of my *curriculum vitae* is attached hereto as **Exhibit 1** of this Declaration.

3. I am one of the named inventors of the above-identified application, and I am familiar with the application.

4. I have been asked by counsel for Prana to prepare a hydrate of a compound within the scope of the invention described in the above-identified application and to comment upon whether the procedure used was known to one of ordinary skill in the art at the time of the filing of the above-identified application, i.e., on or about July 16, 2003. I was also asked to comment whether one of ordinary skill in the art would have known how to prepare a solvate

of a compound within the scope of the present invention at the time of the filing of the application.

5. The experiments described herein were either conducted by me or were under my direct supervision and control.

6. I have prepared two hydrates. More specifically, I have prepared two different hydrates of the compound

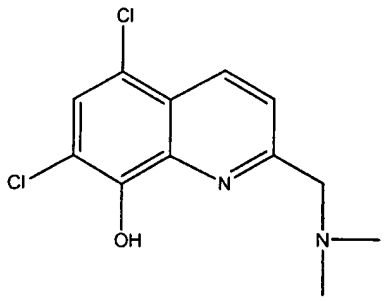

herein designated as 1033.

7. The first hydrate was prepared as follows:

1033.HCl salt (600mg) was diluted with CH_2Cl_2 (50 mL) and saturated aqueous $NaHCO_3$ (50 mL). The resulting mixture was extracted twice into CH_2Cl_2. The combined organic layers were dried over Na_2SO_4, filtered and concentrated to afford a yellow coloured oil. A portion of this material was transferred into a separate flask with CH_2Cl_2 and then concentrated to provide 115mg of the free base. The residue was dissolved in boiling MeOH (2 mL) then hot H_2O (2mL), was added resulting in a pale yellow precipitate forming immediately. The suspension was redissolved by adding warm MeOH (5mL) and transferring the solution to a test tube and allowing it to stand in a fume-hood for 48 hours. Resulting crystals in the test tube were allowed to stand for a further 48 hours, at which time examination of the crystals under a microscope revealed that they were suitable for X-ray

Analysis.

8. Crystals of the protein prepared in the preceding paragraph were grown from Methanol/water. A rod-shaped crystal was selected from the solvent and immediately flash cooled to 130K on the X-ray diffractometer. Intensity data were collected with an Oxford XCalibur X-ray diffractometer with Saphire CCD detector using Cu-Kα radiation (graphite crystal monochromator $\lambda = 1.54184$ Å).

9. The crystal structure of the 1033 hydrate prepared in accordance with the protocol in Paragraphs 7 and 8 is depicted in the crystal-packing diagram in **Exhibit 2** hereto. This diagram is annotated to show the water molecules and in particular the hydrogen atoms hydrogen bonding with the quinoline nitrogen and the 8-hydroxy group and the amine moiety at positions 2 and 8 of the hydroxyquinoline.

10. From the X-Ray diffraction, it was determined that the product is a hydrate of 1033 having one molecule of water associated with one molecule of 1033 in the crystal structure, i.e., a 1:1 molar ratio of 1033 and water.

11. The second product was prepared as follows:

1033.HCl salt (600mg) was diluted with CH_2Cl_2 (50 mL) and saturated aqueous $NaHCO_3$ (50 mL). The resulting mixture was extracted twice into CH_2Cl_2. The combined organic layers were dried over Na_2SO_4, filtered and concentrated to afford a yellow coloured oil. A portion of this material (106mg) was dissolved in EtOAc (5 mL) and hot anhydrous MeOH (0.5 mL) was added. The orange solution was transferred to a test tube and allowed to evaporate slowly. Brick-like orange crystals formed in approximately (1mL) of solvent. The crystals were examined under a microscope and were found to be suitable for X-ray analysis.

12. The crystal structure of this product is depicted in the crystal-packing diagram of **Exhibit 3** attached hereto. This diagram is also annotated to show the position of water molecules hydrogen-bonding with the quinoline nitrogen, 8- hydroxyl group and the amine

moiety at position 2 of the 8-hydroxyquinoline. A crystal packing diagram depicting the hydrogen bonding interactions between the water molecules and the 8-hydroxy quinoline is depicted in **Exhibit 4**.

13. From the X-Ray diffraction, it was determined that the product is a hemi hydrate, i.e., in the crystal structure, there are two molecules of 1033 per one molecule of water.

14. As shown in Figures 1-3, the OH group and the quinoline nitrogen hydrogen bond with the hydrogen atoms of the water molecules. If the compound also contains other electronegative atoms, such as the amine moiety at position 2 of 1033, then another atom for hydrogen bonding is available for such bonding to occur.

15. This ability for the 8-hydroxy quinoline molecules to form hydrates was known at the time of the filing of the application. In addition, the process of preparing a hydrate of an 8-hydroxy-quinoline compound, using the procedure outlined above in paragraphs 7 and 11, was known to one of ordinary skill in the art at the time of the filing of the application. For example, I refer to an extract from the following text book regarding recrystallization techniques: *Vogel's Textbook of Practical Organic Chemistry Fifth Edition*; Vogel, Arthur Israel Furniss, B. S; Hannaford, A. J.; Smith, P.W.G.; Tatchell, A. R. Ed. Longman Group UK Limited, 1989, Chapter 2.20, pages 135 to 153 attached hereto as **Exhibit 5**. This common text book outlines standard recrystallization procedures and confirms that the employed techniques were well established in organic chemistry and have been in existence before the filing date of the above-identified patent application.

16. Since water is a solvent, the preparation of hydrates hereinabove also illustrates the formation of solvates.

17. The process for the formation of other solvates was also known to one of ordinary skill in the art at the time of the filing of the application. In fact, actual solvates of 8-hydroxy-quinoline derivatives were known to one of ordinary skill in the art at the time of the filing of the application.

18. To illustrate the literature in the field of solvates and hydrates of 8-hydroxyquinoline compounds I have located 3 references showing that solvates with a range of solvents, including water, DMSO and ethanol can be formed between the polar atoms of the solvent and nitrogen atom and/or the hydroxyl group on the 8-hydroxy quinoline scaffold using the same protocol as described for the production of the hydrates set out hereinabove.

19. I refer to the paper of Bardez et al, 1997, referenced in **Exhibit 6** and attached hereto. The purpose of this study was to clarify the behavior of the 8-hydroxy quinoline scaffold in neat solvents. The paper discusses this behavior in both aqueous and organic solvent solutions from pages 7787 to 7792. Bardez et al. disclose on page 7792 that the 8-hydroxy group and the pyridyl nitrogen of 8-hydroxy quinoline scaffolds provide for intermolecular proton transfer between each of these moieties. The 8–OH group of 8-hydroxyquinoline consistently seeks hydrogen bonding partners to generate low energy stable structures. In the absence of suitable solvents (i.e., polar solvents) that allows for such bonding, dimers of quinoline molecules are formed.

20. I also refer to the paper of Santo *et al*, 2001, attached hereto as **Exhibit 7**. The purpose of this study was to perform solvatochromic studies on compounds, including 8-hydroxy quinoline in pure solvents such as alkanols and alcohol-cyclohexane mixtures. Pages 1550 and 1551 disclose the NMR studies on the types of solvates produced and their localities in relation to each compound studied. The NMR studies confirm that there is electrostatic and hydrogen bonding interactions between 8-hydroxy quinoline and alkanols, also that such solvates are localized in relation to the azaromatic nitrogen of the quinoline ring. The nature of the interactions between 8-hydroxy quinoline and alkanols are similar to those that we have observed between 1033 and water as shown in Figures 2 and 3 as attached.

21. Although published after the filing of the application, the following article confirms that solvates can be prepared from 8-hydroxy quinoline compounds utilizing procedures, which were routine to one ordinary skill in the art at the time of the filing of the above-

identified application. I refer to the paper of Albrecht *et al*, 2007, referenced in **Exhibit 8** and attached hereto. The purpose of this study was to determine the anion binding properties of substituted quinoline derivatives when they function as receptors. The authors synthesized the DMSO adduct of 5,7-dibromo-8-hydroxyquinoline-2-carboxylic acid as described on page 2855 of this paper. The process used was fairly routine, in my opinion, and one of ordinary skill in the art could have prepared the solvate described therein without difficulty. The X-ray crystal structure of this DMSO adduct is shown on page 2851 of this paper. Albrecht *et al* confirm that there is intramolecular hydrogen bonding interactions to the quinoline nitrogen atom, and solvent hydrogen bonds to the 8–OH group and the OH group of the 2-carboxylic acid group, as taught by Bardez *et al* and Santo *et al* in paragraphs 19 and 20, respectively above and as shown by the crystal structures of the 1033 hydrate and hemi-hydrate attached hereto as **Exhibits 2, 3 and 4**.

22. Thus, based on the above, it is my opinion that one of ordinary skill in the art had the wherewithal to prepare solvates of the compounds of the present invention, and as described in the Bardez et al. and Santo et al., such preparation was routine for one of ordinary skill in the art at the time of the filing of the above-identified application.

23. I have shown that the syntheses of hydrates and hemi-hydrates of 1033 can be achieved using routine techniques such as those described in **Exhibit 5**. In my opinion, similar intramolecular hydrogen bonding which exists between the N atom and 8-OH groups of the 8-hydroxy quinoline scaffold and the water molecules in the hydrates would be expected to occur with other solvents such as alkanols and DMSO, based on the teachings in the scientific publications attached in **Exhibits 6 and 7** and discussed hereinabove. Further it is my opinion that hydrates and solvates of the 8-hydroxy quinoline derivatives described in the above referenced application could have been prepared at the time of the filing of the instant application based on the information available in the literature on or before the filing date using techniques which were routine to one of ordinary skill in the art at the time of the filing.

24. I declare that all statements made herein of my own knowledge are true and that all

statements made on information and belief are believed to be true; and that those statements were made with the knowledge that willful false statements and the like so made are punishable by fine or imprisonment, or both, under Section 1001 of Title 18 of the United States Code, and that such willful false statements may jeopardize the validity of the application or any patent issuing thereon.

By: _____ Dated: 16 SEPTEMBER 2008

CURRICULUM VITAE

NAME

Kevin J Barnham

POSITION TITLE

Principal Research Fellow

Work Address:

Department of Pathology

The University of Melbourne

Level 5, Medical Centre

cnr Grattan St and Royal Parade

Victoria, 3010 Australia

Phone (work): (+613)-8344 2555

Fax (work): (+613)-9347 6750

E.mail: kbarnham@unimelb.edu.au

EDUCATION/TRAINING

INSTITUTION AND LOCATION	DEGREE	YEAR(s)	FIELD OF STUDY
University of Queensland, Australia	PhD	1993	Chemistry
University of Queensland, Australia	BSc(Hons)	1986	Chemistry

Positions

1987-1988	Chemist Queensland Alumina Ltd.Gladstone, Queensland 4680
1986, 1989-1992	Tutorial Assistant/Tutorial Fellow, Department of Chemistry, University of Queensland
1992-1995	MRC Research Fellow The University of London, Birkbeck College
1995-2000	Research Scientist BRI, Project Leader 1998-2000
2001-	Senior Research Fellow, the University of Melbourne
2003-2005	NH&MRC RD Wright Fellow
2006-	NH&MRC Senior Research Fellow
2007-	Principal Research Fellow

Publications (in chronological order).):

1. Appleton T.G., **Barnham K.J.**, Hall J.R., Mathieson M.T. Reactions of nitroplatinum complexes. 1. ^{15}N and ^{195}Pt NMR spectra of platinum(II) nitrite complexes. *Inorg. Chem.* **1991**, *30(13)*, 2751-2756.

2. Appleton T.G., Bailey A.J., **Barnham K.J.**, Hall J.R. Aspects of the solution chemistry of trans-diammineplatinum(II) complexes. *Inorg. Chem.* **1992**, *31(14)*, 3077-3082.

3. **Barnham K.J.**, Djuran M.I., Frey U., Mazid M.A., Sadler P.J. [Pd(CBDCA-O,O')(NH_3)$_2$]: The Pd(II) analogue of a platinum anticancer drug (CBDCA=cyclobutane-1,1-dicarboxylate). *J. Chem. Soc. Chem. Comm.* **1994**, 65-66.

4. **Barnham K.J.**, Djuran M.I., Murdoch P.D., Sadler P.J. Intermolecular displacement of S-bound L-methionine on platinum(II) by guanosine 5'-monophosphate. Implications for the mechanism of action of anticancer drugs. *J. Chem. Soc. Chem. Comm.* **1994**, 721-722.

5. **Barnham K.J.**, Frey U., Murdoch P-D.S., Ranford J.D., Sadler P.J., Newell D.R. Pt(CBDCA-O)$(NH_3)_2$(L-Methionine-*S*)]: Ring-opened adduct of the anticancer drug Carboplatin (Paraplatin)-Detection of a similar complex in urine by NMR spectroscopy. *J. Am. Chem. Soc.* **1994**, *116(24)*, 11175-11177.

6. **Barnham K.J.**, Bauer C.I., Djuran M.I., Mazid M.A., Rau T., Sadler P.J. Outer-sphere macrochelation in [Pd(en)(5'-GMP-N7)$_2$].9H_2O and [Pt(en)(5'-GMP-N7)$_2$].9H_2O: X-ray crystallography and NMR spectroscopy in solution. *Inorg. Chem.* **1995**, *34*, 2826-2832.

7. **Barnham K.J.**, Djuran M.I., Murdoch P-D.S., Ranford J.D., Sadler P.J. L-Methionine increases the rate of reaction of 5'-guanosine monophosphate with the anticancer drug cisplatin: Mixed ligand adducts and reversible methionine binding. *J. Chem. Soc. Dalton Trans.* **1995**, 3721-3726.

8. **Barnham K.J.**, Berners-Price S.J., Frenkiel T.A., Frey U, Sadler P.J. Platination pathways for reactions of cisplatin with GG single-stranded and double-stranded decamer oligonucleotides. *Angew. Chem.* **1995**, *34*, 1874-1877.

9. Appleton T.G., **Barnham K.J.**, Byriel K.A., Hall J.R., Kennard C.H.L., Mathieson M.T., Penman K.G. Reactions of nitroplatinum compounds. 2. Reactions of $K_2[Pt(NO_2)_4]$ and related complexes with aqueous acids (CH_3CO_2H, $HClO_4$, CF_3SO_3H, HNO_3, and H_2SO_4): Pathways to Platinum(III) Compounds with acetate bridges. The crystal structure of $K_2[\{Pt(NO_2)_2(\mu\text{-}CH_3CO_2)\}_2].H_2O$. *Inorg. Chem.* **1995**, *34*, 6040-6052.

10. **Barnham K.J.**, Djuran M.I., Murdoch P-D.S., Ranford J.D., Sadler P.J. Ring-opened adducts of the anticancer drug carboplatinum with sulfur amino acids. *Inorg. Chem.*, **1996**, *35(4)*, 1065-1072.

11. Berners-Price S.J., **Barnham K.J.**, Frey U., Sadler P.J. Kinetic analysis of the stepwise platination of single- and double-stranded GG oligonucleotides with cisplatin and $[PtCl(H_2O)(NH_3)_2]^+$ *Chem. Eur. J.* **1996**, *2(10)*, 1283-1291.

12. Arpallahti, J., Sillanpaa, R., **Barnham, K.J.**, Sadler, P.J. X-Ray crystal structure determination and spectroscopic characterisation of Trans-diamminedihydroxoplatinum (II) dihydrate. *Acta Chem. Scand.* **1996**, *50(2)*, 181-184.

13. **Barnham K.J.**, Guo, Z.J., Sadler, P.J. Stabilisation of monofunctional platinum-nucleotide adducts of N-acetyl-L-methionine complexes with guanosine 5′-monophosphate and guanylyl(3′-5′)guanosine. *J. Chem. Soc. Dalton Trans.* **1996**, 2867-2876.

14. Berners-Price S., **Barnham K.J.**, Corrazza A., Guo Z, Sadler, P.J., Leng M., Locker L.Structural transitions of a GG-platinated DNA duplex induced by pH, temperature and Box A of high-mobility-group protein 1. *Eur. J. Biochem.* **1997**, *243*, 782-791.

15. **Barnham, K.J.**, Dyke, T.R., Kem, W.R., Norton, R.S. Structure of the neurotoxin B-IV from the marine worm *Cerebratulus lacteus*: □-Helical hairpin stabilised by disulfide bonding. *J. Mol. Biol.* **1997**, *268*, 886-902.

16. **Barnham, K.J.**, Monks, S.A., Hinds, M.G., Azad, A.A., Norton R.S.Solution structure of a polypeptide from the N-terminus of the HIV protein Nef. *Biochemistry* **1997**, *36*, 5970-5980.

17. Barton, S.J., **Barnham, K.J.**, Habtemariam, A., Sue, R.E., Sadler, P.J. pK_a values of aqua ligands on platinum(II) anticancer complexes: [^{1}H, ^{15}N] and ^{195}Pt NMR studies of *Cis-* and *Trans-*

[$PtCl_2(NH_3)$(cyclohexylamine)] *Inorg. Chim. Acta* **1998**, *273*, 8-13.

18. Ivanov, A.I., Christodoulou, J., Parkinson, J.A., **Barnham, K.J.**, Tucker, A., Woodrow, J., Sadler, P.J. Cisplatin binding sites on human albumin. *J. Biol. Chem.* **1998**, *273*, 14721-14730.

19. **Barnham, K.J.**, Torres, A.T., Alewood, D., Alewood, P.F., Domagala, T., Nice, E.C., Norton, R.S. Role of the 6-20 disulfide bridge in the structure and activity of epidermal growth factor. *Protein Sci.* **1998**, *7*, 1738-1749.

20. Barton S.J., **Barnham K.J.**, Frey U., Habtemariam A., Sue R.E., Sadler P.J. [^1H,^{15}N] NMR kinetic studies of reactions of *cis* and *trans*-[$PtCl_2(^{15}NH_3)(c\text{-}C_6H_{11}{}^{15}NH_2)$] with guanosine-5′-monophosphate *Aust. J. Chem* **1999**, *52*, 173-177.

21. Cox M.C., **Barnham K.J.**, Frenkiel T.A., Hoeschele J. D., Mason A.B., He·Q.-Y., Woodworth R.C., Sadler P.J. Identification of platination sites on human serum transferrin using ^{13}C and ^{15}N NMR spectroscopy. *J. Bio. Inorg. Chem.* **1999**, *4*, 621-631.

22. **Barnham, K.J.**, Catalfamo, F., Pallaghy, P.K., Howlett, G.J., Norton, R.S. Helical structure and self-association in a 13 residue neuropeptide YY2 receptor agonist: Relationship to biological activity. *BBA-Protein Struct.* **1999**, *1435*, 127-137.

23. Cherny, R.A., **Barnham, K.J.**, Lynch, T., Volitakis, I., Li, Q-X., McLean, C.A., Multhaup, G., Beyreuther, K., Tanzi, R.E., Masters, C.L., Bush A.I. Chelation and intercalation: Complimentary properties in a compound for the treatment of Alzheimer's disease. *J. Struct. Biol.* 2000, *130*, 209-216.

24. Thompson, A.J., **Barnham, K.J.**, Norton, R.S., Barrow, C.J. The Val-210-Ile pathogenic Creutzfeld-Jakob disease mutation increases both the helical and aggregation propensities of a sequence corresponding to helix-3 of PrP. *BBA-Protein Struct.* 2001, *1544*, 242-254.

25. Jobling, M.F., Huang, X., Stewart, L.R., **Barnham, K.J.**, Curtain, C.C., Volitakis, I., Perugini, M., White, A.R., Cherny, R.A., Masters, C.L., Barrow, C.J., Collins, S.J., Bush, A.I., Cappai, R. Copper and zinc binding modulates the aggregation and neurotoxic properties of the prion peptide PrP106-126. *Biochemistry* 2001, *40*, 8073-8084.

26. Cherny, R.A., Atwood, C.S., Xilinas, M.E., Gray, D.N., Jones, W.D., McLean, C.A., **Barnham, K.J.**, Volitakis, I., Fraser, F.W., Kim, Y.-S., Goldstein, Huang, X., L.E., Moir, R.D., Lim, J.T., Beyreuther, K.T., Zheng, H., Tanzi, R.E., Masters, C.L., Bush, A.I. Treatment with a copper-zinc chelator markedly and rapidly inhibits beta-amyloid accumulation in Alzheimer's disease transgenic mice. *Neuron* 2001, *30*, 665-676.

27. Curtain, C.C., Ali, F., Volitakis, I., Cherny, R.A., Norton, R.S., Beyreuther, K., Barrow, C.J., Masters, C.L., Bush, A.I., **Barnham. K.J.** Alzheimer's disease amyloid-□ binds Cu and Zn to generate an allosterically ordered membrane-penetrating structure containing SOD-like subunits. *J. Biol. Chem.* 2001, *276*, 20466-20473.

28. Gorman, J.J., McKimm-Breschkin J.L., Norton R.S., **Barnham K.J.** Antiviral Activity and Structural Characteristics of the Non-Glycosylated Central Subdomain of Human Respiratory Syncytial Virus Attachment (G) Glycoprotein. *J.Biol. Chem.* 2001, *276*, 38988-38994.

29. Corzo, G., Escoubas, P., Villegas, E., **Barnham, K.J.**, He, W., Norton, R.S., Nakajima, T. Pandinins, novel amphipathic antimicrobial peptides from venom of the scorpion *Pandinus imperator*. *Biochem. J.* **2001**, *359*, 35-45.

30. Pannequin J, **Barnham K.J.**, Hollande F., Shulkes A., Norton R.S., Baldwin G.S. Ferric ions are essential for the biological activity of the hormone glycine-extended gastrin. *J. Biol. Chem.* **2002**, *277*,

48602-48609.

31. Miles L.A., Dy C.Y., Nielsen J., **Barnham K.J.**, Hinds M.G., Olivera B.M., Bulaj G., Norton R.S. Structure of a novel P-superfamily spasmodic conotoxin reveals an inhibitory cystine knot motif. *J. Biol. Chem.* 2002, *277*, 43033-43040.

32. Hewish D.R., **Barnham K.J.**, Werkmeister J.A., Kirkpatrick A., Bartone N., Liu S.T., Norton R.S., Curtain C.C., Rivett D.E. Structure and activity of D-Pro(14) melittin. *J. Prot. Chem.* **2002**, *21,* 243-253.

33. Curtain C.C., Ali F.E., Smith D.G., Bush A.I., Masters C.L., **Barnham K.J.** Metal ions, pH and cholesterol regulate the interactions of Alzheimer's disease amyloid-□ peptide with membrane lipid. *J. Biol. Chem.* **2003**, *278*, 2977-2982.

34. Kourie, J.L. Kenna, B.L. Tew, D. Jobling, M.F. Curtain, C.C. Masters, C.L. **Barnham, K.J.** Cappai, R. Copper modulation of ion channels of PrP[106-126] mutant prion peptide fragments. *J. Membrane Biol.* **2003**, *193*, 35-45.

35. **Barnham, K.J.**, McKinstry, W.J., Multhaup, G., Galatis, D., Morton, C.J., Curtain, C.C., Williamson, N.A., White, A.R., Hinds, M.G., Norton, R.S., Beyreuther, K., Masters, C.L., Parker, M.W., Cappai, R. Structure of the Alzheimer's disease amyloid precursor protein copper binding domain: a regulator of neuronal copper homeostasis. *J. Biol. Chem.* **2003**; *278*: 17401-17407.

36. Evin, G., Sernee, M.F, **Barnham, K.J.**, Holsinger, R.M.D, Culvenor, J.G., Hoke, D.E., Li, Q-L., Smith, D.G., Maynard, C., Tickler, A., Huang, X., Opazo, C., Carrington, D., Kocak, G., Volitakis, I., Mok, S.S, Ciccotosto, G, Williamson, N.A., Beyreuther, K., Wade, J., Curtain, C.C., Cherny, R.A., Bush, A.I., Masters, C.L., Cappai, R. Modulation of Alzheimer's Disease Aβ pathways for rational therapeutic intervention: secretase inhibition and metalloprotein active compounds. in *Alzheimer's Disease and Related Disorders: Research Advances.* Khalid Iqbal, and Bengt Winblad, Eds. Aslan International Academy of Aging, Bucharest, Romania, **2003**

37. Lau,T-L., **Barnham, K.J.**, Curtain, C.C, Masters, C.L., Separovic, F. Magnetic Resonance Studies of the β-Amyloid Peptide *Aust. J. Chem.* **2003**, *56*, 349-356.

38. Curtain, C.C., **Barnham, K.J.**, Bush, A.I. A□ Metallobiology and the Development of Novel Metal-Protein Attenuating Compounds (MPACs) for Alzheimer's disease. *Curr. Med. Chem. – Imun., Endoc. & Metab. Agents,* **2003**, 3, 309-315.

39. Bahadi, R. Farrelly, P.V. Kenna, B.L. Curtain, C.C. Masters, C.L. Cappai, R. **Barnham, K.J.** Kourie, J.I. Cu^{2+}-induced modification of the kinetics of A□1-42 channels. *Am. J. Physio-Cell Physio.* **2003**, *285*, C873-C880.

40. **Barnham, K.J.**, Ciccotosto, G.D., Tickler, A.K., Ali, F.E., Smith, D.G., Williamson, N.A., Lam. Y-H., Carrington D., Tew, D., Kocak, G., Volitakis, I., Separovic, F., Barrow, C.J, Wade, J.D., Masters, C.L., Cherny, R.A., Curtain, C.C., Bush, A.I., Cappai, R. Neurotoxic, redox-competent Alzheimer's □-amyloid is released from lipid membrane by methionine oxidation. *J. Biol. Chem.* **2003**, *278*, 42959-42966.

41. Ali, F.E., **Barnham, K.J.**, Barrow, C.J., Separovic, F. Metal Catalyzed Oxidation of Tyrosine Residues by Different Oxidation Systems of Copper/ Hydrogen Peroxide. *J. Inorg. Biochem.* **2004**, *1*, 173-188.

42. **Barnham, K.J.**, Cherny, R.A., Cappai, R., Melov, S., Masters, C.L., Bush, A.I. Metal-protein attenuating compounds (MPACs) for the treatment of Alzheimer's disease. *Drug Design Reviews-Online,* **2004**, *1*, 75-82.

43. Tickler, A.K., **Barnham, K.J.**, Wade, J.D. Metal-mediated peptide-lipid interactions of the amyloid-□ peptide. In: Innovation and Perspectives in Solid Phase Synthesis & Combinatorial Libraries 2004. R.

Epton (ed.), Mayflower Worldwide, England. pp. 309-310.
44. Yao, S., Cherny,R.A., Bush, A.I., Masters, C.L., **Barnham, K.J.** Characterizing Bathocuproine Self-association and Subsequent Binding to Alzheimer's Disease Amyloid-□ Peptide by NMR. *J. Pept. Sci.* **2004**, *10*, 210-217.

45. Pannequin, J., Kovac, S., Tantiongco, J.-P., Norton, R.S., Shulkes, A., **Barnham, K.J.**, Baldwin, G.S. A novel effect of bismuth Ions: Selective inhibition of the biological activity of glycine-extended gastrin. *J. Biol. Chem.* **2004**, *279*, 2453-2460.

46. **Barnham, K.J.**, Masters, C.L., Bush, A.I. Neurodegenerative diseases and oxidative stress. *Nature Rev. Drug Disc.*, **2004**, *3*, 205-214.

47. White, A.R., **Barnham, K.J.**, Huang, X., Voltakis, I., Beyreuther, K., Masters, C.L., Cherny, R.A., Bush, A.I., Cappai, R. Iron inhibits neurotoxicity induced by trace copper and biological reductants. *J. Biol. Inorg. Chem.*, **2004**, *9*, 269-280.

48. Ali, F.E, **Barnham, K.J.**, Barrow, C.J., Separovic, F. Metal Catalyzed Oxidative Damage and Oligomerization of the Amyloid-□ Peptide (□□) of Alzheimer's Disease *Aust. J. Chem.* **2004**, *57*, 511-518.

49. Ali, F.E., **Barnham, K.J.**, Barrow, C.J., Separovic, F. Copper catalysed oxidation of amino acids and Alzheimer's disease. *Letters Pept. Sci.* **2004**, 10, 405-412.

50. **Barnham, K.J.**, Haeffner, F., Ciccotosto, G.D., Curtain, C.C., Tew, D., Mavros, C., Beyreuther, K., Carrington, D., Masters, C.L., Cherny, R.A., Cappai, R., Bush, A.I. Tyrosine gated electron transfer is key to the toxic mechanism of Alzheimer's disease □-amyloid. *FASEB J.* **2004**, doi:10.1096/fj.04-1890fj6e. *FASEB J express* **2004**: *18*, 1427-1429.

51. Ciccotosto, G.D., **Barnham, K.J.**, Cherny, R.A., Masters, C.L., Bush, A.I., Curtain, C.C., Cappai, R., Tew, D. Methionine oxidation: Implications for the mechanism of toxicity of the □-amyloid peptide from Alzheimer's disease. *Letters Pept. Sci.* **2004**, 10, 413-417

52. Rekas, A., Adda, C.G., Aquilina, J.A., **Barnham, K.J.**, Sunde, M., Galatis, D., Williamson, N.A., Masters, C.L., Anders, R.F., Robinson, C.V., Cappai, R., Carver, J.A. Interaction of the molecular chaperone □B-crystallin with □-synuclein: effects on amyloid fibril formation and chaperone activity. *J. Mol. Biol.*, **2004**, 340, 1167-1183.

53. Ciccotosto, G.D., Tew, D., Curtain, C.C, Smith, D., Carrington, D., Masters, C.L., Bush, A.I., Cherny, R.A., Cappai, R., **Barnham, K.J.** Enhanced toxicity and cellular binding of a modified Amyloid □ Peptide with a methionine to valine substitution. *J. Biol. Chem.* **2004**, *279*, 42528-42534.

54 He, H., Shehan, B.P., **Barnham, K.J.**, Norton, R.S., Shulkes, A., Baldwin, G.S. Biological activity and ferric ion binding of fragments of glycine-extended gastrin. *Biochemistry*, **2004**, 43, 11853-11861.

55. Ali, F.E., Separovic, F., Barrow, C.J., Cherny, R.A., Fraser, F., Bush, A.I., Masters, C.L., **Barnham, K.J.** Methionine regulates copper/hydrogen peroxide oxidation products of A□ *J. Pept. Sci.* **2005**, *11*, 353–360

56. Crouch, P.J., Blake, R., Duce, J.A., Ciccotosto, G.D., Li, Q.X., **Barnham, K.J.**, Curtain, C.C, Cherny, R.A., Cappai, R., Dyrks, T., Masters, C.L., Trounce, I.A. Copper-dependant inhibition of human cytochrome c oxidase by a dimeric conformer of A□1-42. *J. Neurosci.* **2005**; *25*: 672-679

57. Kong, G.K.W., Galatis, D., **Barnham, K.J.**, Polekhina, G., Adams, J.J., Masters, C.L., Cappai, R., Parker, M.W., McKinstry, W.J. Crystallisation and preliminary crystallographic studies of the copper binding domain of the amyloid precursor protein of Alzheimer's disease. *Acta Crystallographica D*, **2005**, *F61*, 93-95

58. Tickler A.K., Smith D.G., Ciccotosto G.D., Tew D.J., Curtain C.C., Carrington D., Masters C.L., Bush A.I., Cherny R.A., Cappai R., Wade J.D., **Barnham K.J.** Methylation of the imidazole sidechains of the Alzheimer's disease amyloid-β peptide results in abolition of SOD-like structures and inhibition of neurotoxicity. *J Biol Chem* **2005,** *280*, 13355–13363

59. Ambroggio, E.E. Kim D.H., Separovic F., Barrow C.J, **Barnham, K.J.**, Bagatolli, L.A., Fidelio G.D. Surface behavior and lipid interaction of Alzheimer □-amyloid peptide 1-42: a membrane-disrupting peptide. *Biophys. J.* **2005,** *88*, 2706–2713

60. Cappai R, Leck S-L, Tew D.J., Williamson N.A., Smith D.P., Galatis D., Sharples R.A., Curtain C.C., Ali F.E., Cherny R.A., Culvenor J.G., Bottomly S.P., Masters C.L., **Barnham K.J.**, Hill A.F. Dopamine promotes α–synuclein aggregation into SDS-resistant soluble oligomers via a distinct folding pathway. *FASEB J* **2005,** 19 (8): doi:10.1096/fj.04-3437fje

61. Puglielli L, Friedlich A.L, Setchell K.D.R., Nagano S., Opazo C, Cherny R.A., **Barnham K.J.**, Wade J.D., Melov S., Kovacs, D.M., Bush A.I. Cholesterol oxidase mimetic activity of Alzheimer's Disease β-amyloid. *J. Clin. Invest.* **2005**, 115: 2556-2563.

62. Haeffner, F., Smith, D.G., **Barnham, K.J**, Bush, A.I. Model Studies of Cholesterol and Ascorbate Oxidation by Copper Complexes: Relevance to Alzheimer's Disease □–amyloid Metallochemistry. *J. Inorg. Biochem* **2005**, *99*: 2403-2422

63. Ali, F.E., Leung, A., Cherny, R.A., Mavros, C., **Barnham, K.J**, Separovic, F., Barrow, C.J. Dimerisation of N-Acetyl-L-Tyrosine Ethyl Ester and A□ Peptides via Formation of Dityrosine. *Free Radical Res.* **2006,** *40*, 1-9

64. Opazo, C., Luza, S., Villemagne, V.L., Volitakis, I., Rowe, C., **Barnham, K.J.**, Strozyk, D., Masters, C.L., Cherny, R.A., Bush, A.I. Radioiodinated clioquinol as a biomarker for □-amyloid:Zn^{2+} complexes in Alzheimer's disease. *Aging Cell*, **2006,** *5*, 69-79

65. Lau, T.-L., Ambroggio, E.E., Tew, D.J., Cappai, R.; Masters, C.L.; Fidelio, G.D.; **Barnham, K.J.**; Separovic, F. Amyloid-□ peptide disruption of lipid membranes and the effect of metal ions. *J. Mol. Biol.* **2006,** *356*, 759-770.

66. Ali, F.E., Separovic, F., Barrow, C.J, Yao, S., **Barnham, K.J.** Copper and Zinc Mediated Oligomerisation of A□ Peptides. *Int. J. Pept. Res. Ther.* **2006,** 12 (2): 153-164

67. Smith, D.P.; Smith, D.G.; Curtain, C.C.; Boas, J.F; Pilbrow, J.R.; Ciccotosto, G.D.; Lau, T.-L.; Tew, D.J.; Perez, K.; Wade, J.D.; Bush, A.I.; Drew, S.C.; Separovic, F.; Masters, C.L.; Cappai, R.; **Barnham, K.J.** Copper mediated amyloid-□ toxicity is associated with an intermolecular histidine bridge *J. Biol. Chem.* **2006**, *281*, 15145–15154.

68. White, A.R., **Barnham, K.J.**, Bush, A.I. Metal homeostasis in Alzheimer's disease *Expert Review of Neurotherapeutics;* **2006**, *6*, 711-722.

69. **Barnham, K.J.**; Cappai, R.; Beyreuther, K.; Masters, C.L.; Hill, A.F. Delineating common molecular mechanisms in Alzheimer's and prion diseases. *Trends in Biochem. Sci.* **2006**, *31*, 465-472.

70. Masters, C.L.; Cappai, R.; **Barnham, K.J.**; Villemagne, V.L. Molecular mechanisms for Alzheimer's disease: Implications for neuroimaging and therapeutics. *J. Neurochem.* **2006**, *97*, 1700-1725.

71. Crouch, P.J.; **Barnham, K.J.**; Duce, J.A.; Blake, R.E.; Masters, C.L.; Trounce, I.A. Copper-dependent inhibition of cytochrome *c* oxidase by $A\beta_{1-42}$ requires reduced methionine at residue 35 of the A□ peptide. *J. Neurochem.* **2006**, 99, 226-236.

72. Villemagne, V.L., Ng, S., Cappai, R., **Barnham, K.J.**, Fodero-Tavoletti, M.T., Rowe, C.C., Masters,

C.L. La Lunga Attesa: Towards a molecular approach to neuroimaging and therapeutics in Alzheimer's disease. *The Neuroradiology J.* **2006**, *19*, 453-474.

73. Crouch, P.J, **Barnham, K.J.**, Bush, A.I., White, A.R. Therapeutic treatments for Alzheimer's disease based on metal bioavailability. *Drug News Perspect.* **2006**, *19*, 469-474

74. Smith, D.P., Ciccotosto, G.D., Tew, D.J., Fodero-Tavoletti, M., Johanssen, T., Masters, C.L., **Barnham, K.J.**, Cappai, R. Concentration dependent Cu^{2+} induced aggregation and dityrosine formation of the Alzheimer's disease Amyloid-□ peptide. *Biochemistry*, **2007**, *46*, 2881-2891.

75. Smith, D.G., Cappai, R., **Barnham, K.J.** The redox chemistry of the Alzheimer's disease Amyloid □peptide. *Biophys. BioChim. Acta Biomembranes*, **2007** (Accepted Jan) in press

76. Kong G.K., Adams J.J., Harris H.H., Boas J.F., Curtain C.C., Galatis D., Masters C.L., **Barnham K.J.**, McKinstry W.J., Cappai R., Parker M.W. Structural Studies of the Alzheimer's Amyloid Precursor Protein Copper-binding Domain Reveal How it Binds Copper Ions. *J Mol Biol.* **2007**, *367*, 148-161.

77. Lau T.L, Gehman J.D., Wade J.D., Perez K., Masters C.L., **Barnham K.J,** Separovic F. Membrane interactions and the effect of metal ions on the amyloidogenic fragment A□(25-35) in comparison to A□(1-42). *Biochimica et Biophysica Acta – Biomembranes.* **2007** in press (May 4)

78. Cappai, R. **Barnham K.J**. Molecular determinants of Alzheimer's disease A□ peptide neurotoxicity. *Future Neurol.* **2007**, *4*, 397-409

79. Curtain C.C., **Barnham, K.J.**, Copper coordination by □-amyloid and the neuropathology of Alzheimer's disease. In "A□ peptide and Alzheimer's disease" Eds Barrow, C.J, Small D.H.; Spinger-Verlag London

80. Villemagne, V.L., Cappai, R.; **Barnham, K.J.**; Cherny, R.A.; Opazo, C.; Novakovic, K.; Rowe, C.C.; Masters, C.L. The A□centric pathway of Alzheimer's disease. In "A□ peptide and Alzheimer's disease" Eds Barrow, C.J, Small D.H.; Spinger-Verlag London

81. **Barnham, K.J.**, Curtain C.C., Bush, A.I. Free radicals, metal ions and A□ aggregation and neurotoxicity In "Protein Misfolding, Aggregation and Conformational Diseases" Eds Uversky, V.N., Fink, A.L. Kluwer Academic/Plenum Publishers USA

82. Fodero-Tavoletti, M.T., Smith, D.P., McLean, C.A., Adlard, P.A., **Barnham, K.J.**, Foster, L.E., Leone, L., Cortés, M., Culvenor, J.G., Li, Q-X., Laughton, K.M., Rowe, C.C., Masters, C.L., Cappai, R., Villemagne, V.L. In vitro characterisation of Pittsburgh Compound-B (PIB) binding to Lewy Bodies. *J. Neurosci.* **2007**, *27*, 10365-10371.

83. Hill AF, **Barnham KJ** Response to Ji et al: Why prion diseases are precluded by non-mammals *Trends in Biochem. Sci.* **2007**, *32*, 208-208

84. Caragounis, A., Du, T., Filiz, G., Laughton, K.M., Volitakis, I., Sharples, R.A., Cherny, R.A., Masters, C.L., Drew, S.C., Hill, A.F., Li, Q.-X., Crouch, P.J., **Barnham, K.J.**, White, A.R. Differential modulation of Alzheimer's disease amyloid beta peptide accumulation by diverse classes of metal ligands. *Biochem. J.* **2007**, *407*, 435-450.

85. Lau, T.-L.; Gehman, J.D.; Wade, J.D.; Masters, C.L.; **Barnham, K.J.**; Separovic, F. Cholesterol and Clioquinol modulation of A□(1-42) interaction with phospholipid bilayers and metals *Biochim. Biophys. Acta - Biomembranes* **2007**, *1768*, 3135-3144

86. Harrison, C.F., **Barnham, K.J**, Hill, A.F. Neurotoxic species in prion disease: a role for PrP isoforms? *J. Neurochem.* **2007**, *3*, 1709-1720

87. Tew D.J., Bottomley S.P., Smith D.P., Ciccotosto G.D., Babon J., Hinds M.G., Masters C.L., Cappai R.,. **Barnham K.J.** Stabilization of neurotoxic soluble □-sheet-rich conformations of the Alzheimer's disease amyloid-□ peptide. *Biophys. J.* **2008**, *94*, 2752-2766.

88. Smith, D.P., Tew, D.J., Hill, A.F., Bottomley, S.P., Masters, C.L., **Barnham, K.J.**, Cappai, R. Formation of a high affinity lipid-binding intermediate during the early aggregation phase of □–synuclein. *Biochemistry*, **2008**, *47*, 1425-1434.

89. Naylor, R., Hill, A.F., **Barnham, K.J.** Neurotoxicity in Alzheimer's disease-Is covalently crosslinked A□ responsible? *Eur. J. Biophys.* **2008**, *37*, 265-268.

90. Cappai R., **Barnham, K.J.** Delineating the mechanism of Alzheimer's disease Ab peptide neurotoxicity *Neurochem. Res.* **2008**, *33*, 526-532.

91. Kong, G.K.-W., Miles, L.A., Crespi, G.A.N., Morton, C.J., Ng, H.L., **Barnham, K.J.**, McKinstry, W.J., Cappai, R., Parker, M.W. Copper binding to the Alzheimer's disease amyloid precursor protein *Eur. J. Biophys.* **2008**, *27*, 269-279

92. Sharples R.A., Vella L.J., Nisbet R.M., Naylor R., Perez K., **Barnham K.J.**, Masters C.L., Hill A.F. Inhibition of □-secretase causes increased secretion of amyloid precursor protein (APP) C-terminal fragments in association with exosomes. *FASEB J.* in press Nov 2007

93. Miles L.A., Wun K.S., Crespi G.A.N., Fodero-Tavoletti M., Galatis D., Bagley C.J., Beyreuther K., Masters C.L., Cappai R. McKinstry W., **Barnham K.J.**, Parker M.. Amyloid-β-Anti-Amyloid-β Complex Structure reveals an Extended Conformation in the Immunodominant B Cell Epitope. *J Mol. Biol* **2008**, *377*, 181-192.

94. Donnelly P.S., Caragounis A., Du T., Laughton K.M., Volitakis I., Cherny R.A., Sharples R.A., Hill A.F., Li Q-X., Masters C.L., **Barnham K.J.**, White A.R. Selective intracellular release of copper and zinc ions from bis(thiosemicarbazonato) complexes reduces levels of Alzheimer's disease amyloid-beta peptide. *J. Biol. Chem.* **2008**, *283*, 4568-4577

95. Price K.A., Filiz G., Caragounis A., Du T., Laughton, K.M., Masters C.L., Sharples R.A., Hill A.F., Li Q.-X., Donnelly P.S., **Barnham K.J.**, Crouch P.J., White A.R. Activation of epidermal growth factor receptor by metal-ligand complexes decreases levels of extracellular amyloid beta peptide *The International Journal of Biochemistry & Cell Biology* In press Jan 30 **2008.**

965. Giannakis E., Pacifico J., Smith D.P., Hung, L.W., Masters, C.L., Cappai R., Wade J.D., **Barnham K.J.** Dimeric structures of α-synuclein bind preferentially to lipid membranes. *Biochim. Biophys. Acta-Biomembranes*, in press Jan 7 **2008**

97. **Barnham K.J.**, Bush A.I. Metals in Alzheimer's and Parkinson's Diseases. *Current Opin. Chem. Biol.* **2008**, *12*, 222–228

98. **Barnham K.J.**, Kenche V.B, Ciccotosto G.D., Smith D.P., Tew D.J., Liu X., Perez K., Cranston G.A., Johanssen T.J., Volitakis I, Bush A.I., Masters C.L., White A.R., Smith J.P., Cherny R.A., Cappai R. Platinum based inhibitors of amyloid-□ as therapeutic agents for Alzheimer's disease *Proc. Natl. Acad Sci USA* **2008**, in press March

99. Drew, S.; Leong, S.-L; Pham, C.; Tew, D.J.; Masters, C.L.; Miles, L.A.; Cappai, R.; **Barnham, K.J.** The Cu^{2+} Binding Modes of Recombinant □-Synuclein – Insights from EPR Spectroscopy. *J. Am. Chem. Soc.* **2008** In press March

100. Drew S.C., Djoko K.Y., Zhang L., Koay M., Boas J.F., Pilbrow J.R., Xiao Z., **Barnham K.J.**, Wedd A.G. Electron paramagnetic resonance characterization of the copper-resistance protein PcoC from

Escherichia coli. *J. Biol. Inorg. Chem.* **2008**, in press March

Research Support. (last 3 years)
2002-2005 NHMRC Program Grant, "Diseases of the aging Brain" C.L. Masters, A.I. Bush, R. Cappai, G. Evin, A.F. Hill. K.J. Barnham, D.H. Small. S.J. Collins, E. Storey, I Trounce
2003 RD Wright NH&MRC Fellowship "Biophysical approaches to understanding the role of metal ions and membranes in protein folding and their role in neurodegenerative diseases."
2005-2010 NHMRC Program Grant, "Diseases of the aging Brain" (K.J. Barnham, A.I. Bush, R. Cappai, R.A. Cherny, S.J. Collins, A.F. Hill. C.L. Masters, A.R. White)
2005-2010 NHMRC Senior Research Fellowship

SCULLY, SCOTT, MURPHY & PRESSER PC
INTELLECTUAL PROPERTY LAW

400 GARDEN CITY PLAZA
SUITE 300
GARDEN CITY, NY 11530
516-742-4343
FAX: 516-742-4366
E-MAIL: INTPROP@SSMP.COM
WWW.SSMP.COM

September 23, 2008

Mr. Stanley Gouldson
Spotless Enterprises Incorporated
100 Motor Parkway, Suite 155
Hauppauge, NY 11788

Re: Annuities

Dear Mr. Gouldson,

The annuities (tax maintenance fees) for the patents and/or applications set forth on the attached lists become due from 01-Dec-2008 to 31-Dec-2008. We would appreciate receiving your instructions regarding the payment of annuities as soon as possible but before 01-Nov-2008.

Sincerely,

Polly Stevens

Polly Stevens

cc: Anna Young, Esq.

Client: 506 Spotless Enterprises Incorpor

Case Number	Country Name	Sub Case	CPI Code	Owner	Case Type	Application Number	Patent Number	Due Date	No	Amount
15162	Brazil		SJ		DES	DI6304524-9	DI6304524-9	23-Dec-2008	QUIN2	439.00
				CPI Status: Granted			Your Instruction			
				Client Reference:			☐ Pay	☒ Abandon		
15162	European Community		SJ		DES	000115514-000	000115514-0001	19-Dec-2008	REN 6	359.00
				CPI Status: Granted			Your Instruction			
				Client Reference:			☒ Pay	☐ Abandon		
				Title: GARMENT SET DOUBLE HANGER AND METHOD OF HANGING						
				Abstract: "CABIDE DUPLO DE CONJUNTO DE PE‡AS DE VESTU RIO E M,TODO DE PENDURAR". Sòo descritos, um cabide duplo de conjunto de pe‡as de vestu rio e m,todo que sòo adequados para pendurar e expor um conjunto de pe‡as dc vestu rio superiores combinadas ou coordenadas , tal como um conjunto combinado dc pe‡as de vestu rio superior de homens ou mulheres, que nòo oculte cada uma das pe‡as de vestu rio individual quc formam o conjunto dc pe‡as de vestu rio coordenado, e que , desenhada para tornar mais f cil montar o conjunto combinado de pe‡as dc vestu rio coordenadas no cabide. O cabidc duplo de conjunto de pe‡as de vestu rio inclui um cabide superior que , desenhado para suportar uma primcira pe‡a de vestu rio do conjunto combinado de pe‡as de vestu rio e um cabide inferior, suportado abaixo do cabide superior por um elemento de arma‡òo vertical pendente, que , desenhada para suportar e expor uma segunda pc‡a de vestu rio do conjunto combinado de pc‡as de vestu rio.					
16838	Bangladesh		SJ		DES	D/313/2004	06221	10-Dec-2008	REN 6	566.00
				CPI Status: Granted			Your Instruction			
				Client Reference:			☐ Pay	☒ Abandon		
				Title: INTIMATE APPARREL HANGER						
				Abstract:						
8596	Germany		SJ		DES	49811950.5	49811950.5	01-Dec-2008	REN11	809.00
				CPI Status: Granted			Your Instruction			
				Client Reference:			☐ Pay	☒ Abandon		
8596	Hong Kong		SJ		DES	811552.0M001	811552.0M001	01-Dec-2008	REN11	559.00
				CPI Status: Granted			Your Instruction			
				Client Reference:			☐ Pay	☒ Abandon		
8596	Hong Kong	1	SJ		DES	811552.0M002	811552.0M002	01-Dec-2008	REN11	559.00
				CPI Status: Granted			Your Instruction			
				Client Reference:			☑ Pay	☐ Abandon		
8596	Hong Kong	2	SJ		DES	811552.0M003	811552.0M003	01-Dec-2008	REN11	559.00
				CPI Status: Granted			Your Instruction			
				Client Reference:			☑ Pay	☐ Abandon		

8596 Please explain 3 variances?

Client: 506 Spotless Enterprises Incorpor

Case Number	Country Name	Sub Case	CPI Code	Owner	Case Type	Application Number	Patent Number	Due Date	No	Amount
	Title: GARMENT HANGER									
	Abstract:									
9843	Canada	5	SJ	Spotless Plastics Pty., Ltd.	ORD	2365072		14-Dec-2008	8	552.00
				CPI Status: Pending				Your Instruction		
				Client Reference:				[X] Pay [ ] Abandon		
9843	United Kingdom	5	SJ	Spotless Plastics Pty., Ltd.	ORD	0130227.2	2370498	18-Dec-2008	8	436.00
				CPI Status: Granted				Your Instruction		
				Client Reference:				[X] Pay [ ] Abandon		
9843	Hong Kong	5	SJ	Spotless Plastics Pty., Ltd.	ORD	02108570.9	HK1049099	18-Dec-2008	8	337.00
				CPI Status: Granted				Your Instruction		
				Client Reference:				[X] Pay [ ] Abandon		
9843	South Africa	5	SJ	Spotless Plastics Pty., Ltd.	ORD	2001/10317	2001/10317	14-Dec-2008	8	248.00
				CPI Status: Granted				Your Instruction		
				Client Reference:				[ ] Pay [X] Abandon		

Title: GARMENT HANGER

Abstract: A molded plastic garment hanger as is widely used for the purpose of shipping and displaying garments, comprising a unitary plastic central hook and arms extending in opposite directions from the base of the central hook to facilitate a garment to be suspended therefrom by garment clips. The garment clips enable the attachment of various kinds of garments thereto, such as underwear, slips, brassieres, swimwear and the like, and are particularly adapted to secure the shoulder straps of such garments. The garment hanger has an improved garment retaining clip wherein as a garment strap is inserted into the garment retaining clip, the garment receiving channel of the clip first opens to allow the garment strap to enter, and then closes to securely retain the garment and to prevent it from becoming accidentally dislodged therefrom. The clip further defines a stop formation that is not substantially aligned with the free end of said inner arm, which blocks access to said free space by a garment strap secured by the clip.

Client Total: 5,423.00

Excited-State Processes in 8-Hydroxyquinoline: Photoinduced Tautomerization and Solvation Effects

Elisabeth Bardez,* Isabelle Devol, Bernadette Larrey, and Bernard Valeur

Laboratoire de Chimie Générale, Conservatoire National des Arts et Métiers, 292 rue Saint-Martin, 75003 Paris, France, and Laboratoire de Photophysique et Photochimie Supramoléculaires et Macromoléculaires (CNRS URA 1906), Ecole Normale Supérieure de Cachan, 61 Avenue du Président Wilson, 94235 Cachan Cedex, France

Received: April 15, 1997; In Final Form: July 18, 1997[⊗]

8-Hydroxyquinoline (8-HQ), referred as to oxine in analytical chemistry, is a fluorogenic ligand. Its lack of fluorescence in water and alkanes, and its low quantum yield in many other organic solvents, are rationalized in the present study in terms of photoinduced formation of a nonfluorescent tautomeric form 8-HQ(T*). In water, intermolecular proton transfers with surrounding water molecules are expected, but intrinsic intramolecular proton transfer between the −OH and ⩾N functions cannot be ruled out because the presence of a weak internal H bond can be inferred from the ground-state properties of 8-HQ such as pK_a values or solubility. In organic solvents, vapor pressure osmometry measurements in conjunction with infrared spectra allow us to show that (i) in alkane solvents, a very stable dimer is formed in the ground state ($K_{dim} = 7 \times 10^7$ at 25 °C); biprotonic concerted proton transfers are then expected to occur within the dimer upon excitation, as was previously reported for 7-azaindole; (ii) in chlorinated solvents (CH_2Cl_2, $CHCl_3$), hydration by residual water molecules likely leads to a nonnegligible fraction of hydrated open structures where excited-state proton transfer is impaired; a weak fluorescence can then be observed ($\Phi_F \approx 4 \times 10^{-3}$).

1. Introduction

Photoinduced proton-transfer reactions are of fundamental importance in photochemical and photobiological processes. Numerous studies have been devoted to monofunctional compounds able to exhibit excited-state intermolecular proton transfers[1−4] and the impact of solvation on these processes has been pointed out.

The behavior of amphoterous bifunctional molecules whose functions become very acidic and very basic, respectively, upon excitation is not necessarily relevant to the behavior of monofunctional compounds. Bifunctional compounds are likely to undergo photoinduced tautomerization and, in this respect, three types of compounds can be distinguished. First are the compounds whose donor acidic and acceptor basic groups are in close proximity and hydrogen-bonded to each other. Upon excitation, an excited-state proton transfer (ESPT) occurs intramolecularly between the two functions leading to a phototautomer. During this intrinsic ESPT, a single proton is transferred. Back to the ground state, reverse tautomerization occurs and leads to the initial form. The earliest compound where this phenomenon was reported is methyl salicylate in the pioneering work of Weller.[5] The compounds undergoing intrinsic ESPT form a wide class and, even nowadays, are by far the most studied, for example, 3-hydroxyflavone or 2-(2-hydroxyphenyl)benzothiazole and derivatives.[6,7]

The second category is made up of compounds whose functions are in such positions that photoinduced tautomerization results from a concerted double-proton transfer from one function to the other in hydrogen-bonded complexes. This may occur in doubly hydrogen-bonded dimers as for example in the case of 7-azaindole.[8−10] Proton transfer may also be relayed by a bridge of solvent molecules in a cyclically hydrogen-bonded solvent/solute complex as it occurs for instance with 7-hydroxyquinoline (7-HQ) in alcoholic solutions or in apolar solvents in the presence of low fractions of alcohol.[11−14] In both cases, the prerequisite of hydrogen bonds linking the acidic and basic groups, via solvent molecules or not, can be fulfilled only in the absence of water because water is considered to favor polyhydration of the prototropic groups, thereby inhibiting the solvent arrangement necessary for this concerted mechanism.

The third kind of compounds that can undergo phototautomerization possesses on the contrary very distant functions from each other. The excited-state proton transfers likely to occur are then unconcerted intermolecular transfers between each of the two functions and the surrounding solvent molecules. Because of the amphiprotonic character of the water molecule, aqueous or water containing media are therefore suitable. Nevertheless, few recent studies are devoted to such compounds.[15−17] In a previous paper dealing with 6-hydroxyquinoline (6-HQ) in aqueous media, proton transfers between each of the −OH and ⩾N functions and the surrounding water molecules were shown by us to consist in a one-way reaction whatever the acidity, basicity, or ionic strength of the medium.[16] The reason is a coupling of the ESPT with an intramolecular electron transfer from one ring to the other which removes the resulting charge from the initial prototropic site at a faster rate than any back ESPT reaction.[16] Moreover, the structure of the resulting phototautomer was proved to be ketonic (quinonoid), and not zwitterionic as claimed by others.[17,18] We suggested that these results could be transposable to hydroxyquinolines possessing each of their two functional groups on neighboring rings, especially 8-hydroxyquinoline (8-HQ).[16]

The fluorescence behavior of 8-HQ in aqueous media is in fact quite similar to that of 6-HQ (see below).[16] However, the proximity of the two functions is similar to that observed in 7-azaindole and allows one to expect concerted ESPT mechanisms in contrast to 6-HQ. Besides, in the ground state, the reactivities of both functions are already exhibited in a cooperative way especially when 8-HQ form complexes with metal ions; 8-HQ is an outstanding complexing agent, a bidentate ligand,

[⊗] Abstract published in *Advance ACS Abstracts*, September 1, 1997.

S1089-5647(97)01293-5 CCC: $14.00

considered as the second chelating agent in importance after EDTA.[19]

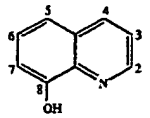

In analytical chemistry, 8-HQ is referred to as *oxine*. Many derivatives can be used, with improvement of either the water solubility of the ligand and chelates (5-sulfonic-8-hydroxyquinoline), or the selectivity vs some metal ions (5,7-dihalogeno-8-hydroxyquinoline or 2- and/or 7-methyl-8-hydroxyquinoline, for instance).[20] 8-HQ itself and its uncharged chelates are very poorly water soluble, which leads to use them in extraction, mainly liquid−liquid extraction.[21,22] In this respect, the 7-(4-ethyl-1-methyloctyl)-8-hydroxyquinoline is the major complexing reagent (82%) of the industrial extractant Kelex 100.[23,24]

Besides its chelating properties, 8-HQ is a fluorogenic ligand; i.e., it shows a very low quantum yield in aqueous and organic solutions, and fluorescence arises from cation binding with most metal ions. It is then used for fluorimetric determination of metals.[25] However, this fluorogenic character is not yet fully understood. In particular, the very low fluorescence emission in most media has never been really explained.

The purpose of the present study is therefore to clarify the behavior of 8-HQ in neat solvents, with the aim to understand why it is weakly or practically nonfluorescent in aqueous *and* organic solvents. First, several ground-state properties of 8-HQ in aqueous medium will be collected in order to take into consideration the possibility of hydrogen bonding between the −OH group and the N atom in a five-membered ring, even in water. The consequences on the excited-state behavior will be drawn. Then, attention will be directed to solvation in organic solvents, especially in chlorinated solvents (e.g. dichloromethane and chloroform) and alkanes. It is worthwhile to mention that chlorinated solvents, and especially chloroform, are widely used in extraction processes of metals from aqueous phases by means of oxine 8-HQ and many of its derivatives.[22] With regard to alkanes, they can be used as oil phases when inverted microemulsions are employed in extraction[26] or in fluorogenic determination of metals.[27] In each case, molecular modeling calculations will be used in support of the proposed interpretations.

2. Materials and Methods

8-Hydroxyquinoline was purchased from Aldrich and twice recrystallized from hexane-ethyl acetate, dried in a vacuum and kept in a desiccator over $CaCl_2$. Elementary analysis results (C % 74.38; H % 4.84; N % 9.60; O % 10.95) show that 8-HQ is anhydrous and does not contain any crystallization water molecule. 8-Methoxyquinoline was purchased from Lambda probes and used as received. All organic solvents for spectroscopic measurements were of spectrograde quality and were used without further purification. In particular, dichloromethane and chloroform are certified to contain less than 0.02 wt % water, i.e., 1.47×10^{-2} and 1.66×10^{-2} mol·dm^{-3}, respectively. This was checked by a Karl-Fischer titration on a spectrograde CH_2Cl_2 sample whose water content was found to be $(1.06 \pm 0.04) \times 10^{-2}$ mol·dm^{-3}. Chloroform for vapor pressure lowering measurements was from Merck and of high purity, containing water contents lower than 0.1 wt % (8.3×10^{-2} mol·dm^{-3}).

Vapor pressure lowering measurements were performed on a KNAUER vapor pressure osmometer, using benzile and 8-methoxyquinoline as standard compounds for measurements in chloroform (at 35 °C), and benzile and anthracene as standard compounds in heptane (at 40 °C). Chloroform as a chlorinated solvent was preferred to dichloromethane according to the recommendations of the osmometer manufacturer.

TABLE 1: Ground-State pK_a Values of Hydroxyquinolines (20 °C)[31]

	pK_a (≥NH$^+$/≥N)	pK_a (−OH/−O$^-$)
5-HQ	5.20	8.54
6-HQ	5.17	8.88
7-HQ	5.48	8.85
8-HQ	5.13	9.89

The infrared absorption spectra were recorded on a single beam UNICAM Mattson 1000 FTIR spectrometer. The near IR spectra were recorded on a double beam CARY 5 "E-Line" spectrometer.

Light-scattering measurements were conducted on a SPEX Fluorolog 2 spectrofluorimeter employing a synchronous-scan protocol and right-angle geometry.[28]

The UV−vis absorption spectra were recorded on a KONTRON Uvikon-940 spectrophotometer. Corrected fluorescence spectra were obtained with a SLM 8000 C spectrofluorometer. Fluorescence quantum yields were measured using PPO in undegassed cyclohexane as the standard ($\Phi_F = 0.90$).

Time-resolved fluorescence experiments were carried out with our multifrequency (0.1−200 MHz) phase-modulation fluorometer described elsewhere.[29] The samples were excited at 325 nm with an Omnichrome He−Cd laser. The data were analyzed by a nonlinear least-squares method using Globals software (Globals Unlimited, University of Illinois at Urbana−Champaign, Laboratory for Fluorescence Dynamics).

The Hyperchem software (Hypercube Inc.) was used for molecular modeling calculations.

3. Properties of 8-HQ in Aqueous Solutions

Ground-State pK_a Values and Prototropic Forms of 8-HQ. The ground-state pK_a values of 8-HQ in aqueous solutions at 20 °C are 5.13 (≥NH$^+$/≥N) and 9.89 (−OH/−O$^-$) (Table 1).[30,31] Both functions, ≥N and −OH, appear then as either a weak base or a weak acid, respectively. At pH values lower than pH = 3, 8-HQ is exclusively in the protonated quinolinium form 8-HQ(C), whereas it is in the deprotonated quinolinate form 8-HQ(A) at pH values larger than 12. In neutral water, the predominant form is the neutral enolic 8-HQ(N) form.

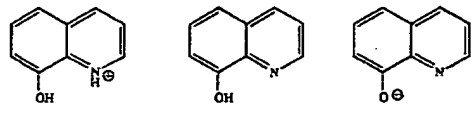

It is generally observed for bifunctional compounds that the coexistence of a tautomeric form in equilibrium with the neutral form in the ground state results in an additional band on the absorption spectrum at wavelengths longer than those of the N, C, and A bands. According to Mason in the case of hydroxyquinolines,[32] the tautomer band peaks at $\lambda_{max} \geq 400$ nm, as observed for example with 7-hydroxyquinoline. For 8-HQ in water, such a band is hardly noticeable. At pH ≈ 7 the lowest energy band is in fact located at 305 nm and is ascribed to the neutral enolic N form which then appears more stable than the tautomer in the ground state.

Comparison between the pK_a values of 8-HQ with those of 5-, 6-, and 7-HQ (Table 1) shows that the pK_a (≥NH$^+$/≥N) value is nearly the same for the four compounds, whereas for

8-HQ, the pK_a (−OH/−O$^-$) value is larger than those of the other hydroxyquinolines, the difference being at least one unit.[31] The mobility of the hydrogen atom is then reduced in 8-HQ in comparison with the three other hydroxyquinolines. A similar observation is made when comparing the acidities of the hydroxyl groups of 7-hydroxyflavone (III) (pK_a = 7.39) and 3-hydroxyflavone (I) (pK_a = 9.6).[33] The moderate increase in the pK_a values is ascribed to the existence of a H bond between the hydroxyl and the carbonyl groups of 3-hydroxyflavone, but this bond is rather weak because it takes place in a five-membered ring. The same explanation can be put forward for 8-hydroxyquinoline in which a weak H bond between the −OH group and the pyridinic nitrogen atom must then be taken into account, even in water. It is noteworthy that hydrogen bonding occurring in six-membered rings is stronger as exemplified by larger increases in the pK_a values than above: for example, the pK_a of 5-hydroxyflavone (II) is 11.56, and the pK_a of the well-known intramolecularly H-bonded 2-hydroxybenzoic acid (salicylic acid) is 13.4 whereas it is 9.9 and 9.3 for the 3- and 4-hydroxy derivatives.[34]

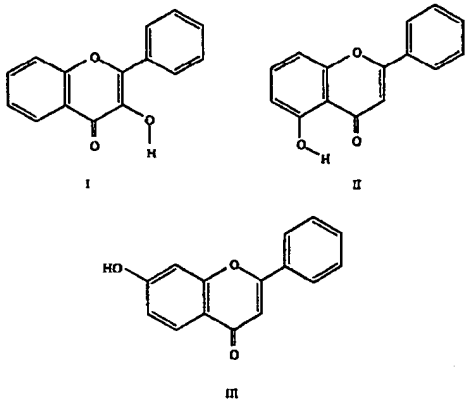

I II III

Solubility. The solubility of the neutral form 8-HQ(N) in neutral water is low. A solubility value of 4.7×10^{-3} mol·dm^{-3} is reported at 25 °C in water at pH = 7,[35] whereas the ionized forms 8-HQ(C) and 8-HQ(A) are of course much more soluble. Moreover, we have observed in this work that solubilization in neutral water at room temperature is unexpectedly slow. For instance, dissolution of 8-HQ at a concentration of 9×10^{-7} mol·dm^{-3} cannot be completed within 5 to 6 h, under magnetic stirring. On the contrary, 5-, 6-, and 7-HQ can be solubilized in neutral water under stirring without observing long delays for solubilization, and their solubility appears to be at least 2 or 3 times larger than that of 8-HQ. Comparison can be made again with the hydroxybenzoic acids. At 20 °C, salicylic acid is 3.9 and 2.3 times less soluble than 3- and 4-hydroxybenzoic acids, respectively, because of the intramolecular hydrogen bond.[34] The behavior of 8-HQ can then be, once again, accounted for by intramolecular H-bonding.

Molecular Modeling Calculations. After energy minimization performed in vacuum by using the semiempirical method AM1, a 8-HQ molecule was put in a "periodic box" of water whose size was chosen to be 12 × 10 × 12 Å (so that it contains 37 water molecules). The molecular mechanics method MM+ was then used to optimize the geometry. The distance between the hydrogen atom of the hydroxyl group and the heterocyclic nitrogen atom was found to be 2.43 Å which is consistent with the existence of a hydrogen bond linking these atoms. It is worth making a comparison with the optimized geometry of glycine under exactly the same molecular modeling conditions because the number of bonds separating the hydrogen and

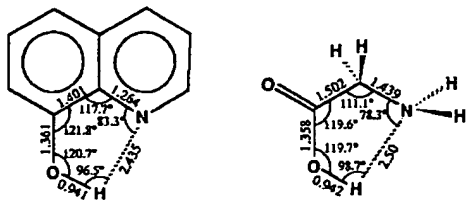

Figure 1. Energy-minimized geometries of 8-HQ (left) and glycine (right) in the presence of water molecules.

nitrogen atoms involved in an intramolecular hydrogen bond, (i.e., the hydrogen atom of the carboxylic group and the nitrogen atom of the amino group) is the same as in 8-HQ; the existence of a hydrogen bond in glycine was demonstrated by Tortonda et al.[36] In spite of some differences between our data and those of these authors owing to the different methods of calculations, Figure 1 clearly shows the strong analogy between 8-HQ and glycine in terms of spatial arrangement of atoms (five-membered ring). These considerations further support the existence of an intramolecular hydrogen bond in 8-HQ.

Fluorescence. It was mentioned in the Introduction that 8-HQ is nearly nonfluorescent in water. In fact, the fluorescence intensity is very weak in the acidity range $H_0 = -6$ to pH = 13 (H_0 is the Hammett acidity function). The quantum yield Φ_F is reported to be lower than 2×10^{-4}.[37] Fluorescence emission appears in very concentrated acidic ($H_0 < -6$)[38] or basic (pH >13)[39] solutions. Then, Φ_F increases when the concentration of acid or base increases. For instance, the fluorescence of the excited 8-quinolinate 8-HQ(A*) is increased 100-fold in NaOH solutions when going from pH ≈ 13 to $H_- \approx$ 17.5 (H_- is the Hammett acidity function for strongly basic media).[39] In concentrated acidic media, the increase of fluorescence is observed when H_0 decreases from −6 to −10. Such acidities can be obtained only with concentrated sulfuric acid. However, sulfonation occurs and leads to a sulfo derivative whose fluorescence properties are different from those of the parent hydroxyquinoline.[38,40,41] That may be the reason why the only two published values of the quantum yield of 8-HQ-(C*) in sulfuric acid available are quite different: 0.31 in 98% H_2SO_4,[37] or 0.565 in 97% H_2SO_4.[42]

The interpretation of the observed phenomena and especially of the fluorescence quenching in the major part of the acidity and pH range must take the nature of the excited form into account. Two cases are to be considered: the excited form is either the cationic 8-HQ(C) or the anionic 8-HQ(A) form, or on the contrary, it is the neutral form 8-HQ(N) (the pH ranges for the predominance of each form can be inferred from the above pK_a values).

When the excited forms are C or A, the analysis and conclusions proposed by us for 6-HQ[16] are transposable to 8-HQ. Thus, the fluorescent 8-HQ(C*) form is proved to be an outstanding photoacid: excited-state deprotonation of the −OH group occurs even in concentrated acidic media as soon as dilution releases from hydration shells water molecules able to accept the ejected proton, the ionic strength of the medium being very high. In the same way, the fluorescent 8-HQ(A*) form is an outstanding photobase, and protonation of the ≥N group occurs even in concentrated basic media as soon as water molecules exist that are able to give a proton, again because of the high ionic strength of the medium. These reactions are intermolecular monoprotonic transfers between either 8-HQ-(C*) or 8-HQ(A*) and water. They were shown to be one-way reactions because they are coupled with a simultaneous charge transfer from the prototropic site to the adjacent ring. They take place on the nanosecond scale and compete with

direct deexcitation of C* and A*. In each case, the photoproduct is 8-HQ(T*), whose structure is a ketotautomer of the neutral enolic form, and in which deexcitation takes place preponderantly via a nonradiative way, as for 6-HQ(T*). When dilution provides enough free water, the ESPT reactions become the preponderant phenomena: fluorescence is then quenched.

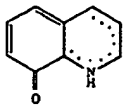

8-HQ(T*)

When the excited form is the neutral 8-HQ(N) form, it undergoes both deprotonation of −OH group and protonation of ≥N atom, coupled to the intramolecular charge transfer from one ring to the other. The question now is: are the ESPT reactions mostly intermolecular ones with the surrounding water molecules in polysolvated structures, or can they partially consist of intrinsic intramolecular proton transfers between −OH and ≥N hydrogen-bonded functions? This latter mechanism is usually discarded as soon as solvents (or impurities) with H-bonding abilities can interact with the functional groups via external H bonds. Nevertheless, the experimental considerations on pK_a and solubility, together with the calculation results, do not allow to discard the assumption of an intrinsic proton transfer process within the molecule. In fact, only dynamic characterization of the process would allow one to answer, because intrinsic ESPT occurs generally on the picosecond or subpicosecond time scale while intermolecular proton transfers are slower.[6] Unfortunately, time-resolved measurements turned out to be impossible because the fluorescence quantum yield is too low ($\Phi_F < 2 \times 10^{-4}$), and due to lack of kinetic data we can only say that the assumption of two competing, unconcerted intermolecular ESPT on the one hand, and intrinsic intramolecular ESPT according to Scheme 1 on the other hand, is not deprived of physical meaning.

4. Properties of 8-HQ in Organic Solvents

The structure of 8-HQ dissolved in organic solvents should be clearly established for the understanding of the excited-state processes leading to the poor fluorescence emission in these solvents. Before describing our own results and interpretations, it is worth relating what was the situation when we started studying 8-HQ. As far as we are aware, the related papers were published between 1957 and 1961,[43−46] and when referring to them, it can be noted that intramolecular hydrogen bonding in 8-HQ dissolved in organic solvents was commonly accepted. Two major arguments were put forward for this:

(i) In the solid state, the intramolecular hydrogen bond is unquestionable: the infrared absorption spectrum shows a broadband due to −OH stretching vibrations in the range 3100−3200 cm^{-1} which is characteristic of the hydrogen bonding between the −OH groups and the ≥N atoms. Moreover, the low melting point of 8-HQ (72−74 °C) compared to those, for instance, of 2-HQ (198−199 °C), 5-HQ (223−226 °C), 6-HQ (193 °C), or 7-HQ (235−238 °C), means that hydrogen bonds in solid 8-HQ are mainly intramolecular. Such internal hydrogen bonds are expected to be partially retained upon dissolution at least in solvents with low hydrogen-bonding power.

(ii) In solutions of organic solvents, the −OH stretching vibration frequency $\bar{\nu}_{OH}$ is reported to progressively decrease from 3418 to 3400 cm^{-1} when going from hexane to dioxane via carbon tetrachloride, chloroform, benzene, toluene, and

SCHEME 1

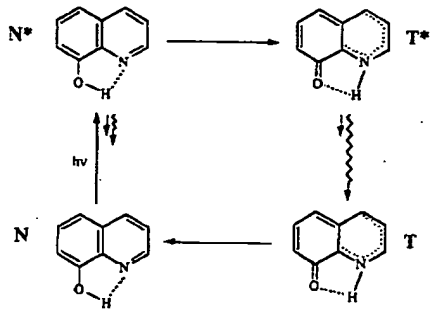

diethyl ether. Furthermore, $\bar{\nu}_{OH}$ is independent of the concentration of 8-HQ below 0.1 mol·dm^{-3}.[44,45] Vibration frequencies lower than those of a free −OH group (typically in the 3600 cm^{-1} region) are a criterion for the presence of either inter- or intramolecular hydrogen bonding, but the absence of dependence on the concentration led the authors to think that the observed phenomena resulted in fact from intramolecular hydrogen bonding (favoring then the cis structure of 8-HQ rather than the trans isomer). Moreover, the small shift (18 cm^{-1}) when going from hexane to dioxane was compared to the shift of the phenol −OH stretching band in the same solvents, i.e., 307 cm^{-1}. Phenol self-associates to give dimers, trimers, and polymers and also exhibits intermolecular bonding with the solvent when possible. The 307 cm^{-1} shift indicates the increasing contribution of intermolecular binding with the solvent when the strength of the solvents to act as proton acceptors in hydrogen bonding increases. On the contrary, the small variation, 18 cm^{-1} for 8-HQ, rules out a change from intramolecular to intermolecular hydrogen bonding in spite of dissolution in solvents possessing increasing hydrogen-bonding power. 8-HQ was then considered to be intramolecularly hydrogen bonded whatever the solvents.

However, several experimental observations in the present study will be shown to refine the above interpretation of −OH···N≤ internal hydrogen bonding of 8-HQ whatever the organic solvents. That is why the behavior of 8-HQ solubilized in chlorinated or alkane solvents will be carefully examined because the mechanism of the excited-state processes depends on the solvation modes.

Solubility of 8-HQ in Dichloromethane and in Alkane Solvents. It is surprising at first sight that, in dichloromethane as well as in heptane and cyclohexane, 8-HQ is much more soluble than 5-, 6-, and 7-HQ (by a factor of at least 10^3 at room temperature). But, on the other hand, the rates of solubilization at room temperature do not vary in a similar way in these two kinds of solvents: in dichloromethane, the rate of solubilization decreases when both 8-HQ and solvent are dried (water content lower than 0.015 wt %); in alkanes, it decreases when 8-HQ has not been dried prior to dissolution.

Considering the large solubility of 8-HQ in the solvents used in this study, once more salicylic acid can be used as a reference compound as concerns its solubility in an organic solvent. Thus, it is reported that salicylic acid is nearly 100 times more soluble than 3-hydroxybenzoic acid, and 300 times more soluble than 4-hydroxybenzoic acid in benzene at 20 °C.[35] Consequently, the solubility due to intramolecular hydrogen bond in salicylic acid increases by a factor which is not at all in the same range as the factor 10^4 observed when comparing 8-HQ with its isomers. Therefore, the question arises as to whether in the case of 8-HQ, intramolecular hydrogen bonding or other phenomena, for example self-association of 8-HQ molecules, may be responsible for such enhancements of solubility as

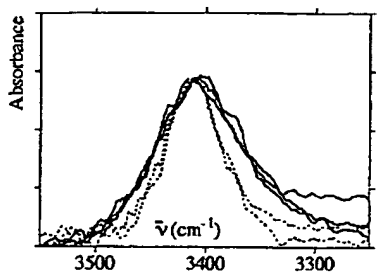

Figure 2. Normalized infrared absorption spectra of 8-HQ (−OH stretching vibration range): (—) in CH_2Cl_2, $CHCl_3$, and CH_3CN; (- - -) in benzene and toluene.

compared with the other hydroxyquinolines. Moreover, the observations on the rates of solubilization show that the presence of dissolved water plays a different role according to the solvents. It is now worth considering separately the two kinds of solvents.

Behavior of 8-HQ in Chlorinated Solvents. *Infrared Absorption Spectra.* The near-IR and IR spectra of 8-HQ were recorded in dichloromethane, chloroform, and carbon tetrachloride. The observed −OH stretching band is located at 6622 cm^{-1} (1510 nm) and 3410−3412 cm^{-1}, respectively. This band is quite similar in shape in both solvents CH_2Cl_2 and $CHCl_3$, and somewhat narrower in CCl_4. Its shape and frequency were checked to be independent of the 8-HQ concentration in the $2 \times 10^{-2} - 0.2$ mol·dm^{-3} range. Figure 2 shows the IR −OH vibration band of 8-HQ in CH_2Cl_2 and $CHCl_3$. On the contrary, 5-, 6-, and 7-HQ spectra exhibit in CCl_4 the free −OH stretching band at 3600 cm^{-1}.[43] This difference confirms the previous interpretation of the abovementioned hydrogen bonding. Moreover, we have also recorded the spectra in acetonitrile on the one hand, in benzene and toluene on the other hand (Figure 2). In CH_3CN we have found that the −OH band is exactly similar in shape and position to the one observed in CH_2Cl_2 and $CHCl_3$, with a half-width of 95 cm^{-1}. In benzene or toluene, the maxima remain in the range 3409−3410 cm^{-1}, but the −OH band is a bit narrower than in CH_2Cl_2, $CHCl_3$, or CH_3CN, with a half-width of ≈63 cm^{-1}, respectively. The slight differences on the maxima wavelengths reported previously (see above)[45] seem in fact to be deprived of physical meaning. It is striking that no environmental effects due the nature of the solvents appear on the −OH stretching frequencies and that the influence on the band shape is of minor importance. In order to better characterize the solvation state of 8-HQ in chlorinated solvents, we have turned to molecular mass determination of dissolved 8-HQ.

Vapor Pressure Osmometry. The sensitivity of this technique is well-known for the determination of the average molecular weight of small macromolecules or micellar systems. Consequently, this technique was used here in order to provide some information about a possible self-association of 8-HQ leading to the outstanding solubility reported above by comparison with the other hydroxyquinolines. The measurements were performed on solutions of 8-HQ in chloroform at a concentration ranging from 1.03×10^{-2} to 5.14×10^{-2} mol·dm^{-3}. A molecular weight of 163.2 ± 6.0 g·mol^{-1} was found using benzil as a reference compound, and 169.1 ± 6.3 g·mol^{-1} using 8-methoxyquinoline. These values are not consistent with any aggregated form of 8-HQ (molecular weight 145.16 g·mol^{-1}). Nevertheless, they are consistent with a 8-HQ monohydrate, 8-HQ·H_2O whose molecular weight is 163.16 g·mol^{-1} and whose stability would be sufficient to make it observable by this technique. Measurements in other chlorinated solvents were not done, but remembering the exact similarity of the IR spectra

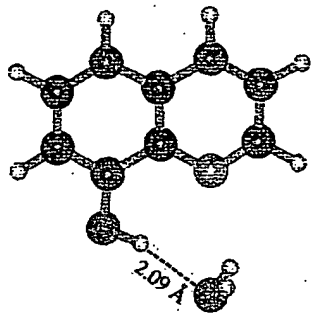

Figure 3. 3-D energy-minimized structure of a 8-HQ·H_2O complex obtained by the semiempirical method AM1.

in $CHCl_3$ and CH_2Cl_2, the results obtained in $CHCl_3$ can be transposable to CH_2Cl_2. Moreover, owing to the role of water in the solubilization rate, it seems reasonable to consider that 8-HQ is solvated in the chlorinated solvents under hydrated structures, at least 8-HQ·H_2O. In particular, when the 8-HQ concentration is lower than those used in vapor pressure osmometry experiments, for example in fluorescence measurements where typical concentrations used in the present study are ≈5×10^{-5} mol·dm^{-3} in spectrograde CH_2Cl_2 (residual water ≈ 10^{-2} mol·dm^{-3}, see Experimental Section), the residual water content of the solvent may induce polyhydrate structures.

Molecular modeling calculations were then performed in order to see whether it is possible to propose the structure 8-HQ·H_2O inferred from osmometry, and how one H_2O molecule could be located.

Molecular Modeling Calculations. Geometry optimization of a single 8-HQ molecule was first performed by using the semiempirical methods AM1 and PM3. Then, an optimized 8-HQ molecule was allowed to interact with a water molecule; the same semiempirical method was again used for geometry optimization. AM1 finds a single hydrogen-bonded structure involving the hydrogen atom of the −OH group (Figure 3), whereas PM3 predicts a double hydrogen-bonded species in which a water molecule forms a bridge between the −OH group and the heterocyclic nitrogen atom. The same kind of discrepancy between the results obtained by AM1 and PM3 was reported by Kim and Bernstein[47] in the case of 7-azaindole interacting with a water molecule. In its studies on the same system, Gordon[48] found that the results obtained by PM3 were in better agreement with its ab initio calculations.

Therefore, it is difficult to draw a reliable conclusion from these calculations on the interaction between 8-HQ and one water molecule.

Fluorescence. It is surprising to observe some fluorescence emission of the 8-HQ form in CH_2Cl_2 (λ_{max} = 391 nm) compared to the very poor fluorescence in water, and as will be seen below, in alkanes (with quantum yields lower than 2×10^{-4} at room temperature).[37] The quantum yield of 8-HQ in spectrograde CH_2Cl_2 was measured and found to be equal to $(3.8 \pm 0.2) \times 10^{-3}$ at 25 °C. This value is of the same order of magnitude as the quantum yields in acetonitrile or dimethylformamide, for example.[37]

In order to attribute with certainty the fluorescence of 8-HQ to the N* form (as expected from the emission wavelength), comparison with the fluorescence emission of 8-methoxyquinoline (8-MeOQ) in CH_2Cl_2 was made because this compound cannot undergo any excited-state prototropic reaction in neutral medium and is then supposed to mimic the 8-HQ(N) form. Figure 4 shows that the emission spectra of 8-HQ and 8-MeOQ are quite similar in shape. The blue shift of ≈10 nm observed when going from 8-HQ to 8-MeOQ is comparable to the shift

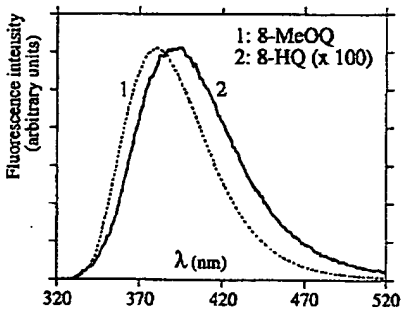

Figure 4. Fluorescence spectra of 8-methoxyquinoline and 8-hydroxyquinoline in dichloromethane (≈5 × 10^{-5}M). Concentrations are chosen such as the optical densities are the same at the excitation wavelength: 305 nm. The spectra are intensity normalized at the maximum emission wavelength.

in their absorption spectra: λ_{max} = 309 and 302 nm for 8-HQ and 8-MeOQ, respectively, in CH_2Cl_2 (spectra not shown). These shifts can reasonably be accounted for by the substitution of the −OH group in 8-HQ by the $-OCH_3$ group in 8-MeOQ. Hence the emission of 8-HQ in CH_2Cl_2 can be ascribed to the only neutral form 8-HQ(N*).

Nevertheless, the lack of any fluorescence band of the 8-HQ-(T*) form must not be interpreted by the absence of photoinduced tautomerization but rather by the fact that deexcitation of 8-HQ(T*) is nearly nonradiative as in water. The extent of phototautomerization N* → T* is in fact to be correlated with the decrease in the N* fluorescence quantum yield because of its conversion to T*. 8-MeOQ, which cannot undergo phototautomerization, fluoresces indeed much more efficiently than 8-HQ(N*). We have determined its quantum yield in CH_2Cl_2 (0.38 ± 0.02) which is 100 times larger than the quantum yield of 8-HQ in the same solvent (see above). This is exhibited in Figure 4 by the normalization factor of 100 between the spectra of 8-MeOQ and 8-HQ. It is then concluded that 8-HQ undergoes phototautomerization in CH_2Cl_2. However, when the fluorescence quantum yields in CH_2Cl_2 and in water are compared along this line, phototautomerization can be thought to be really less efficient in CH_2Cl_2 than in aqueous solution.

As concerns 8-HQ(N*) fluorescence decay, measurements performed using multifrequency phase-modulation fluorometry show that it is composed of a main component of about 15 ns and a much shorter one (with a fractional intensity of a few percents) which cannot be determined accurately owing to the very low level of light. Remembering that coupled electron transfer and proton transfer in excited-state tautomerization[16] result in a one-way reaction whatever the solvent, those two decays can be understood as arising from two kinds of solvated molecules that are both excited: (i) polyhydrate open structures where water is attached to the hydroxyl group of 8-HQ but not bridging the two functions; such structures are expected to compete with the intramolecular H bonding (which is essential for intrinsic ESPT), precluding then excited-state proton transfer; they may exhibit consequently a noticeable fluorescence (let us note that a similar interpretation has already be put forward in the case of 3-hydroxyflavone);[49] (ii) intramolecularly H-bonded molecules leading, within a short time scale, to excited-state nonfluorescent tautomers.

Behavior of 8-HQ in Alkane Solvents. *Infrared Absorption Spectra.* The spectra of 8-HQ in solutions of *n*-heptane or cyclohexane are basically the same: narrow −OH stretching bands are observed at 6605 cm^{-1} (1514 nm), and 3419−3421 cm^{-1} (Figure 5). The half-width of the latter band is ≈25 cm^{-1} and its location is in agreement with measurements of Bellamy and Hallam in *n*-hexane.[45] In addition to the different frequency

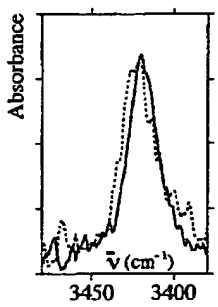

Figure 5. Normalized infrared absorption spectra of 8-HQ (−OH stretching vibration range): (—) in cyclohexane; (- - -) in *n*-heptane.

range, the narrowness of the bands distinguishes them from the previous spectra recorded in chlorinated solvents, acetonitrile, benzene, or toluene (see above). It may signify that the 8-HQ molecules fit in a well-defined and rigid structure where hydrogen bonds involving the −OH groups are responsible for self-association and indicates anyway quite a different behavior in alkanes than in the other organic solvents. Other examples of self-association through hydrogen bonding can be found in the literature (e.g. concerning aminoacridines[50] or azaindole[51]).

UV−Visible Absorption Spectra. Absorption spectra of 8-HQ in *n*-heptane and cyclohexane were recorded at various concentrations ranging from 9 × 10^{-7} to 2 × 10^{-3} mol·dm^{-3}. It turned out that the spectral changes were very small and the Beer−Lambert law was obeyed.

Resonance Light Scattering. This technique is suitable for the characterization of aggregates of chromophores that are strongly interacting via electronic coupling.[28] For instance, Pasternack and co-workers successfully applied this method to porphyrin arrays.[52,53] Unfortunately, in the present study, no significant signal was observed which may be due to the small size of the aggregates or to insufficient electronic coupling.

Vapor Pressure Osmometry. The measurements were performed on solutions of 8-HQ in *n*-heptane at concentrations ranging from 4.7 × 10^{-3} to 9.4 × 10^{-3} mol·dm^{-3}. A molecular weight of 282.5 ± 10.0 g·mol^{-1} was found using benzil as a reference compound, and 283.5 ± 10.0 g·mol^{-1} using anthracene. These values are close (within 2.5%) to twice the molecular weight of 8-HQ (145.16 g·mol^{-1}); we can thus conclude the presence of *dimers* in *n*-heptane solutions. Measurements in other alkanes, in particular cyclohexane, were not performed, but according to the strong analogies of the properties of 8-HQ in this solvent and in *n*-heptane, dimers certainly exist in cyclohexane as well.

Stability Constant of the Dimers. The stability constant K_{dim} of the dimer is not measurable by using the UV absorption spectra because of the lack of changes in these spectra in the considered concentration range (see above). The stability constant was then indirectly measured upon studying association of 8-HQ to the AOT (sodium bis(2-ethylhexyl) sulfosuccinate) surfactant molecule in *n*-heptane.[27] The experimental results obtained by fixed wavelength absorbance or stationary fluorescence intensity measurements were fitted by a model in which dimerization and association of 8-HQ monomer to the surfactant compete. The obtained value is K_{dim} = (7.0 ± 1.5) × 10^7 at 25 °C. This value shows that in a 8-HQ solution in *n*-heptane whose concentration is 10^{-6} mol·dm^{-3}, 92% of 8-HQ is under the dimer form. In view of this calculation, one can understand why no UV-absorption spectral change could be detected: the concentration range where the measurement could be performed was larger than 9 × 10^{-7} mol·dm^{-3}.

It is interesting to compare the stabilities of the 8-HQ and 7-azaindole dimers, the latter being the reference aggregates in

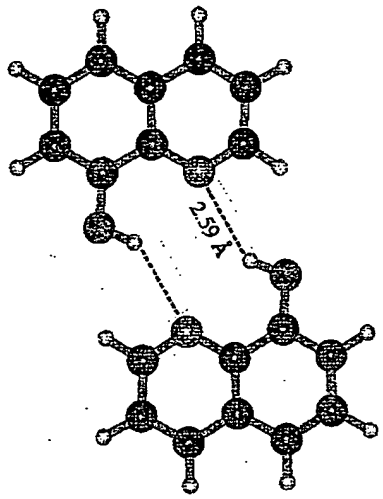

Figure 6. 3-D energy-minimized structure of a 8-HQ dimer obtained by the semiempirical method AM1.

which concerted excited-state biprotonic transfers occur. The stability constant determined by Ingham and El-Bayoumi for 7-azaindole dimers is 1.8×10^3 in 3-methylpentane at 25 °C.[51] This value shows that the 8-HQ dimers are 4×10^4 times more stable than the 7-azaindole dimers in alkane solvents. The outstanding stability of the 8-HQ dimers deserves consequently to be emphasized. It may be linked to the observation of narrow IR bands consistent with narrow energy distribution of the −OH stretching vibration within well-defined structures as the dimers. This prompted us to perform molecular modeling calculations.

Molecular Modeling Calculations. Geometry optimization of a single 8-HQ molecule was first performed by using the semiempirical methods AM1 or PM3. Then, two optimized 8-HQ molecules were allowed to interact, AM1 (or PM3) being used again for geometry optimization. Energy minimization by both methods leads to a dimer involving two intermolecular hydrogen bonds −OH···N≤. It should be noted that AM1 predicts longer hydrogen bonds (2.6 Å) than PM3 (1.8 Å); the fact that nonbonded interactions are less repulsive in PM3 than in AM1 may account for this difference. Moreover, the dimer predicted by AM1 is planar in contrast to that obtained by PM3. The 3-D energy-minimized structure found by AM1 is shown in Figure 6. The calculations were performed in vacuum, and a better description would be obtained by simulation of the apolar solvent molecules, but the relevant tools are not presently available in our software package. The conformation of the dimer could then be somewhat different, but there is no doubt on the existence of an energy minimum corresponding to dimers.

Fluorescence. The fluorescence quantum yield of 8-HQ in alkane solvents is very low ($<2 \times 10^{-4}$ at room temperature), and in particular much lower than that of 5-HQ in isopentane (0.30) or that of 8-methoxyquinoline in isopentane (0.05).[37] It is moreover noteworthy that decreasing the temperature to 77 K does not improve the fluorescence emission, the quantum yield remaining lower than 2×10^{-4}.[37] The weak fluorescence emission was tentatively explained in the following way: the intramolecular hydrogen bond between the −OH and ≥N groups, which is stronger in the excited state, would favor the deexcitation $S_1^* \rightarrow S_0^*$ via internal conversion.[37]

The presence of dimers in alkanes, as demonstrated above, together with our findings on the mechanism of coupled proton and electron transfers, lead us to give a different explanation for the very low fluorescence quantum yield of 8-HQ in these solvents: light excitation induces a double concerted proton transfer within the dimer, coupled to an intramolecular electron transfer within each 8-HQ moiety. The efficiency of the process is very high at room temperature and at 77 K as well. The proton transfers in the excited state seems then to be barrier-free or to involve a barrier ineffective at 77 K. The excited-state phenomena within 8-HQ dimers may match the concerted biprotonic proton transfers within 7-azaindole dimers[8-10,51,54-56] occurring at a rate larger than 2×10^{11} s^{-1} in hydrocarbon solvents at room temperature.[10,57] Moreover, dimers are almost solely present at the usual concentration where the measurements are carried out (10^{-5}–10^{-4} mol·dm^{-3}). The probability of finding and consequently exciting a monomer is so low that the phenomena occurring in the monomers are not detectable.

5. Conclusion

The poor fluorescence emission of 8-HQ has been shown to result in all cases from a photoinduced tautomerization reaction followed by deexcitation of the tautomer which occurs mainly via a nonradiative route. Various solvated structures have been proposed according to the solvent in which the ESPT reaction can occur in different ways.

(i) In water, it is likely that the tautomerization mainly results from intermolecular proton transfers between each of the two functions (−OH and ≥N) and surrounding water molecules. However, it has been shown that the properties of 8-HQ are consistent with the existence of a weak intramolecular hydrogen bond in a five-membered ring. An intrinsic intramolecular proton transfer between the two functions is thus likely to occur as well.

(ii) In alkane solvents, 8-HQ molecules self-associate to form highly stable dimers which can undergo concerted biprotonic transfer in the excited state as in 7-azaindole. The efficiency and the extent of this process is related to the stability of the dimers consistently with a very low quantum yield which is not improved by lowering the temperature down to 77 K.

(iii) In dichloromethane and chloroform, a monohydrated form has been detected at high concentrations by vapor pressure osmometry. The existence of polyhydrates at lower concentrations in 8-HQ cannot be discarded. In some of these structures, hydration of the −OH group may occur without a bridge between the two functions. Consequently, the photoinduced tautomerization is less efficient than in pure water and fluorescence emission is detectable ($\Phi_F \approx 4 \times 10^{-3}$).

The results as a whole show that 8-HQ is a prototype compound where all possible modes of ESPT can be observed. The conceptual interest of this molecule is then remarkable. Unfortunately, the lack of fluorescence of the tautomer precludes time-resolved fluorescence experiments, but ultrafast transient absorption spectroscopy may provide in the future further insight into the excited-state processes. Time-resolved infrared or Raman spectroscopy is also to be considered. On the other hand, analytical applications take advantage of the lack of fluorescence since complexation with some metal ions induces a fluorescence enhancement (fluorogenic effect); in fact, the structure of a complex with a cation resembles the cationic form of 8-HQ and is thus fluorescent.

The present study is the first one aiming to rationalize and understand the excited-state behavior of the 8-HQ ligand, mainly in organic solvents where it is generally used.

Acknowledgment. The authors thank Dr. N. Goasdoué for helpful discussions on infrared spectra, and J.-P. Lefèvre for his assistance in time-resolved measurements. Vapor pressure osmometry experiments were performed in Collège de France,

Laboratoire des Interactions Moléculaires; Dr. V. Marchi-Artzner is gratefully acknowledged for her welcome and help.

References and Notes

(1) Ireland, J. F.; Wyatt, P. A. H. *Adv. Phys. Org. Chem.* **1976**, *12*, 131.
(2) Hibbert, F. *Adv. Phys. Org. Chem.* **1986**, *22*, 113.
(3) Gutman, M.; Nachliel, E. *Biochim. Biophys. Acta* **1990**, *1015*, 391.
(4) Formosinho, S. J.; Arnaut, L. G. *J. Photochem. Photobiol. A: Chem.* **1993**, *75*, 1.
(5) (a) Weller, A. *Naturwissenschaften* **1955**, *42*, 175. (b) Weller, A. *Z. Elektrochem.* **1956**, *60*, 1144.
(6) Kasha, M. *J. Chem. Soc., Faraday Trans. 2* **1986**, *82*, 2379.
(7) Arnaut, L. G.; Formosinho, S. J. *J. Photochem. Photobiol. A: Chem.* **1993**, *75*, 21, and references therein.
(8) Taylor, C. A.; El-Bayoumi, A. M.; Kasha, M. *Proc. Natl. Acad. Sci. U.S.A.* **1969**, *65*, 253.
(9) Ingham, K. C.; Abu-Elgheit, M.; El-Bayoumi, M. A. *J. Am. Chem. Soc.* **1971**, *93*, 5023.
(10) Hetherington, W. M., III; Micheels, R. H.; Eisenthal, K. B. *Chem. Phys. Lett.* **1979**, *66*, 230.
(11) Itoh, M.; Adachi, T.; Tokumura, K. *J. Am. Chem. Soc.* **1984**, *106*, 850.
(12) Nakagawa, T.; Kohtani, S.; Itoh, M. *J. Am. Chem. Soc.* **1995**, *117*, 7952.
(13) Konijnenberg, J.; Ekelmans, G. B.; Huizer, A. H.; Varma, C. *J. Chem. Soc., Faraday Trans. 2* **1989**, *85*, 39.
(14) Chou, P. T.; Martinez, S. S. *Chem. Phys. Lett.* **1995**, *235*, 463.
(15) Bardez, E.; Boutin, P.; Valeur, B. *Chem. Phys. Lett.* **1992**, *191*, 142.
(16) Bardez, E.; Chatelain, A.; Larrey, B.; Valeur, B. *J. Phys. Chem.* **1994**, *98*, 2357.
(17) (a) Lee, S. I.; Jang, D. J. *J. Phys. Chem.* **1995**, *99*, 7537. (b) Kim, T. G.; Lee, S. I.; Jang, D. J.; Kim, Y. *J. Phys. Chem.* **1995**, *99*, 12698.
(18) Mason, S. F.; Philp, J.; Smith, B. E. *J. Chem. Soc. A* **1968**, 3051.
(19) Soroka, K.; Vithanage, R. S.; Phillips, D. A.; Walker, B.; Dasgupta, P. K., *Anal. Chem.* **1987**, *59*, 629.
(20) Hollingshead, R. G. W. *Anal. Chim. Acta* **1958**, *19*, 447.
(21) Stary, J. *Anal. Chim. Acta* **1963**, *28*, 132.
(22) Laing, M. *Educ. Chem.* **1996**, 157.
(23) Demopoulos, G. P.; Distin, P. A. *Hydrometallurgy* **1983**, *11*, 389.
(24) Cote, B.; Demopoulos, G. P. *Solvent Extr. Ion Exch.* **1993**, *11*, 2, 349.
(25) Dowling, S. D.; Seitz, W. R. *Spectrochim. Acta* **1984**, *40A*, 991.
(26) Boumezioud, M.; Kim, H. S.; Tondre, C. *Colloid Surf.* **1989**, *41*, 255.
(27) Devol, I.; Bardez, E. To be published.
(28) Pasternak, R. F.; Bustamante, C.; Collings, P. J.; Giannetto, A.; Gibbs, E. J. *J. Am. Chem. Soc.* **1993**, *115*, 5393.
(29) Pouget, J.; Mugnier, J.; Valeur, B. *J. Phys. E Sci. Instrum.* **1989**, *22*, 855.
(30) Hollingshead, R. G. W. *Oxine and its derivatives*; Butterworths: London, 1954; Vol. I-IV.
(31) Albert, A.; Phillips, J. N. *J. Chem. Soc.* **1956**, 1294.
(32) Mason, S. F. *J. Chem. Soc.* **1957**, 5010.
(33) Wolfbeis, O. S.; Leiner, M.; Hochmuth, P.; Geiger, H. *Ber. Bunsen-Ges. Phys. Chem.* **1984**, *88*, 759.
(34) *Traité de Chimie Organique*; Grignard, V., Dupont, G., Locquin, R., Eds.; Masson: Paris, 1945; Vol. XI.
(35) *Solubilities of inorganic and organic compounds*; Stephen, H., Stephen, T., Eds.; Pergamon Press: London, 1964; Vol. 2, Part 1.
(36) Tortonda, F. R.; Pascual-Ahuir, J. L.; Silla, E.; Tunon, I. *Chem. Phys. Lett.* **1996**, *260*, 21.
(37) Goldman, M.; Wehry, E. L. *Anal. Chem.* **1970**, *42*, 1178.
(38) Ballard, R. E.; Edwards, J. W. *J. Chem. Soc.* **1964**, 4868.
(39) Schulman, S. G. *Anal. Chem.* **1971**, *43*, 285.
(40) Schulman, S. G.; Fernando, Q. *Tetrahedron* **1968**, *24*, 1777.
(41) Bratzel, M. P.; Aaron, J. J.; Winefordner, J. D.; Schulman, S. G.; Gershon, H. *Anal. Chem.* **1972**, *44*, 1240.
(42) Onoue, Y.; Hiraki, K.; Morishige, K.; Nishikawa, Y. *Nippon Kagaku Kaishi* **1978**, *9*, 1237.
(43) Mason, S. F. *J. Chem. Soc.* **1957**, 4874.
(44) Badger, G. M.; Moritz, A. G. *J. Chem. Soc.* **1958**, 3442.
(45) Bellamy, L. J.; Hallam, H. E. *Trans. Faraday Soc.* **1959**, *55*, 220.
(46) Richards, J. H.; Walker, S. *Trans. Faraday Soc.* **1961**, *57*, 399.
(47) Kim, S. K.; Bernstein, E. R. *J. Phys. Chem.* **1990**, *94*, 3531.
(48) Gordon, M. S. *J. Phys. Chem.* **1996**, *100*, 3974.
(49) McMorrow, D.; Kasha, M. *J. Phys. Chem.* **1984**, *88*, 2235.
(50) Albert, A. *The Acridines*; Edward Arnold: London, 1966.
(51) Ingham, K. C.; El-Bayoumi, M. A. *J. Am. Chem. Soc.* **1974**, *96*, 1674.
(52) Pasternak, R. F.; Schaefer, K. F. *Inorg. Chem.* **1994**, *33*, 2062.
(53) Pasternak, R. F.; Collings, P. J. *Science* **1995**, *269*, 935.
(54) Tokumura, K.; Watanabe, Y.; Udagawa, M.; Itoh, M. *J. Am. Chem. Soc.* **1987**, *109*, 1346.
(55) Chou, P. T.; Wei, C. Y.; Chang, C. P.; Meng-Shin, K. *J. Phys. Chem.* **1995**, *99*, 11994.
(56) Nakajima, A.; Hirano, M.; Hasumi, R.; Kaya, K.; Watanabe, H.; Carter, C. C.; Williamson, J. M.; Miller, T. A. *J. Phys. Chem. A* **1997**, *101*, 392.
(57) Share, P. E.; Sarisky, M. J.; Pereira, M. A.; Repinec, S. T.; Hochstrasser, R. M. *J. Lumin.* **1991**, *48/49*, 204.

ELSEVIER

Spectrochimica Acta Part A 57 (2001) 1541–1553

SPECTROCHIMICA ACTA PART A

www.elsevier.nl/locate/saa

Hydrogen bonding and dipolar interactions between quinolines and organic solvents. Nuclear magnetic resonance and ultraviolet–visible spectroscopic studies

Marisa Santo, Rosa Cattana, Juana J. Silber *

Departamento de Química y Física, Universidad Nacional de Río Cuarto, Agencia Postal Nro. 3, 5800, Río Cuarto, Argentina

Received 12 September 2000; accepted 2 November 2000

Abstract

Solvatochromic studies on quinoline (Q), 3-cyanoquinoline (CNQ), 3-bromoquinoline (BrQ) and 8-hydroxyquinoline (OHQ) in pure solvents and alcohol–cyclohexane mixtures have been performed. The results are compared with Proton Nuclear Magnetic Resonance, ^{1}H NMR, studies and AM1 calculations. Taft and Kamlet's solvatochromic comparison method was used to disclose solvent effects in pure solvents. These studies shows that the hydrogen bond acceptor ability of the Q ring is diminished and its polarity is increased by the presence of the cyano group in CNQ and the bromo group in BrQ. In OHQ, intramolecular hydrogen bonding has been observed. This interaction is weakened by the interaction with protic solvents. The studies in binary mixtures, alcohol–cyclohexane, show solute–solvent interactions, which compete with solvent self-association in the preferential solvation phenomena. Alcohols with strong ability to self-associate have less preference toward solvation of these compounds. The association constants for solute–ethanol systems were determined by ^{1}H NMR. The results show that the solvent hydrogen bond donor ability is the main factor involved in the interaction with these solutes at the aza aromatic site.

Keywords: Solvatochromism; Quinolines; Solvent effects; Intermolecular interactions; Hydrogen bonding

1. Introduction

The nature and extent of solute–solvent interactions are able to affect various properties of some compounds in solution. The search for a better understanding of the effect that this factor has on property variations has been an active area of research [1].

The position and intensity of absorption bands in Ultraviolet visible (UV–visible), Infrared Resonance (IR), Nuclear Magnetic Resonance (NMR) spectroscopy are solvent dependent [2]. The solvent effects on the electronic spectrum of a molecule are referred as 'solvatochromism'. The solvatochromic shifts are indicative of interactions between the solvent and the solute in the immedi-

* Corresponding author. Tel.: +54-358-467157; fax: +54-358-4680280.

E-mail address: jsilber@exa.unrc.edu.ar (J.J. Silber).

1386-1425/01/$ - see front matter © 2001 Elsevier Science B.V. All rights reserved.
PII: S1386-1425(00)00478-9

ate vicinity of the solute, this region being referred as the solute cybotactic region [3]. The interactions can be classified into: (i) non-specific solute–solvent association caused by polarity–polarizabitity effects; and (ii) specific solute–solvent association such as hydrogen bonding or electron donor–acceptor interactions. In order to analyse the interactions, one of the most successful approaches is the solvatochromic comparison method of Kamlet, Taft et al. [4]. In this method empirical parameters are used to quantify specific interactions and to separate them from polarity–polarizability effects. Another methodology for the study of solute–solvent interactions is the use of binary mixtures of solvents. In solvent mixtures a preferential enrichment by one of the solvent components in the cybotactic region of a compound is often observed. The fact that the solvent shell has a composition other than the macroscopic ratio is termed selective or preferential solvation [5].

In previous works, we have used the concept of preferential solvation to characterise and quantify specific interactions such as electron-donor–acceptor complexation between solutes that may act as π-acceptors, and n-donor solvents [6]. We also analysed hydrogen bond interactions between nitroanilines and hydrogen-bond acceptor solvents [7–9].

In this paper we report the solvation and preferential solvation studied, by solvatocromism and ^{1}H NMR, of quinoline (Q), 3-cyanoquinoline (CNQ), 3-bromoquinoline (BrQ) and 8-hydroxyquinoline (OHQ) in pure solvents and alcohol–cyclohexane mixtures.

The substituent effects on the quinoline spectrum depend how strong is it interaction with the conjugated systems [10]. The cyano and bromo group are widely recognised as a electron withdrawing groups in conjugated molecules. A vast experimental database exists on their role in altering a number of standard physical properties of π electronic systems such as electronic spectra [11]. The hydroxy group makes important changes in the spectrum of the aromatic system. In OHQ it is of particular interest because it is in position to give intramolecular hydrogen bonding with the azaromatic nitrogen [12].

The quinoline ring systems have always attracted a considerable amount of attention because it is present in many compounds, both natural and synthetic, which exhibit a wide range of biological activities. This structure has a high degree of importance among heterocyclic compounds such as those, which reveal strong cytotoxic and/or antimicrobial properties [13,14]. Also, quinoline derivatives represent the effective moiety in some antimalarial drugs [15].

The study of dipolar interactions and hydrogen bonding with the medium in pharmacological active compounds is pertinent because non-covalent interactions have been shown physiologically important [16]. Moreover the studies in binary mixtures allow detecting the mixture composition with maximum solute–medium interaction. These results have relevant application in the development of chromatographic techniques [17] used in separation and characterisation of biologic systems.

The solvatocromic studies performed in this work are compared with ^{1}H NMR studies and AM1 calculations. The results show that hydrogen bond interaction is the main factor responsible of the observed solvent effects in the analysed solutes.

2. Experimental section

Quinoline (Q) from Fluka was purified by the method reported in [18]. 3-Cyano-quinoline (CNQ) obtained from Aldrich Chemical Co., was purified by vacuum sublimation, m.p. 105°C [19]. 3-Bromo-quinoline (BrQ) obtained from Fluka was purified by vacuum distillation [20], and its purity was tested by HPLC in 90:10 hexane/ethylacetate and also by it refractive index, $n = 1.6641$, which was concordant with literature data [21]. 8-Hydroxyquinoline (OHQ) obtained from Sigma was purified by vacuum sublimation, m.p. 75.3°C [21].

The solvents used, cyclohexane (CHx), hexane (Hx), methanol (MeOH), ethanol (EtOH), 1-propanol (1-PrOH), 1-butanol (BuOH), 2-

propanol (2-PrOH), acetonitrile (ACN), tetrahydrofuran (THF), ethyl ether (EE), dimethylformamide (DMF) were purified to spectroscopic quality by standard methods [22]. Water was first distilled over potassium permanganate and then bidistilled. The UV cut-off point of the solvents in a UV cell of 10 mm against air was used as purity criteria.

The UV–visible spectroscopic measurements were performed using a Cary 17 spectrometer at a temperature of 25 ± 0.2°C. ν_{max} was measured by taking the middle point between the two positions of the band where the absorbance is equal to 0.90 A_{max} [23]. Thus, the uncertainties in ν_{max} are 100 cm^{-1}. The solute concentration was $\cong 10^{-5}$ M. The ^1H NMR measurements were performed using NMR Bruker (200 MHz) with tetramethysilane (TMS) as internal reference, the uncertainties are ± 0.5 Hz, 8% of the average shift observed. The solute concentration was 10^{-2} M in pure solvents determinations and change from 10^{-6} to 10^{-2} M in EtOH–CHx mixture. The AM1 calculations were carried out using the HyperChem software, version 3.1, running in a Pentium III 500 MHz personal computer.

3. Results and discussion

3.1. UV–visible studies in pure solvents

Quinolines show two bands, assigned to ^1L_b and ^1L_a transitions, respectively [24]. The absorption maxima obtained for quinoline and substituted quinolines, in all solvents used, are gathered in Table 1. The frequencies of the ^1L_a bands are more solvent sensitive than those of the ^1L_b band.

Taft and Kamlet's solvatochromic comparison method [4] was used to analyse the solvatochromism of the ^1L_a band for Q, CNQ, BrQ and OHQ. This method rationalises solvent effects in terms of a linear combination, which depends on three fundamental indexes: The scale π^* of solvent dipolarity/polarizability parameter, which measures the ability of the medium to stabilise the charge on a dipole by virtue of its dielectric effects; the α scale of solvent hydrogen bond donor acidity, which describes the solvent's ability to donate a proton in a solvent to solute hydrogen bond; the β scale of hydrogen bond acceptor basicities, which provides a measure of the solvent's ability to accept a hydrogen bond.

Table 1
Maximum absorption frequencies [a] of Q CNQ, BrQ and OHQ in pure solvents [a]

	Q		CNQ		BrQ		OHQ
Solvent	$\nu_{max}L_a$ [a]	$\nu_{max}L_b$	$\nu_{max}L_a$	$\nu_{max}L_b$	$\nu_{max}L_a$	$\nu_{max}L_b$	ν_{maxII}
CHx	37.20	32.05	35.61	30.64	36.79	31.02	31.68
Hx	37.20	32.06	35.63	30.66	36.75	31.09	31.72
DMF	36.88	32.05	35.20	30.63	36.29	31.06	31.93
THF	37.04	31.97	35.34	30.65	36.59	31.07	31.75
EE	37.12	32.12	35.52	30.64	36.72	31.09	31.63
DCE	36.78	31.92	35.20	30.58	36.33	31.01	31.64
DCM	36.59	[b]	35.02	[b]	36.25	30.94	32.05
Chl	36.44	31.94	35.97	30.51	36.34	31.02	31.54
Cl_4C	36.62	[b]	35.26	[b]	36.28	30.91	31.32
ACN	36.91	32.06	35.36	30.70	36.64	31.11	32.99
W	35.71	32.08	34.69	30.74	35.34	30.99	32.88
MeOH	36.11	32.09	35.08	30.77	35.95	31.08	31.81
EtOH	36.28	32.04	35.05	30.77	35.83	30.98	32.74
PrOH	36.06	31.99	35.00	30.63	35.77	30.99	31.71
BuOH	36.14	31.90	34.98	30.69	35.65	30.89	31.49
2-PrOH	36.36	32.10	35.06	30.66	35.95	31.02	31.68

[a] Values given in 10^{-3} ν_{max} cm^{-1}.
[b] Shoulder.

Table 2
Results of the regression analysis in the ν_{max} of the ^1L_a band by using Eq. (2) [a]

Solute	ν_o 10^{-3}/cm^{-1}	s	A	r	n [b]
Q	37.19 ± 0.05	-0.27 ± 0.08	-1.01 ± 0.06	0.9790	12
CNQ	35.60 ± 0.04	-0.38 ± 0.08	-0.42 ± 0.05	0.9463	12
BrQ	36.78 ± 0.09	-0.32 ± 0.1	-0.88 ± 0.09	0.9186	12

[a] Confidence level greater than 99.99%, according to Student test.
[b] Number of points.

These solvatochromic parameters are used in linear solvation energy relationships of the general form in Eq. (1).

$$XYZ = XYZo + s\pi^* + a\alpha + b\beta \quad (1)$$

where XYZ is the property to be correlated; s, a and b coefficients measure the relative susceptibilities of XYZ to the indicated solvent property scales. The parameters of organic solvents, π^*, α, β are reported in [25].

The results of the stepwise regression applied to Eq. (1) with the values of ν_{max} for the ^1L_a band in different pure solvents are collected in Table 2. The correlations are good with π^* and α parameter. The b values are smaller than the error, no statistical significance was observed for β, according the test utilised [26].

The negative values of the s coefficients are expected, considering the increase of dipole moment upon excitation for these solutes [27]. The magnitude of the s values shows also that the bromo and cyano derivatives are more sensitive to solvent polarity than the unsubstituted compound. On the other hand all the solutes are quite sensitive to the hydrogen bond donor ability of the solvent.

In order to analyse the effect that the heteroatom in the aromatic ring has on the solvation properties the results are compared with similar studies on π-isolectronic compounds such as naphthalene (Np) and cyanonaphthalene (CNNp) [28]. The sensitivity to the dipolarity–polarizability parameter in CNNp is quite significant, $s_{CNNP} = 0.63 \pm 0.08$, while no dependence on ν_{max} of CNNp with the α parameter has been observed [28], since a has a value smaller than the error. This suggests that the cyano group increases the polarity of Np without increasing the hydrogen bond acceptor ability. Similar results were obtained in our studies with other cyanoaromatic compounds [6]. Thus, it is assumed that the hydrogen bond effects produced by hydrogen bond donor solvents in quinoline derivatives are only due to interactions with the aza group. The order in values of 'a' coefficient are Q > BrQ > CNQ, as expected, because bromo and cyano groups decrease the basicity of the aza nitrogen atom as a result of inductive and resonance electron-withdrawing effects. Both bromine and cyano groups have similar electro negativities [29] but the electron-withdrawing effect of the cyano group, as measured by σ_m constant, is greater than that of the bromine atom [30].

Semiempirical molecular orbital calculations AM1 [31] have been performed in order to obtain more information about the structural features in the studied systems. Calculations were performed starting from standard bonds lengths and bond angles. All geometries were fully optimised by minimising the energy with respect to geometrical variables without symmetry constraint, using gradient 0.01 Kcal mol^{-1} and Polak–Ribierie algorithm as convergence criterion. This semi-empirical method does not describe the solvating processes, but it may provide some information about the interaction centres, changes in the charge distribution and in the bond distance when different groups are present in the main structure. Semi-empirical AM1 method provides a good description of charge distribution, and is acceptable for systems of the given size. Its merit is an improved treatment of van der Waals interactions and, in particular, of the hydrogen bonds [32] due to a new expression for the core–core repulsion.

Table 3
Calulated charge density and dipole moment, μ_{cal}, for Q, CNQ, BrQ and OHQ

Solute		Q	CNQ	BrQ	OHQ
Charge density	N	−0.130	−0.126	−0.125	−0.148
	N C–C_3		−0.027		
	C_2	−0.054	−0.023	−0.029	−0.053
	C_3	−0.185	−0.072	−0.231	−0.177
	C_4	−0.080	−0.031	−0.049	−0.083
	C_5	−0.111	−0.105	−0.107	−0.154
	C_6	−0.127	−0.126	−0.126	−0.087
	C_7	−0.124	−0.112	−0.117	−0.172
	C_8	−0.099	−0.103	−0.101	0.116
	Br			0.073	
μ_{cal}		1.88 D	3.50 D	2.04 D	2.45 D

AM1 semiempirical calculations (Table 3) show an increment of the dipole moment (μ) in BrQ ($\mu = 2.04$ D) and CNQ ($\mu = 3.50$ D) with respect to the non-substituted compounds Q ($\mu = 1.88$ D). This effect is in accord with the different 's' values obtained from Eq. (1) for Q and substituted Qs, (Table 2). The π^* parameter measures dipolarity and polarizability, and μ measures only dipolarity. Then, the order of s values of CNQ and BrQ does not show an exact correlation with the calculated μ, probably due to the different polarizability of the solutes not considered in μ.

The solvent effect on the intramolecular hydrogen bonding, of OHQ, has been the subject of many studies, however the nature of the interaction and the influence of solvents on the hydrogen bond strength still have not been unequivocally elucidated [33].

Negative solvatochromism is observed for OHQ bands, (Table 1). This behaviour indicates an increase of the dipole moment upon electronic transition. In water, a strong hydrogen bond donor solvent, two bands are observed in the region 260–340 nm. As noticed in Fig. 1, in the other hydrogen bond donor solvents only one band is detected at 310–320 nm. The changes in the shape bands observed in the OHQ spectra in different hydrogen bond donor solvents may be due to the splitting of electronic levels by vibrational states. This precludes any analysis of the solvatochromism of OHQ [34]. Actually, as observed in Table 1, with the exception of water, the shifts of the band are very small when changing the solvent properties. This low sensitivity may be attributed to the formation of intramolecular hydrogen bond in OHQ, between the proton in hydroxyl group and the aromatic nitrogen. The intramolecular hydrogen bond interaction is expected preferentially in weak- or non-hydrogen-bond-donor solvents. The AM1 semiempirical calculations show than the OHQ conformer with intramolecular hydrogen bonding is 3.41 Kcal mol^{-1} more stable than the anti conformer without hydrogen bonding. A distance of 2.40 Å between H of OH and aza nitrogen and an angle between the oxygen in the donor group, the proton, and the aza aromatic nitrogen acceptor,

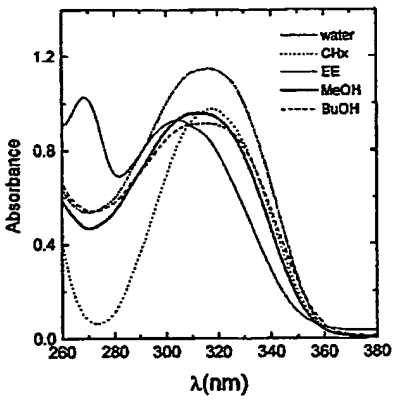

Fig. 1. Absorption spectra of OHQ: (a) in water (-------); (b) Chl (.....); (c) E.E. (-·-·-·-); (d) MeOH (—); (e) BuOH (—·—).

O–H···N, $\theta = 110.1°$ are calculated. These data are the same order as those observed in similar systems with intramolecular hydrogen bonding [35]. Enthalpies for hydrogen bond formation, ΔH_f, were calculated for the complex OHQ–W, OHQ–MeOH and OHQ–EtOH giving the values of -5.40, -3.03 and -2.91 kcal mol^{-1}, respectively. ΔH_f for the hydrogen bonding interaction was obtained as the difference between the enthalpy of the formation of the complex and the enthalpy of formation of each of the molecules involved in the complex. These enthalpies were compared with the calculated ΔH_f for hydrogen-bonded interactions in the W–W, MeOH–MeOH, EtOH–EtOH complexes. The interaction energies are -5.38, -2.42 and -2.48 kcal mol^{-1}, respectively. It must however be borne in mind that this analysis is only qualitative because it is based on calculations that neglect the energy required to break the pre-existing hydrogen bonding between the solvent molecules themselves. Nevertheless the ΔH_f calculated provides evidence that only OHQ–W hydrogen bonding is stronger than the intramolecular hydrogen bonding in OHQ. The intramolecular interaction is probably broken in strong hydrogen bond donor solvents as water and weaken, but do not break, in low hydrogen bond acceptor solvents as alcohols. Studies developed by Holzer et al. [36] by ^{1}H NMR in similar systems show than only strongly interacting solvents have the capacity to break the intramolecular hydrogen bonding.

Evidences of intramolecular hydrogen bonding have been reported for Bardez in OHQ. They also detect in alkane solvents, a very stable dimer [37]. At this point there is not enough evidence to determine if the cause of the OHQ behaviour is intramolecular hydrogen bonding or dimer formation, but at the low concentrations used dimer formation is not favoured.

3.2. UV–visible studies in solvent mixtures

In order to obtain more insight about the interactions between quinolines and alcohols, their spectral behaviour was studied in alcohol–CHx binary mixtures. The alcohols used were EtOH, 1-PrOH, 2-PrOH and 1-BuOH. CHx is considered quite an 'inert' solvent. However, in these solvent mixtures self-associations between alcohol molecules through hydrogen bonding usually occur. Then, these solutions are non-ideal despite the fact that hydrocarbons do not form complexes with alcohol [38]. A dynamic equilibrium in pure liquid alcohol is assumed to exist as hydrogen bonds are broken and formed at a high rate. If an inert solvent is added the dynamic equilibrium continues until the limit of an infinitely dilute solution is reached, in this point the concentration of the hydrogen bonded species becomes infinitesimal [39]. On the other hand, when solute–solvent and solvent–solvent interactions are present in the system both interactions play significant roles in determining the preferential solvation characteristics [40,41].

Fig. 2 shows the plots obtained for ν_{max} of the L_a band of Q as a function of the alcohol concentration. The deviations from the ideal curve shows that, in all the mixtures studied, Q exhibits preferential solvation. The dielectric enrichment model [7] has been used to calculate the preferential solvation caused only by dielectric interaction (dotted line, Fig. 2). In all the mixtures, the experimental preferential solvation interaction is greater than the calculated, showing specific interactions, that is hydrogen bonding, between the alcoholic solvent and the solute Q.

CNQ shows specific interaction with the alcohol as shown for the deviation of the experimental curve with respect to the calculated by dielectric enrichment model. This compound shows preferential solvation only at low concentration of alcohol (Fig. 3a,b). This is an evidence of competition between solute–solvent and solvent–solvent interactions. Solute–alcohol interactions dominate at low concentrations of alcohol and alcohol–alcohol interactions dominate at high concentrations of alcohol. To analyse this behaviour it is convenient to consider the self-association constants (K_{AA}) of the alcohol used, listed in Table 4. The plots in Fig. 3 show that the X_A of the alcohol in the mixtures at which preferential solvation of CNQ becomes negligible, follows a reverse order relative to the association constants of the alcohols. Thus, preferential solvation can be observed at X_A lower than 0.7 for EtOH, $K_{AA} = 134$, while

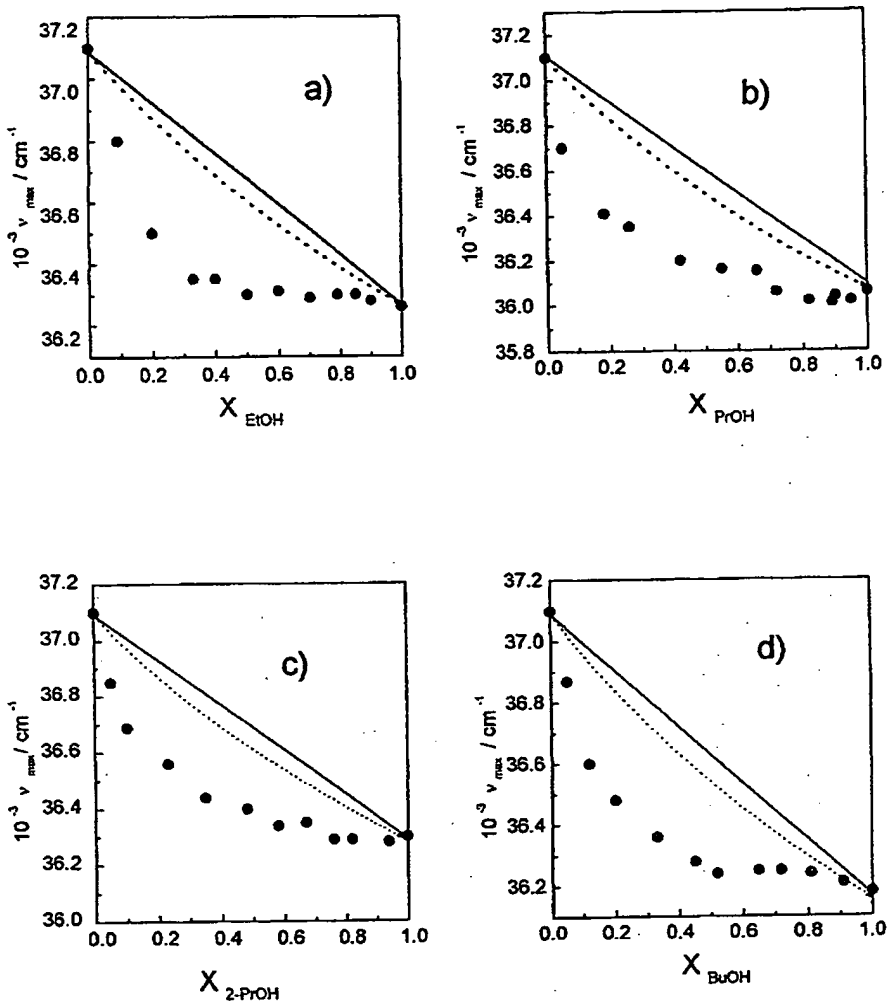

Fig. 2. ν_{max} of the ^1L_a band of Q vs. molar fraction of the alcohol in alcohol–CHx binary mixtures: (a) EtOH; (b) 1-PrOH; (c) 2-PrOH; (d) 1-BuOH. (●) Experimental points; (----) DE curves.

for 1-BuOH, $K_{AA} = 73$, the preferential solvation is observed almost in all range of concentration, X_A lower than 0.9.

BrQ shows preferential solvation in almost the whole range of alcohol concentration in the mixtures (Fig. 4a,b). Since the experimental curve shows deviation from the dielectric enrichment curves, specific interaction with the alcohol is observed.

In OHQ–alcohol systems small preferential solvation is detected, and it is close to the calculated by dielectric enrichment model, as shown in Fig. 5 for CHx–EtOH mixtures. This result could be indicating the absence of hydrogen bonding interaction between OHQ and the alcohol, and reinforces the previous conclusion that intramolecular hydrogen bond present in OHQ is only weakened, but not break, by the interaction with the solvent. The absence of hydrogen bonding interaction between OHQ and the alcohol may be also due to the dimer formation of OHQ [37] through intermolecular solute–solute hydrogen bond, in the

whole range of the solvent mixture. Another possibility that can not be roulette out is that the studied band is not sensitive to hydrogen bonding formation. Thus, the studies in the mixtures do not give enough information for make a conclusion about inter or intramolecular interactions in OHQ.

In order to analyse the interaction observed the preferential solvation could be quantified using the following approach. If the ν_{max} in the solvent mixture (ν_{AB}) can be expressed by Eq. (2),

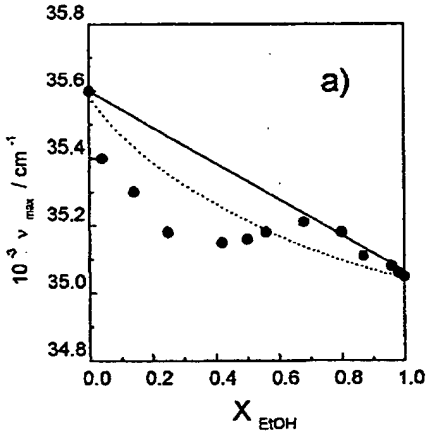

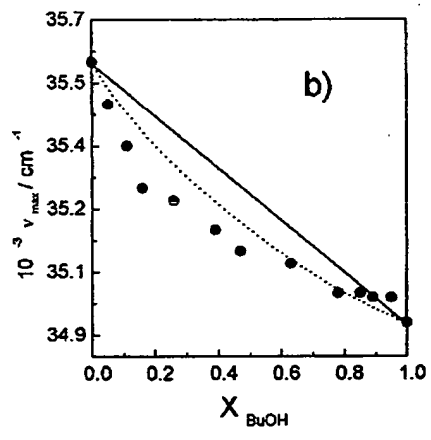

Fig. 3. ν_{max} of the ^1L_a band of CNQ vs. molar fraction of the alcohol, X_A: (a) EtOH; and (b) 1-BuOH, in alcohol–CHX binary mixtures. (●) Experimental points; (----) DE curves.

Table 4
Kamlet Taft's parameters and self-association constants, K_{AA}, of the alcohols used

Alcohol	α [a]	π^* [a]	K_{AA} (50°C) [b]
EtOH	0.83	0.54	134
n-PrOH	0.76	0.52	93
n-BuOH	0.78	0.47	73
2-PrOH	0.77	0.48	50

[a] [25].
[b] [46].

$$\nu_{AB} = X_A^L \nu_A + X_B^L \nu_B \quad (2)$$

where X_A^L and X_B^L are the solvent composition, in molar fraction, in the immediate neighbourhood of the solute, and ν_A and ν_B are the position of the maximum in the pure solvents, alcohol and CHx, respectively. Then, the alcohol composition, X_A^L, can be calculated by Eq. (3)

$$X_A^L = (\nu_{AB} - \nu_B)/(\nu_A - \nu_B)\ . \quad (3)$$

A parameter δ [42] which can be used to quantify the extent of preferential solvation is defined as

$$\delta = X_A^L - X_A$$
$$= (\nu_{AB} - X_A\,\nu_A - X_B\,\nu_B)/(\nu_A - \nu_B) \quad (4)$$

where X_A and X_B are the bulk molar fractions of the solvents in the mixture.

Q shows preferential solvation in the whole range of X_A, and consequently δ is zero only at $X_A = 0$ and 1 and goes through a maximum when the molar fraction of the alcohol, X_A, is less than 0.5 (Fig. 6). Similar curves are obtained for CNQ and BrQ. The maximum values of δ, δ_{max}, and the corresponding X_A are shown in Table 5. For Q the values of δ_{max} correlate well with the hydrogen bond donor ability of the alcohols as measured by the α-coefficient. Consequently, EtOH has a higher δ_{max} value than the other alcohols, (Table 5).

For CNQ the δ_{max} values are smaller than for Q. This is reasonable because the substituted quinolines have less hydrogen bond acceptor ability than Q. In CNQ, δ goes through a maximum when the molar fraction of the alcohol, X_A, is less than 0.4. It should be noticed that for CNQ δ is

zero at X_A values higher than 0.8, because alcohols with a strong hydrogen bond donor ability will relatively prefer other alcohol molecules rather than the solute molecule. Thus, at high X_A, the alcohol–alcohol interaction prevails over the CNQ–alcohol interaction and preferential solvation diminishes.

It should also be noted that the values of δ_{max} for Q and CNQ in the 1-PrOH mixtures are similar. Although CNQ is less basic, it is much more polar than Q and the counterbalance of these effects could account for the observed effects on preferential solvation.

For BrQ the values of δ as a function of the mixture composition are closer to the CNQ ones. The interaction with the alcohol is weaker than for Q as observed by the δ_{max} (Table 5), showing that it is the hydrogen bond acceptor ability of the solute the determining factor of the interaction.

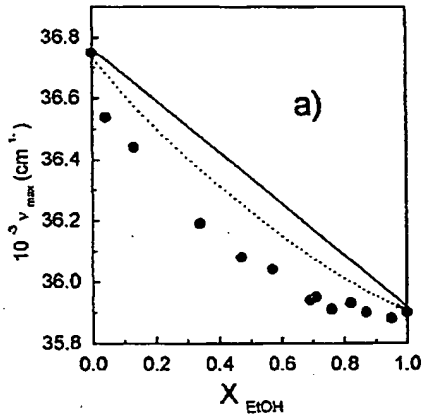

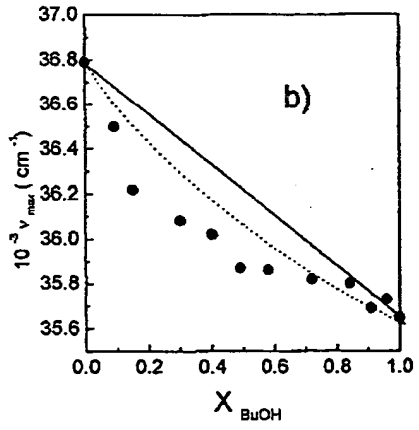

Fig. 4. ν_{max} of the ^1L_a band of BrQ vs. molar fraction of the alcohol, X_A: (c) EtOH; and (d) 1-BuOH, in alcohol–CHX binary mixtures. (●) Experimental points; (----) DE curves.

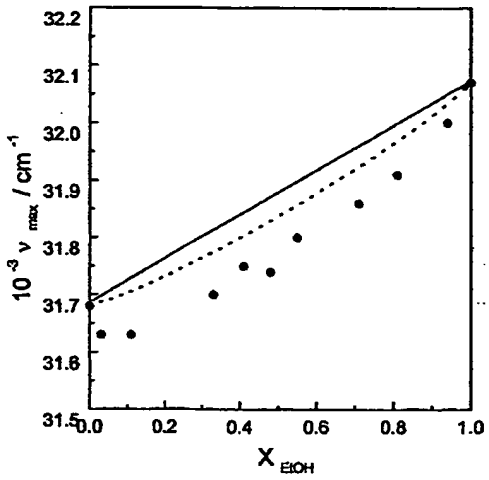

Fig. 5. ν_{max} of the ^1L_a band of OHQ vs. molar fraction of the alcohol, X_A, in EtOH–CHx binary mixtures. (●) Experimental (—) DE curves.

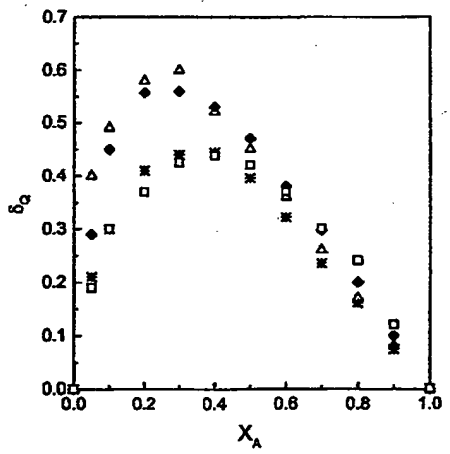

Fig. 6. δ as a function of X_A for Q: (a) in alcohol–CHX mixtures.(△) EtOH;(◆) 1-PrOH; (□) 2-PrOH; (★) 1-BuOH.

Table 5
Extent of preferential solvation measured by δ_{max} for Q, CNQ and BrQ in the alcohol–CHx binary mixtures

Alcohol	δ_{max} Q	$X_{alcohol}$ [a]	δ_{max} CNQ	$X_{alcohol}$ [a]	δ_{max} BrQ	$X_{alcohol}$ [a]
EtOH	0.60	0.25	0.32	0.30	0.32	0.30
1-PrOH	0.56	0.25	0.55	0.3	0.25	0.40
1-BuOH	0.43	0.40	0.26	0.35	0.30	0.30
2-PrOH	0.42	0.40	0.22	0.30	0.20	0.30

[a] $X_{alcohol}$ with maximum preferential solvation.

On the other hand, 1-BuOH and 2-PrOH have the lowest value of K_{AA}, and it will be expected that the preferential solvation would be detected at higher molar fraction than the value actually observed. The values of δ_{max} are lower than for the other alcohols. It is possible that in these alcohols steric problems are preventing complexation. Steric problems are known in self-associations and explain why 1-alkanols form tetramers compared with the trimers or dimers that are formed by secondary alcohols [39].

In summary, the results suggest than alcohols with strong ability to self-associate have less preference toward solvation of these compounds. At low alcohol concentration in the mixture (i.e. X of alcohol < 0.5) solute–solvent interactions are stronger than solvent–solvent interactions. When the alcohol concentration of the mixture increases the self-association of the alcohol determine the preferential solvatation characteristics of the system.

3.3. ^1H NMR studies

In approach to elucidate the type of solute–alcohol interaction and the extent of solvent localization ^{1}H NMR studies were performed. ^{1}H NMR spectra for Q, CNQ and BrQ were measured in CHx and ethanol. The chemical shift of the protons in the solutes are summarised in Table 6. The proton assignments were performed as reported in the literature [43]. No significant chemical shift for proton H_5, H_6, H_7 was observed with the change of solvent. On the other hand, H_2, H_3, H_4 and H_8 are shifted downfield with increasing solvent polarity from CHx to EtOH. The signals of H_2 and H_8 were considered the most convenient to study because they are the closest to the hydrogen bonding interaction area in the different quinolines. However, broadening of the H_2 protons by the electric quadrupole effect of ^{14}N prevented the study with H_2 proton.

To account for the location of the interaction, studies using THF as solvent were performed. This solvent was selected because it has similar polarity to EtOH ($\pi^* = 0.5$), but it is not hydrogen bond donor ($\alpha = 0$). The proton shift for Q, CNQ and BrQ are shown in Table 6. In all the quinolines the proton shift from CHx to EtOH or THF were analysed. H_4, localised far from the interaction area, shows similar downfield shift in EtOH and THF. In this case, solute–solvent dipolar interactions are predominant. The proton shift observed in H_8, closer to the interaction area, is higher in EtOH than THF. This shows that dipolar and hydrogen bonding interactions are present between the solute and EtOH, and just dipolar ones with THF. These results confirm than the solute–solvent interaction is by hydrogen bonding, and the interacting area is localised at the azaromatic nitrogen.

The hydrogen bonding interactions between alcoholic proton and azaromatic nitrogen in quinoline was quantified as follows.

Considering the equilibrium:

$$A\text{–}H + B = A\text{–}H\cdots B \quad (5)$$

Where A–H is the alcohol and B is the aromatic nitrogen of the solute, if the formation of the hydrogen-bond complex is fast, the observed chemical shift of the hydrogen bonding proton δ_{obs} will be a time-weighed average of the chemical shift of the protons in the complex $\delta_{[AH\cdots B]}$ and the chemical shift of the free molecule A–H, δ_f [44] Eq. (6).

$$\delta_{obs} = \frac{[AH]_o - [AH\cdots B]}{[AH]_o}\,\delta_f + \frac{[AH\cdots B]}{[AH]_o}\,\delta_{AH\cdots B}, \quad (6)$$

where $[AH]_o$ is the analytical concentration of hydrogen bonding donor and [A–H···B] is the complex concentration.

Rearranging Eq. (6) gives Eq. (7):

$$[AH\cdots B] = \frac{\delta_{obs} - \delta_f}{\delta_{[AH\cdots B]} - \delta_f}\,[AH]_o \quad (7)$$

The equilibrium expression gives

$$K[AH]_o[B]_o - K[AH\cdots B]$$

$$\{[AH]_o + [B]_o - [AH\cdots B]\} = [AH\cdots B] \quad (8)$$

where K is the equilibrium constant and $[B]_o$ is the initial concentration of hydrogen bonding acceptor. Combining Eq. (7) and Eq. (8) gives:

$$\frac{[B]_o}{\Delta_{obs}} = \frac{1}{\Delta_{[AH\cdots B]}}\{[AH]_o + [B]_o - [AH\cdots B]\} + \frac{1}{K\Delta_{[AH\cdots B]}} \quad (9)$$

where $\Delta_{obs} = \delta_{obs} - \delta_f$, and $\Delta_{[AH\cdots B]} = \delta_{[AH\cdots B]} - \delta_f$. Eq. (9) contains two unknowns, [AH...B] and $\Delta_{[AH\cdots B]}$ which can be calculated by means of an iterative procedure [45]. A plot of $([B]_o/\Delta_{obs})$ versus $([A\text{-}H]_o + [B]_o)$ gives a line with a slope, which is $1/\Delta_{[AH\cdots B]}$. This is substituted into Eq. (7) to obtain an approximate value of [AH···B]. This value of [AH···B] is then used in Eq. (9) to calculate an improved value of the slope. The procedure is repeated until two successive cycles yield identical values for the slope. The final value of the equilibrium constant is calculated from the limiting slope and intercept values.

Increasing the quinoline concentration, changes in the chemical shifts of the ^1H NMR spectra of EtOH were induced. Eq. (9) was used to calculate the association constant between EtOH and quinolines in CHx. The association constant (K) calculated are $K_Q = 110 \pm 20\ M^{-1}$, $R = 0.9989$ and $K_{CNQ} = 140 \pm 10\ M^{-1}$, $R = 0.9998$ and $K_{BrQ} = 120 \pm 15\ M^{-1}$, $R = 0.9978$. The K values observed in solute/EtOH systems are similar for the different solutes within experimental error showing that the solvent hydrogen bond donor ability is the main influence in the interaction with the solute.

4. Conclusions

The spectroscopic studies have shown that the interactions of the solvent with the different quinolines are both specific and non-specific in their nature. The solvent effect depends on the polarity–polarizability, hydrogen-bond donor and acceptor properties of the solvent. AM1 calculations allowed interpreting the most probable sites of interaction. These interactions are complex and vary over the range of the solvents under study. The results suggest that formation of hydrogen bonding between the alkanols as solvents and Q, CNQ and BrQ is significant and dependent on the solute characteristics and the self-association capacity of the alcohol. In OHQ

Table 6
Proton Chemical shift in ν (Hz) for Q, CNQ and BrQ in CHx, EtOH and THF

Solute	Solvent	H_2 (ν Hz)	H_8 (ν Hz)	H_4 (ν Hz)	$H_{5,7,6}$ (ν Hz)	H_3 (ν Hz)
Q	CHx	1759.7	1613.0	1588.4	1534/1467	1435.9
	EtOH	1769.8	1673.1	1616.3	1593/1520	1507.2
	THF	1770.0	1638.3	1610.2	1580/1510	1498.2
BrQ	CHx	1758.0	1612.0	1604.0	1571/1470	–
	EtOH	1765.9	1707.1	1609.1	1584/1517	–
	THF	1775.0	1689.9	1608.1	1578/1512	–
3CNQ	CHx	1784.3	1655.9	1627.3	1550/1497	–
	EtOH	1804.2	1781.7	1629.8	1602/1540	–
	THF	1804.5	1756.2	1624.1	1598/1525	–

intramolecular hydrogen bonding has been observed. This interaction is not broken in CHx-alcohols mixtures, but only weakly debilitated by the interaction with the alcohol.

Acknowledgements

Financial support from the Consejo Nacional de Investigaciones Científicas y Técnicas (CONICET), the Consejo de Investigaciones Científicas y Tecnológicas de la Provincia de Córdoba (CONICOR) and Secretaría de Ciencia y Técnica de la Universidad Nacional de Río Cuarto is gratefully acknowledged. We thank Pedro Rossomando of the Universidad Nacional de San Luis for his help in the measurement of ^{1}H NMR.

References

[1] A.D. Headley, S.D. Starnes, E.T. Cheung, P.L. Malone, J. Phys. Org. Chem. 8 (1995) 26.
[2] C. Reichardt, Chem. Rev. 94 (1994) 2319.
[3] M.L. O'Neill, P. Kruus, R.C. Burk, Can. J. Chem. 71 (1993) 1984.
[4] M.J. Kamlet, J.L.M. Abboud, M.H. Abraham, R.W. Taft, J. Org. Chem. 48 (1983) 2877.
[5] C. Reichardt, Solvents and Solvent Effects in Organic Chemistry, 2nd, V.C.H, Germany, 1990.
[6] N.B. Toselli, J.J. Silber, J.D. Anunziata, Spectrochim. Acta 44A (1988) 829.
[7] R. Cattana, J. Perez, J.J. Silber, J.D. Anunziata, Spectrochim. Acta 47A (1991) 821.
[8] R. Cattana, J.J. Silber, J.D. Anunziata, Can. J. Chem. 70 (1992) 2677.
[9] H. Boggetti, J.D. Anunziata, R. Cattana, J.J. Silber, Spectrochim. Acta 50A (1994) 719.
[10] A.R. Katritzky, Physical Methods in Heterocyclic Chemistry, vol. III, Academic Press, Inc., London, 1971.
[11] M.D. Gordon, Tetrahedron 36 (1980) 2113.
[12] S. Katayama, Y. Arahori, H. Mori, Chem. Pharm. Bull. 21 (12) (1973) 2622.
[13] (a) J.P. Michael, Natural Products Reports, 11 pp.163 (1994) and references therein. (b) H.Z. Alkhathlan, Synth. Commun. 22, 2659 (1992). (c) J.M. Michael. Natural Products Reports.12, pp. 465 (1995) and references therein.
[14] K. Kamienska-Trela, L. Kania, J. Sitkowski, L. Kaczmarek, J. Chem. Soc. Perkin Trans. 2 (1995) 1617.
[15] T.J. Egan, D.C. Ross, P.A. Adams, Febs Lett. 352 (1994) 54.
[16] B. Marchon, L. Bokobza, G. Cote, Spectrochim. Acta 42 (4) (1986) 537.
[17] M. Kamlet, R. Dorherty, J. Abboud, M. Abraham, R. Taft, Chemtech 16 (1986) 566.
[18] A. Komura, K. Uchida, M. Yagi, J. Higuchi, J. Photochem. Photobiol. 42A (1988) 293.
[19] F. Marqez, I. Zabala, F. Tomas, J. Molec. Struct. 293 (1993) 185.
[20] F. Marqez, I. Zabala, F. Tomas, J. Lumin. 54 (1992) 13.
[21] R.C. West, CRC Handbook of Chemistry and Physics, 65th, CRC Press, Boca Raton, FL, 1984.
[22] J.A. Riddick, W.B. Bunger, Techniques of Chemistry, in: Organic solvents, vol. II, 3rd, Wiley Interscience, New York, 1970.
[23] M.J. Kamlet, J.L.M. Abboud, R.W. Taft, J. Am. Chem. Soc. 99 (1977) 6027.
[24] V. Zanker, Z. Physik. Chem. 2 (1954) 52.
[25] Y. Marcus, Chem. Soc. Rev., 409 (1993).
[26] R.H. Myers, Classical and Modern Regression with Applications, P.W.S. Publishers, Boston, 1986.
[27] H.H. Jaffe, M. Orchin, Theory and Applications of Ultraviolet Spectroscopy, Wiley, New York, 1962, p. 303.
[28] M. Santo, R. Cattana, J. Anunziata, J.J. Silber, Spectrochim. Acta 51A (1995) 1789.
[29] S. Marriot, W.F. Reynolds, R.W. Taft, R.D. Topsom, J. Org. Chem. 49 (1984) 959.
[30] G. Consiglio, S. Gronowitz, A.B. Hörnfeldt, N. Noto, D. Sinelli, Chem. Scripta 16 (1980) 117.
[31] M.J.S. Dewar, E.G. Zoebisch, A.F. Healvy, J.J.P. Stewart, J. Am. Chem. Soc. 107 (1985) 3902.
[32] P. Ertl, O. Exner, Structural Chem. 3 (1992) 301.
[33] (a) S. Katayama and Y. Arahori, Chem. Pharm. Bull. 26, 12, (1978) 3758; (b) T. Dziembowska, Z. Malarski, B. Szczodrowska, J. Solut. Chem., 25, 2, (1996) 179.
[34] J. Catalan, E. Mena, W. Meutermans, J. Elguero, J. Phys. Chem. 96 (1992) 3615.
[35] C. Beeson, N. Phan, G. Shipps Jr., T. Dix, J. Am. Chem. Soc. 115 (1993) 6803.
[36] W. Holzer, W. von Philipsborn, Mag. Res. Chem. 27 (1989) 511.
[37] E. Bardez, I. Devon, B. Larrey, B. Valeur, J. Phys. Chem. B101 (1997) 7786.
[38] S.A. Chen, E.B. Bagley, Chem. Eng. Sci. 33 (1978) 153.
[39] (a) S. Perez-Casas, L.M. Trejo and M. Costas, J. Chem. Soc., Faraday Trans., 87 (1991) 1733; (b) L.M. Trejo, S. Perez-Casas, M. Costas and D. Paterson, J. Chem. Soc., Faraday Trans., 87 (1991) 1739; (c) S. Perez-Casas, R. Moreno-Esparza and M. Costas, J. Chem. Soc., Faraday Trans. 87 (1991) 1745.
[40] P. Chatterjee, A.K. Laha, S. Bagchi, J. Chem. Soc., Faraday Trans. 88 (1992) 1675.
[41] C. Lerf, P. Suppan, J. Chem. Soc., Faraday Trans. 88 (1992) 963.
[42] P. Chaterjee, S. Bagchi, J. Chem. Soc., Faraday Trans. 87 (1991) 587.
[43] J. Kidric, D. Hadzi, D. Kocian, V. Rutar, Org. Magn. Reson. 15 (3) (1981) 280.

[44] C.S. Wilcox, in: H. Schneider, H. Durr (Eds.), Frontiers in Supramolecular Organic Chemistry and Photochemistry, VCH Publishers, New York, 1991.
[45] (a) M. Joesten and L. J. Schaad, Hydrogen Bonding. 1974 Marcel Dekker, Inc. New York. 173; (b) R. Foster. In Organic Charge Transfer Complexes. 1969 Ed. A. Blomquist, Academic Press London N.Y.
[46] A. Nath, E. Bender, Fluid Phase Equil. 7 (1981) 275.

DOI: 10.1002/ejoc.200700130

Anion Receptors Based on a Quinoline Backbone

Markus Albrecht,*[a] Triyanti,[a] Stefanie Schiffers,[a] Olga Osetska,[a] Gerhard Raabe,[a] Thomas Wieland,[a] Luca Russo,[b] and Kari Rissanen[b]

Keywords: Anions / Quinoline / Receptors / Ab initio calculations / Fluorescence

2-Amido-8-urea substituted quinoline derivatives are potent receptors for the binding of halide or benzoate anions in chloroform. The selectivity and affinity of the receptors for fluoride can be tuned by variation of the substituents at the receptor side chains. Computational considerations show that the cleft of the receptors provides space for effective binding of F^-, but not bigger anions.

Introduction

Anions play an important role in many biological and chemical processes.[1] For example, the disfunction of anion-channel proteins can be the reason for *cystic fibrosis*, a genetic disease.[2] Despite the importance of the specific recognition and transport of anions, the molecular principles of anion binding and recognition are not fully understood.

The shape of anions is very often overestimated in binding modes; in only a few cases does it strictly follow the lock-and-key principle.[3] Very often, anion binding occurs only as a result of electrostatic attraction and entropic driving forces; shape usually only has a minor influence.[4]

To gain some deeper understanding on processes involving anions, it is necessary to thoroughly investigate the anion binding properties of simple receptor molecules. Therefore, this field of research became an important topic of current supramolecular chemistry.

A series of cationic anion receptors were developed, which can bind simple inorganic but also sophisticated organic anions even in water.[5] Alternatively, neutral receptors can be used to investigate anion binding mechanisms, as demonstrated by the work of Sessler, Schmidtchen, Gale and many others.[6] Recently, we reported a simple quinoline derivative of type **1**, which is able to bind halide anions with moderate affinities in a 1:1 fashion; some selectivity for the smaller anions was discovered.[7] On the basis of those preliminary results, we now describe the synthesis of a series of related quinoline-type receptors **1** and the optimisation of the halide binding properties. In addition, we discuss their ability to bind simple organic (carboxylate) anions. To gain some deeper insight into the interaction between anions and receptors, supporting computational studies were performed.[8]

Results and Discussion

Synthesis of the Receptors

Quinoline derivatives **1** were prepared following the synthetic procedure as described previously for **1a**.[9] The synthesis is depicted in Scheme 1. The reaction sequence starts with Huc's nitroquinoline carboxylic acid **2**.[10] From **2**, amides **3** (a: R′ = C_6H_{13}, b: R = Ph) were prepared by coupling with an appropriate amine, H_2N–R′, in the presence of carbonyl diimidazole (CDI) as the coupling reagent. Hydrogenative reduction of the nitro group with Pd–C as the catalyst afforded amine **4** (a: R′ = C_6H_{13}, b: R = Ph) in quantitative yield as the crude product. Even though this

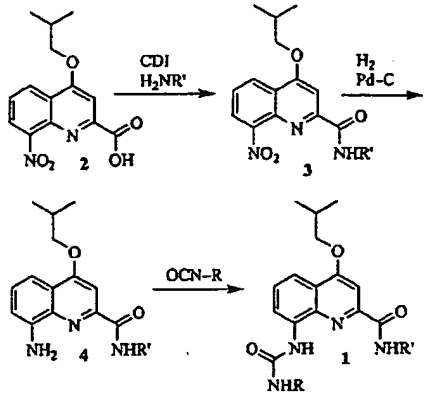

Scheme 1. Synthetic pathway for the preparation of quinoline derivatives **1** (CDI = carbonyl diimidazole).

[a] Institut für Organische Chemie, RWTH Aachen, Landoltweg 1, 52072 Aachen, Germany
E-mail: markus.albrecht@oc.rwth-aachen.de
[b] Nanoscience Centre, Department of Chemistry, University of Jyväskylä, Survontie 9, 40014 Jyväskylä, Finland

amine can be purified, it usually reacts with isocyanates without work up to form desired urea derivatives **1**.

Following this approach, differently substituted compounds **1a** (R = C_8H_{17}, R′ = C_6H_{13}), **1b** (R = C_8H_{17}, R′ = Ph), **1c** (R = C_4H_9, R′ = Ph), **1d** (R = Ph, R′ = C_6H_{13}) and **1e** (R = Ph, R′ = Ph) were prepared in moderate-to-good yields (56–85% overall yield starting from **2**). The compounds were characterised by standard spectroscopic methods (see Experimental Section) and the X-ray structure of **1c**·CH_3CN as well as **1e**·DMSO (vide infra) could be obtained.

Solid State Structures and Conformational Considerations

Figure 1 shows the result of the X-ray structure analysis of the DMSO adduct of 5,7-dibromo-8-hydroxyquinoline-2-carboxylic acid (**5**) from a weakly diffracting crystal. The representation nicely shows the orientation of the two acidic protons (phenol and carboxylic acid) towards the front of the molecule. This front position is enforced by intramolecular hydrogen bonding to the quinoline nitrogen atom,[11] and owing to this, the hydrogen atoms are ideally predisposed for the tweezer-type interaction with hydrogen-bond acceptors — in the present case DMSO. As shown earlier, only weak binding of anions can be expected by derivatives such as **5**. However, by using the intramolecular interactions such as those in **5**·DMSO as a starting point, we developed and optimised anion receptors **1**.

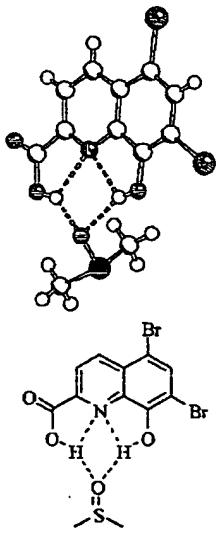

Figure 1. X-ray structure of **5**·DMSO.

Weakly diffracting crystals of **1c**·CH_3CN with only moderate X-ray quality were also obtained. They show the formation of a hydrogen-donor binding pocket, in which, for example, anionic guest species can be introduced. Similar to that observed for model **5**, intramolecular hydrogen bonds between the quinoline N atom and a urea unit and between the quinoline N atom and the amide NH are formed. These contacts fix the molecule in a tweezer-type arrangement with the hydrogen-bond donors pointing to the front of the molecule (Figure 2).

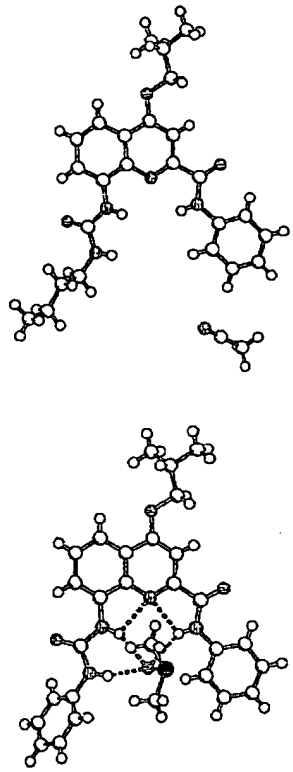

Figure 2. Solid-state structure of **1c**·CH_3CN (top) and **1e**·DMSO (bottom).

The two internal NH units provide the conformational rigidity that positions the remaining NH to form a small cleft. Therefore, this pyridine-bridged amido–urea unit is predisposed to act as an anchor for the fixation of guest species. In the solid phase, the carbonyl oxygen of a second molecule of urea binds in the pocket, which leads to a 1D hydrogen-bonded chain. Acetonitrile is not involved in the H-bonding.

Involvement of solvent molecules in the hydrogen bonding to the receptor is observed in the solid-state structure of **1e**·DMSO. The conformation of receptor **1e** is very similar to that described for **1c**. However, now one molecule of DMSO is bound to the three hydrogen-bond donors and it shows long contacts to the internal hydrogen atoms with the H···O bond lengths equal to 2.48 Å (amide), 2.21 Å (urea) and a shorter one to the external urea proton of 2.00 Å. In addition, one *ortho* proton of the phenyl ring that is attached to the amide is located at a distance of 2.56 Å from the DMSO oxygen atom. This phenyl ring is in the same plane as the amide and quinoline moieties, which probably introduces some steric hindrance, whereas the phenyl group at the urea is twisted out of plane and therefore does not interfere with the binding guest. The DMSO

molecule is located somewhat above the plane of the binding site owing to the size of the oxygen atom, which is too big to allow binding inside the cavity.

Determination of Binding Affinities

In our earlier study, we used receptor **1a** to determine its binding affinities with fluoride, chloride, bromide and nitrate anions by NMR as well as fluorescence spectroscopy in chloroform. Only in the case of fluoride did NMR spectroscopy not allow the determination of the binding constants. With the other anions, only relative binding constants could qualitatively be estimated because of self-aggregation of the receptors at the concentration of the measurement (0.0125 M).

Fluorescence spectroscopy, alternatively, was carried out at a much lower concentration (1 μM) were no self-aggregation of the receptor could take place. Therefore, the observed values are much higher, but they show similar trends in their selectivities.

Following this, we investigated modified receptors **1b–e** to determine their anion binding abilities using both spectroscopic methods. In addition, benzoate as a bigger "organic" anion was studied.

NMR Spectroscopic Investigations

Before starting the titration experiments, we determined the binding stoichiometry between receptors and anions by Jobs method. It was found to be 1:1 (Figure 3).[12]

Titration experiments were performed at a receptor concentration of 0.0125 M in $CDCl_3$ by the successive addition of tetrabutylammonium salts of the anions, and the amide signals, as well as the urea NH signals, were followed. The observation of three different signals allows to estimate the error of the titration to be <25%. The titration curves (e.g. Figure 3) were fitted by standard nonlinear regression methods as described in the literature.[12] The results of the NMR studies are summarised in Table 1. Again, no reliable data could be obtained for fluoride by NMR spectroscopy.

All receptors **1** have a strong preference for the smaller anions over the bigger ones. Therefore, decreasing binding constants can be observed in the series chloride, bromide and nitrate. However, a strong dependence of K_a on the substituents at the receptor side chains can be observed. Starting from our initial receptor **1a**, we introduced a phenyl group at the amide unit to obtain receptors **1b** and **1c**. This does not influence the binding of the anions significantly. In **1d**, we added a phenyl substituent to the urea moiety. This led to a slight increase in the binding affinity of the chloride anion. The most significant increase is found for receptor **1e** with two phenyl substituents. With chloride, a K_a = 7700 M^{-1} was found. This effect is probably due to the increase in the acidity of the two protons close to the phenyl groups and is most effective with chloride, which, because of its size, can come in close contact with the protons.

In the case of benzoate binding,[13] the association constants seem to unsystematically vary with the different receptors **1a–e**. Here, not only the binding of the anionic part is important, but it is additionally influenced by steric interactions of the phenyl group with the receptor and by aromatic–aromatic interactions between the benzoate anion and the receptors.

To summarise the NMR titration experiments, it is seen that quinoline receptors **1a–e** can be used for the binding of anions in chloroform, which shows some selectivity for

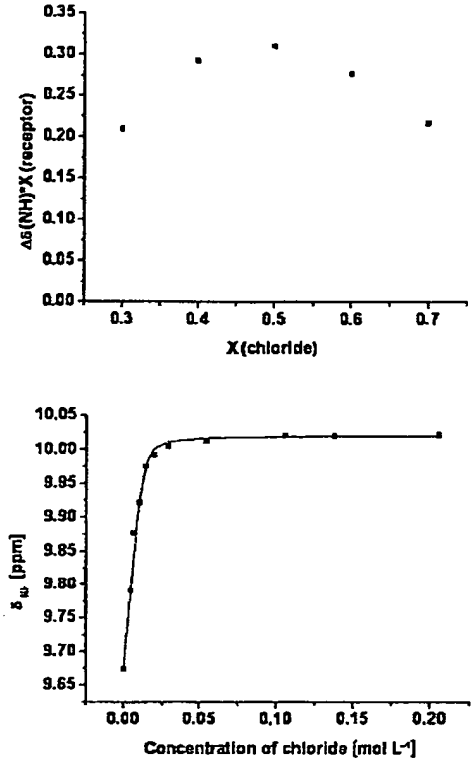

Figure 3. Representation of a selected example of the Jobs plot of receptor **1d** with chloride anions and the corresponding NMR titration curve observed for the amide NH. The solid line represents the simulated curve.

Table 1. Binding constants K_a [M^{-1}] for the 1:1 binding of various anions (as tetrabutyl ammonium salts) with receptors **1a–e** determined by ^1H NMR spectroscopy in $CDCl_3$ at a concentration of 0.0125 M and 296 K. All data are the result of at least two independent measurements. Errors are estimated to be <25%.

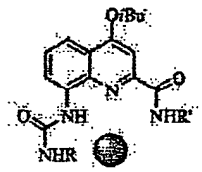

	R	R'	Cl^-	Br^-	NO_3^-	Benzoate
1a	C_8H_{17}	C_6H_{13}	1000	500	420	450
1b	C_8H_{17}	Ph	830	260	320	4000
1c	C_4H_9	Ph	2110	353	412	390
1d	Ph	C_6H_{13}	3333	337	322	600
1e	Ph	Ph	7700	1100	1100	3000

smaller chloride anions over the larger halides. Introduction of phenyl groups increases the acidity of neighbouring NH protons and thus increases the binding affinities of the anions.

Fluorescence Spectroscopic Investigations[14]

As mentioned above, fluorescence spectroscopy has the advantage that the measurements are performed at a concentration where no aggregation of the receptor can occur. This can be shown by concentration-dependent fluorescence studies. In addition, fluoride anion binding can be investigated.

The addition of halide or nitrate anions to receptors **1a–e** leads in all cases to fluorescence enhancement (Figure 4). Only with benzoate quenching occurs probably by the aromatic carboxylate.

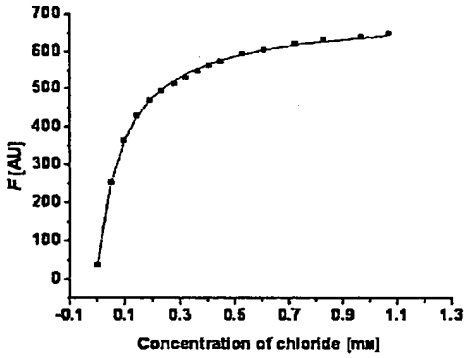

Figure 4. Enhancement of the fluorescence intensity of receptor **1d** (concentration: 1 μM) in chloroform upon addition of tetrabutyl ammonium chloride (excitation wavelength: 323 nm, emission wavelength: 438 nm).

As a disadvantage, no reliable titration curves could be obtained for easily photooxidised receptor **1e**.

The results of the fluorescence titrations are summarised in Table 2. Without competition of receptor self-aggregation, the obtained K_a's are usually higher than the ones obtained by NMR spectroscopy. The relative selectivities of chloride, bromide and nitrate anion binding by **1a–d** are in the same range as observed by NMR spectroscopy (see for comparison Table 1).

The fluoride anion already shows a moderately high binding with receptor **1a** (K_a = 14400 M^{-1}) as well as with **1b** (K_a = 14300 M^{-1}). The K_a = 5000 M^{-1} of **1c** with fluoride seems to be very low, but can be reproduced.

Receptor **1d**, in contrast, shows a very high affinity for the small fluoride anion with K_a = 150000 M^{-1}. This is probably due to the fact that F^- is the ideal size to fit in the cavity of the receptor. In this case, enhancement of the acidity at the urea moiety increases the binding affinity because of the close contact to the anion. Enhancement of the acidity at the amide moiety (receptor **1b/1c**) does not lead to related effects. This binding unit is blocked by the intramolecular hydrogen bonding to the quinoline nitrogen atom. Unfortunately we were not able to obtain association constants of the biphenylated receptor **1e** with fluoride.

Table 2. Binding constants K_a [M^{-1}] for the 1:1 binding of various anions (as tetrabutyl ammonium salts) with receptors **1a–e** determined by fluorescence spectroscopy in $CHCl_3$ at a concentration of 1 μM at 296 K. All data are the result of at least two independent measurements. Errors are estimated to be <25%. Excitation/emission wavelength [nm]: 403/471 (**1a**), 350/462 (**1b**), 387/461 (**1c**), 323/438 (**1d**), and 299/456 (**1e**).

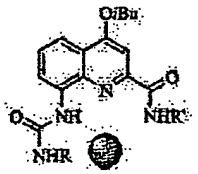

	R	R'	F^-	Cl^-	Br^-	NO_3^-	Benzoate
1a	C_8H_{17}	C_6H_{13}	14400	3100	640	400	6000
1b	C_8H_{17}	Ph	14300	7700	340	1510	4700
1c	C_4H_9	Ph	5000	4630	1050	1630	5080
1d	Ph	C_6H_{13}	150000	10380	1887	1672	
1e	Ph	Ph		receptor is light unstable			

Computational Considerations

Quantum-chemical calculations were performed to acquire some insight into the size-complementarity between model receptor A and different halide anions. Although the applied method is appropriate to gain an impression of the geometry of the interaction between host and guest, it does not allow an estimation of entropic influences or solvent effects.

Unconstrained optimisation for all structures were initially carried out at the Hartree–Fock level of ab initio theory by using the 6-31++G** basis set (HF/6-31++G**). Calculation and diagonalisation of the corresponding force constant matrices showed that all resulting structures were local minima. Starting from these geometries, we then performed final optimisations at the correlated level by employing Møller–Plesset perturbation theory to the second order and the 6-31+G* basis set (MP2/6-31+G*). The Gaussian03 suite of quantum-chemical routines[15] running on the facilities of the Computing and Communication Centre of the RWTH Aachen was used for all of the calculations. Selected structural parameters of the minima are given in Table 3, and the structures optimised at the MP2 level of theory are shown in Figure 5.

The $-C(=O^2)-N^4H_2$ segment of free receptor molecule A has a significantly pyramidalised amino group; it is distinctively turned out of the plane defined by the atoms of the condensed ring system. Except for a pyramidalisation of the N^4H_2 group, the complex $A{\cdot}F^-$ (Figure 5, a) is essentially planar. Whereas the structural features of the host unit are widely retained in $A{\cdot}Cl^-$, the chlorine atom lies significantly (1.114 Å) above the least-squares plane defined by the non-hydrogen atoms of the acceptor part of the complex (cf. Table 3). Elevation of the halogen atom from this plane is even stronger in $A{\cdot}Br^-$ (1.674 Å), where rotation of the $N^3-C(=O)-N^4H_2$ side chain about the bond to the ring system is more pronounced than in the other complexes. The $H^{1a}\cdots X\cdots H^{4a}$ bond angles decrease in the order F > Cl >

Table 3. Selected structural parameters for A·F⁻, A·Cl⁻ and A·Br⁻ obtained at the MP2/6-31+G* level (HF/6-31++G** values in parentheses) (Interatomic distances measured in Å, angles in °). The parameter h is the largest perpendicular distance of an atom (≠X⁻) from the least-squares plane defined by the non-hydrogen atoms of the host part of the complex. The parameter h' is the largest perpendicular distance of the halide anion from the same plane.

	A·F⁻	A·Cl⁻	A·Br⁻
$H^{1a}\cdots X$	1.663(1.718)	2.216(2.418)	2.416(2.560)
$H^{3}\cdots X$	1.758(1.826)	2.401(2.834)	2.534(3.059)
$H^{4a}\cdots X$	1.728(1.753)	2.195(2.283)	2.403(2.426)
$H^{1a}\cdots H^{3[a]}$	2.491(2.559)	2.779(2.833)	2.822(2.840)
$H^{1a}\cdots X\cdots H^{3}$	93.4(92.4)	73.9(64.7)	69.5(59.9)
$H^{3}\cdots X\cdots H^{4a}$	69.5(68.2)	54.9(48.9)	51.7(45.3)
$H^{1a}\cdots X\cdots H^{4a}$	162.9(160.6)	123.8(113.3)	111.6(105.2)
$H^{1a}\cdots N^{2}\cdots H^{3[b]}$	66.4(67.4)	72.9(73.6)	73.7(73.9)
$N^{4}\cdots C\cdots N^{3}\cdots C^{[d]}$	−177.0(179.8)	178.7(178.1)	−173.4(−179.9)
$h^{[c]}$	0.355(0.013)	0.418(0.101)	0.585(0.002)
h'	0.064(0.007)	1.114(0.332)	1.674(0.003)

[a] 2.744 Å in acceptor molecule A. [b] 75.30° in acceptor molecule A. [c] 0.886 Å in acceptor molecule A. [d] 173.8° in acceptor molecule A.

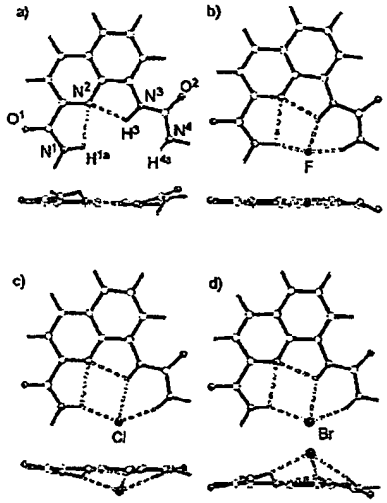

Figure 5. Calculated structures (MP2, top view and side view) of simplified receptor A (a), and its host–guest complex with fluoride A·F (b), chloride A·Cl (c) and bromide A·Br (d).

Br. The bond lengths between the atoms of the heavy-atom skeletons obtained at the MP2/6-31+G* level are very similar in all three complexes. Except for the side chains where the C–NH_2 and the C=O bonds are about 0.020 Å shorter and 0.013 Å longer than in the acceptor molecule, the bonds in A and A·X⁻ are of comparable lengths.

At all levels of accuracy, bonding is the strongest for X = F, followed by X = Cl and finally X = Br.

The energies of the reaction A + X⁻ → A·X⁻ [$\Delta E_b = E_{tot}(A\cdot X^-) - E_{tot}(A) - E_{tot}(X^-)$] obtained at different levels of theory are given in Table 4. The interactions between the halogen anions and A are stabilising even at the HF level. To roughly estimate how much of ΔE_b might be due to a basis set superposition error (BSSE), we applied counterpoise corrections using the method suggested by Boys and Bernardi.[16] These corrections are small at the Hartree–Fock level (cf. Table 4), and although the calculated ΔE_b values are most likely too negative as a result of an overpolarisation of the molecules at the Hartree–Fock level, strong electrostatic and polarisation components are likely to contribute to the total binding energy. As to be expected, the counterpoise corrections are significantly larger when MP2 corrections are included in single-point calculations at the Hartree–Fock-optimised geometries (MP2/6-311++G**// HF/6-31++G**).

Table 4. Energy changes associated with the reaction A + X⁻ → A·X⁻ (ΔE_b; all energies in kcal mol⁻¹); ZPE is the zero-point vibrational energy.

	A·F⁻	A·Cl⁻	A·Br⁻
HF/6-311++G**//HF/6-31++G**	−66.56	−40.67	−35.60
HF/6-311++G**//HF/6-31++G**[a]	−65.16	−40.04	−35.48
MP2/6-311++G**//HF/6-31++G**	−55.73	−34.21	−28.76
MP2/6-311++G**//HF/6-31++G**[a]	−50.46	−28.21	−24.39
MP2/6-31+G*//MP2/6-31+G*	−62.34	−40.97	−40.38
MP2/6-311++G**//MP2/6-31+G*	−61.84	−41.94	−36.32
ZPE+MP2/6-311++G**//HF/6-31++G**	−53.78	−32.61	−26.80
ZPE+MP2/6-311++G**//HF/6-31++G**[a]	−48.51	−26.61	−22.43
ZPE+MP2/6-31+G*//MP2/6-31+G*	−60.39	−39.37	−38.42
ZPE+MP2/6-311++G**//MP2/6-31+G*	−59.89	−40.34	−34.36

[a] Including a counterpoise correction.[16]

NBO calculations[17,18] with the 6-31G** basis set at the HF/6-31++G**- and the MP2/6-31+G*-optimised geometries were performed to elucidate binding between the anions and the acceptor molecule. Independent of the geometry and the halogen atom, the NBO results are qualitatively the same for all three complexes in that *this* analysis of the molecular wave function does not give classical bonds between X and the host unit of the complex. Each of the anions carries four lone pairs (n) with occupation numbers between 1.910 and 2.000 e. These lone pairs strongly interact predominantly with the σ_{NH}* orbitals of the receptor unit, whereas the interaction of highly occupied σ orbitals of the host molecule with *Rydbergs* of the halogen atoms are very weak and can safely be neglected. The energy lowering due to the $n\rightarrow\sigma^*$ interaction ($\Delta E_{n\sigma^*}^{(2)}$) can be estimated by using an energy expression derived from second-order perturbation theory $\Delta E_{n\sigma^*}^{(2)} = -q_n\langle n|F|\sigma^*\rangle^2/(\varepsilon_{\sigma^*}-\varepsilon_n)$, where F is the Fock operator of the molecule and q_n is the occupation number of the lone pair. The parameters ε_{σ^*} and ε_n are the NBO orbital energies of the σ* and nonbonding orbital n, respectively.[17,18] The corresponding values are given in Table 5.

Table 5. Natural atomic charges $q(X^-)$, charge transfer energies (ΔE_{ct}) and $\Delta E_{n\sigma^*}$ calculated at the HF/6-31G**//MP2/6-31+G* level. The numbers in parentheses were obtained at the HF/6-31G**//HF/6-31++G** level (charges in e and energies in kcal mol⁻¹).

X⁻	$q(X^-)$	ΔE_{ct}	$\Delta E_{n\sigma^*}^{(2)}$
F⁻	−0.8304(−0.8492)	−105.1(−91.1)	−108.5(−91.4)
Cl⁻	−0.8870(−0.9283)	−53.5(−31.8)	−61.8(−35.4)
Br⁻	−0.8868(−0.9211)	−47.7(−32.4)	−52.2(−33.4)

At $-108.5\,kcal\,mol^{-1}$, the $n\rightarrow\sigma^*$ interactions are the strongest for X = F, significantly weaker for X = Cl ($-61.8\,kcal\,mol^{-1}$) and the weakest for X = Br ($-52.2\,kcal\,mol^{-1}$). As to be expected, these energies are similar to the energies associated with charge transfer from X^- to acceptor molecule A upon formation of the complex (charge-transfer energy, ΔE_{ct}). The charge-transfer energy was obtained as the difference between the SCF energy of the complex ($A{\cdot}X^-$) calculated with the full Fock matrix and the total energy obtained in a single iteration after deletion of the Fock matrix elements between the donor orbitals of X and the acceptor orbitals of A.[17] The amount of charge transferred to the acceptor molecule (Δq) is relatively small (F: 0.1696 *e*, Cl = 0.1130 *e* and Br: 0.1132 *e*), and the largest transfer occurs from the fluoride anion, which also gives the most negative charge-transfer energy. Owing to similar geometries for $A{\cdot}F^-$ at the Hartree–Fock and the MP2 levels, Δq, ΔE_{ct} and $\Delta E_{n\sigma^*}{}^{(2)}$ are not too different for both sets of structural parameters. The structural differences between the geometries obtained with the HF and MP2 methods are larger for $A{\cdot}Cl^-$ and $A{\cdot}Br^-$. Consequently, the values that were obtained for Δq, ΔE_{ct} and $\Delta E_{n\sigma^*}{}^{(2)}$ for both geometries differ much more for these two molecules than they do for $A{\cdot}F^-$. In general, more negative values of ΔE_{ct} and $\Delta E_{n\sigma^*}{}^{(2)}$ and a more positive Δq value are obtained for the structures optimised at the correlated level.

Conclusions

Starting from solid-state structures such as 5·DMSO, which show the host–guest behaviour of 2-acid substituted 8-hydroxyquinolines, we developed an efficient and selective receptor for the fluoride anion in chloroform. Substitution of the amide moiety for an acid functionality and a urea group instead of the hydroxy group in **5** led to potent halide receptors **1a–c**. However, variation of the substituents at the amide group as well as at the urea caused an enhancement in the acidity of the NH protons and an enhancement in the binding of fluoride anions in chloroform at room temperature to $K_a = 150000\,M^{-1}$ for **1d**.

Computational considerations using model **A** indicate that the binding of the anion is mainly electrostatic and show that receptors **1a–e** provide a cavity that is most appropriate for the binding of the small fluoride. The larger halides (chloride and bromide) do not fit in the provided cavity and therefore have to be located above the plane of receptor molecule **A**.

From our comparative studies by NMR and fluorescence techniques, we can see that fluorescence at lower concentrations leads to more accurate data than the corresponding NMR spectroscopic methods. However, NMR spectroscopy allows an estimation of relative affinities for different anions, if measurements are performed at the same concentration of the receptor.

As pointed out,[19] deprotonation of the receptors by a fluoride anion always has to be considered as a competitive process to the binding of this anion with high basicity. This prevents the determination of reliable data for fluoride anionic binding by NMR spectroscopy. In our computational calculations, this process was not taken into account and only binding of the fluoride anion to the pocket of the receptor was considered.

In an additional preliminary study, the binding of carboxylate anions to the receptors can be shown, which opens up a way for organocatalytic reactions. Therefore, we are now preparing enantiomerically pure chiral derivatives of **1**.

Experimental Section

NMR spectra were recorded with a Varian Mercury 300 or Inova 400 spectrometer. FTIR spectra were recorded with a Perkin–Elmer FTIR 1760 spectrometer (KBr). MS were measured with a Varian MAT 212 spectrometer. Elemental analyses are obtained with a Heraeus CHN-O-Rapid analyser. Melting points were measured with a Büchi B-540 apparatus and are uncorrected. Fluorescence measurements were performed with a Perkin–Elmer LS 50-B spectrofluorometer.

CCDC-633847 to -633849 contain the supplementary crystallographic data for this paper. These data can be obtained free of charge from The Cambridge Crystallographic Data Centre via www.ccdc.cam.ac.uk/data_request/cif.

5,7-Dibromo-8-hydroxyquinoline-2-carboxylic Acid (5): 5,7-Dibromo-8-hydroxyquinoline-2-carboxaldehyde[20] (0.25 g, 0.72 mmol) was dissolved in formic acid (10 mL, 0.26 mol, 1 equiv.) and the suspension was cooled to 0 °C. Cold hydrogen peroxide (16 mL; 30% solution in water, 0.52 mol, 2 equiv.) was slowly added, and the mixture was warmed to room temperature. After stirring for 3 d, water (200 mL) was added, the precipitate was collected by filtration, washed with cold water and dried. The first recrystallisation from DMF/*i*PrOH allowed the recovery of 0.06 g (24%) of the starting material; the second recrystallisation from methanol provided **5** as a yellow solid. Yield: 0.096 g (37%). M.p. 265 °C. ^1H NMR (300 MHz, [D$_6$]DMSO): δ = 13.00 (br. s, 1 H), 11.07 (br. s, 1 H), 8.55 (d, J = 7.0 Hz, 1 H), 8.24 (d, J = 8.8 Hz, 1 H), 8.15 (s, 1 H) ppm. ^{13}C NMR (75 MHz, $CDCl_3$): δ = 164.70 (C), 151.70 (C), 146.15 (C), 138.29 (CH), 137.34 (C), 136.03 (CH), 128.06 (C), 122.23 (CH), 109.29 (C), 106.08 (C) ppm. IR (KBr): $\tilde{\nu}$ = 3309, 1706, 1613, 1572, 1451, 1376, 1245, 1194, 936, 839 cm^{-1}. MS (EI): m/z = 346.8 $[M + H]^+$. $C_{10}H_5Br_2NO_3{\cdot}CH_3OH$ (379.01): calcd. C 34.86, H 2.39, N 3.70; found C 35.09, H 2.68, N 4.08. X-ray quality crystals were obtained from DMSO: Crystal data ($C_{10}H_5NO_3Br_2$)-(SC_2H_6O): FW = 425.10, plate, 0.20×0.10×0.04 mm^3, triclinic, space group $P\bar{1}$, a = 8.6570(17) Å, b = 10.524(2) Å, c = 17.694(4) Å, α = 96.72(3)°, β = 102.80(3)°, γ = 109.81(3)°, V = 1446.1(5) Å^3, Z = 4, $D_{calcd.}$ = 1.952 $g\,cm^{-3}$, $F(000)$ = 832, Mo-K_α radiation, λ = 0.71073 Å, μ = 5.761 mm^{-1}, T = 173(2) K, $2\theta_{max}$ = 55.0°, 12587 reflections collected, 3638 unique (R_{int} = 0.1006), 2158 with $I_o > 2\sigma(I_o)$. Solved by using SHELXS and refined with SHELX-97,[21] full-matrix least-squares on F^2, 392 parameters, 492 restraints, GoF = 1.128, R_1 = 0.1800, wR_2 = 0.2391 (all reflections), 1.24 < $\Delta\rho$ < −1.24 e Å^{-3}.

4-Isobutoxy-8-nitroquinoline-2-carboxylic Acid Hexylamide (3a): A solution of 4-isobutoxy-8-nitroquinoline-2-carboxylic acid (2; 0.6 g, 2.07 mmol, 1.0 equiv.) and carbonyl diimidazole (0.57 g, 3.5 mmol, 1.75 equiv.) in chloroform (20 mL) was heated at reflux for 1.5 h under an atmosphere of Ar. A solution of *n*-hexylamine (0.32 g, 3.18 mmol, 1.5 equiv.) in chloroform (2 mL) was added, and the mixture was heated at reflux for an additional 2 d. After cooling

to room temperature, the organic phase was washed with water and dried ($MgSO_4$), and the solvent was removed in vacuo. After column chromatography (silica gel, CH_2Cl_2) **3a** was obtained in 92% (0.71 g) as a yellow solid. M.p. 97 °C. ^1H NMR (400 MHz, $CDCl_3$): δ = 8.48 (dd, J = 1.5, 8.5 Hz, 1 H), 8.20 (s, NH), 8.11 (dd, J = 1.5, 7.5 Hz, 1 H), 7.81 (s, 1 H), 7.62 (t, J = 8.5 Hz, 1 H), 4.11 (d, J = 6.6 Hz, 2 H), 3.47 (q, J = 7.5 Hz, 2 H), 2.30 (m, 1 H), 1.67 (m, 2 H), 1.37 (m, 2 H), 1.33 (m, 4 H), 1.14 (d, J = 6.6 Hz, 6 H), 0.90 (s, 3 H) ppm. ^{13}C NMR (100 MHz, $CDCl_3$): δ = 163.4, 163.1, 153.4, 126.7 (2 C), 124.9 (2 C), 124.8 (2 C), 123.1, 99.8, 75.6, 39.7, 31.6, 29.7, 28.1, 26.7, 22.5, 19.1, 14.0 ppm. IR (KBr): $\tilde{\nu}$ = 3301 (s), 2959 (s), 2928 (s), 2859 (m), 1667 (vs), 1539 (vs), 1501 (m), 1465 (m), 1354 (s), 1240 (m), 1142 (m), 1014 (s), 873 (m), 758 (m), 729 (m) cm^{-1}. MS (EI, 70 eV): m/z (%) = 373 (7) $[M, C_{20}H_{27}N_3O_4]^+$, 355 (92) $[C_{20}H_{25}N_3O_3]^+$, 300 (22) $[C_{18}H_{26}N_2O]^+$, 282 (17) $[C_{17}H_{20}N_3O]^+$, 246 (100) $[C_{13}H_{14}N_2O_3]^+$, 230 (40) $[C_{13}H_{12}NO_3]^+$, 217 (14) $[C_{12}H_{11}NO_3]^+$, 200 (12) $[C_{12}H_8O_3]^+$, 190 (21) $[C_9H_6N_2O_3]^+$, 173 (6) $[C_9H_5N_2O_3]^+$, 144 (5) $[C_9H_6NO]^+$, 57 (9) $[C_4H_9]^+$. $C_{20}H_{27}N_3O_4$ (373.45): calcd. C 64.32, H 7.29, N 11.25; found C 64.60, H 7.63, N 11.71.

4-Isobutoxy-8-nitroquinoline-2-carboxylic Acid Phenylamide (3b): A solution of 4-isobutoxy-8-nitro-quinoline-2-carboxylic acid (**2**; 0.2 g, 0.69 mmol, 1.0 equiv.) and carbonyl diimidazole (0.196 g, 1.21 mmol, 1.75 equiv.) in chloroform (20 mL) was heated at reflux for 1.5 h under an atmosphere of Ar. A solution of aniline (0.01 g, 0.76 mmol, 1.1 equiv.) in chloroform (2 mL) was added, and the mixture was heated at reflux for an additional 2 d. After cooling to room temperature, the organic phase was washed with water and dried ($MgSO_4$), and the solvent was removed in vacuo. After column chromatography (silica gel, CH_2Cl_2), **3b** was obtained in 80% (0.2 g) as a white solid. M.p. 188.5 °C. ^1H NMR (400 MHz, $CDCl_3$): δ = 10.18 (s, NH), 8.52 (dd, J = 1.4, 8.5 Hz, 1 H), 8.19 (dd, J = 1.4, 7.4 Hz, 1 H), 7.88 (s, 1 H), 7.81 (d, J = 7.4 Hz, 2 H), 7.66 (t, J = 7.9 Hz, 1 H), 7.42 (t, J = 7.9 Hz, 2 H), 7.19 (t, J = 7.4 Hz, 1 H), 4.15 (d, J = 6.7 Hz, 2 H), 2.33 (m, 1 H), 1.17 (d, J = 6.7 Hz, 6 H) ppm. IR (KBr): $\tilde{\nu}$ = 3743 (m), 3350 (w), 2958 (m), 2361 (vs), 2339 (vs), 1692 (s), 1525 (vs), 13674 (m), 1110 (m), 1018 (m), 752 (m), 669 (m) cm^{-1}. MS (EI, 70 eV): m/z (%) = 365 (85) [M, $C_{20}H_{19}N_3O_4]^+$, 309 (7) $[C_{16}H_{13}N_3O_4]^+$, 280 (2) $[C_{15}H_{12}N_3O_3]^+$, 262 (5) $[C_{16}H_{10}N_2O_2]^+$, 246 (40) $[C_{13}H_{14}N_2O_3]^+$, 190 (100) $[C_9H_6N_2O_3]^+$, 173 (4) $[C_9H_5N_2O_2]^+$, 143 (3) $[C_9H_5NO]^+$, 115 (5) $[C_8H_5N]^+$, 93 (3) $[C_6H_5O]^+$, 77 (4) $[C_6H_5]^+$, 57 (5) $[C_4H_9]^+$. $C_{20}H_{19}N_3O_4$ (365.39): calcd. C 65.75, H 5.21, N 11.5; found C 65.37, H 5.73, N 11.96.

8-Amino-4-isobutoxyquinoline-2-carboxylic Acid Hexylamide (4a): A mixture of nitro precursor **3a** (0.6 g, 1.66 mmol) dissolved in EtOAC (20–30 mL) and 10% Pd/C was stirred at ambient temperature under an atmosphere of hydrogen (5 bar) for 4 h. The solution was filtered through Celite, and the solvent was evaporated. Yield:0.55 g (1.60 mmol, 98%). M.p. 121 °C. ^1H NMR (300 MHz, $CDCl_3$): δ = 8.10 (s, NH), 7.67 (s, 1 H), 7.60 (dd, J = 1.0, 8.2 Hz, 1 H), 7.36 (t, J = 8.2 Hz, 1 H), 6.99 (dd, J = 1.0, 6.9 Hz, 1 H), 4.91 (br. s, 2 H), 4.05 (d, J = 6.5 Hz, 2 H), 3.52 (q, J = 6.9 Hz, 2 H), 2.27 (m, 1 H), 1.69 (m, 2 H), 1.36 (m, 4 H), 1.13 (d, J = 6.5 Hz, 6 H), 0.92 (s, 3 H) ppm. ^{13}C NMR (75 MHz, $CDCl_3$): δ = 167.8, 164.8, 163.1 (2 C), 148.9, 143.7, 127.5, 111.3, 110.6, 108.4, 98.8, 75.0, 39.7 (2 C), 31.6, 29.8, 28.2, 26.7, 22.6, 19.2, 14.0 ppm. IR (KBr): $\tilde{\nu}$ = 3491 (m), 3332 (s), 3257 (m), 2957 (s), 2926 (s), 2851 (m), 1650 (s), 1614 (m), 1510 (m), 1510 (vs), 1469 (m), 1422 (m), 1355 (m), 1275 (m), 1150 (m), 1065 (m), 1012 (m), 878 (m), 747 (s) cm^{-1}. MS (EI, 70 eV): m/z (%) = 343 (82) [M, $C_{20}H_{29}N_3O_2]^+$, 300 (1) $[C_{18}H_{26}N_3O]^+$, 286 (4) $[C_{18}H_{26}N_2O]^+$, 272 (8) $[C_{17}H_{24}N_2O]^+$, 258 (3) $[C_{16}H_{22}N_2O]^+$, 243 (5) $[C_{13}H_{11}N_2O_3]^+$, 216 (100) $[C_{11}H_8N_2O_3]^+$, 187 (10) $[C_{10}H_7N_2O_2]^+$, 160 (27) $[C_9H_6NO_2]^+$, 130 (4) $[C_9H_6O]^+$, 100 (9) $[C_8H_4]^+$, 77 (1) $[C_6H_5]^+$, 57 (1) $[C_4H_9]^+$. $C_{20}H_{29}N_3O_2 \cdot 1/2H_2O$ (352.47): calcd. C 68.15, H 8.58, N 11.92; found C 68.17, H 8.67, N 11.82.

4-Isobutoxy-8-amine-quinoline-2-carboxylic Acid Phenylamide (4b): A mixture of nitro precursor **3a** dissolved in CH_2Cl_2 (20–30 mL) and 10% Pd/C was stirred at ambient temperature under an atmosphere of hydrogen (5 bar) for 1 d. The solution was filtered through Celite. The solution was used in the next step without isolation of the amine.

4-Isobutoxy-8-(3-octylureido)quinoline-2-carboxylic Acid Hexylamide (1a): A solution of 8-amino-4-isobutoxyquinoline-2-carboxylic acid hexylamide (**4a**; 0.53 g, 1.55 mmol, 1.0 equiv.) and *n*-octyl isocyanate (0.51 g, 3.29 mmol, 1.5 equiv.) in chloroform (30 mL) was heated at reflux for 3 h. After cooling to room temperature, the solvent was removed in vacuo. After column chromatography (silica gel, CH_2Cl_2), **1a** was obtained as a yellow solid. Yield: 0.66 g (1.32 mmol, 85%). M.p. 135 °C. ^1H NMR (400 MHz, $CDCl_3$): δ = 9.69 (s, NH), 9.23 (s, NH), 8.73 (d, J = 7.7 Hz, 1 H), 7.75 (d, J = 8.5 Hz, 1 H), 7.67 (s, 1 H), 7.49 (t, J = 8.2 Hz, 1 H), 6.37 (s, NH), 3.98 (d, J = 6.6 Hz, 2 H), 2.32 (q, J = 6.7 Hz, 2 H), 2.25 (m, 1 H), 1.64 (s, 4 H), 1.39 (m, 4 H), 1.15 (d, J = 6.6 Hz, 6 H), 1.10 (d, J = 6.9 Hz, 6 H) ppm. ^{13}C NMR (100 MHz, $CDCl_3$): δ = 165.0, 163.5, 163.2, 137.4, 136.3, 127.9, 123.5, 121.9, 100.2, 98.4, 76.1, 40.2, 31.6, 31.4, 30.4, 30.2, 29.2, 29.1, 28.2, 26.9, 26.7, 22.5, 22.4, 19.0, 14.0, 13.8 ppm. IR (KBr): $\tilde{\nu}$ = 3348 (vs), 2928 (vs), 2858 (s), 1646 (s), 1528 (vs), 1460 (m), 1416 (m), 1384 (w), 1360 (m), 1321 (m), 1274 (m), 1224 (m), 1144 (w), 1045 (m), 865 (w), 817 (w), 762 (m), 725 (w), 544 (w) cm^{-1}. MS (EI, 70 eV): m/z (%) = 498 (7) [M, $C_{29}H_{46}N_4O_3]^+$, 370 (22) $[C_{21}H_{30}N_4O_2]^+$, 343 (100) $[C_{20}H_{29}N_3O_2]^+$, 314 (10) $[C_{19}H_{28}N_3O]^+$, 242 (42) $[C_{15}H_{20}N_3]^+$, 216 (53) $[C_{12}H_{20}N_2]^+$, 185 (12) $[C_{10}H_5N_2O_2]^+$, 159 (13) $[C_9H_5NO_2]^+$, 100 (11) $[C_8H_4]^+$, 85 (1) $[C_6H_{13}]^+$, 57 (4) $[C_4H_9]^+$. $C_{29}H_{46}N_4O_3 \cdot 1/2H_2O$ (509.71): calcd. C 68.60, H 9.33, N 11.04; found C 68.83, H 9.03, N 10.90.

8-(3-Octylureido)-4-isobutoxy-quinoline-2-carboxylic Acid Phenylamide (1b): A solution of 4-isobutoxy-8-aminoquinoline-2-carboxylic acid phenylamide (**4b**; 0.28 g, 0.89 mmol, 1.0 equiv.) and *n*-octyl isocyanate (0.179 g, 1.155 mmol, 1.5 equiv.) in dichloromethane (30 mL) was heated at reflux for 1 d. After cooling to room temperature, the solvent was removed in vacuo. After column chromatography (silica gel, CH_2Cl_2), **1b** was obtained as a yellow solid. Yield: 0.302 g (0.62 mmol, 80%). M.p. 155 °C. ^1H NMR (300 MHz, $CDCl_3$): δ = 10.02 (s, NH), 8.95 (s, NH), 8.58 (dd, J = 1.0, 8.0 Hz, 2 H), 7.74 (dd, J = 1.0, 6.7 Hz, 2 H), 7.67 (s, NH), 7.43 (t, J = 8.0 Hz, 1 H), 7.21 (t, J = 7.4 Hz, 2 H), 7.04 (t, J = 7.4 Hz, 1 H), 5.87 (s, 1 H), 3.95 (d, J = 6.5 Hz, 2 H), 3.11 (m, 2 H), 2.23 (q, J = 6.7 Hz, 1 H), 1.33 (m, 2 H), 1.19 (m, 10 H), 1.09 (d, J = 6.5 Hz, 6 H), 0.83 (m, 3 H) ppm. ^{13}C NMR (100 MHz, $CDCl_3$): δ = 155.8, 148.9, 137.3, 135.7, 134.9, 128.6 (2 C), 127.7, 124.4, 122.0, 120.5 (2 C), 116.0 (2 C), 113.9, 98.8, 75.1, 40.5, 31.7 (2 C), 30.1, 29.2 (2 C), 28.1, 26.9, 22.6, 19.2 (2 C), 14.0 ppm. IR (KBr): $\tilde{\nu}$ = 3746 (w), 3335 (s), 2928 (s), 1686 (s), 1643 (m), 1526 (vs), 1449 (m), 1320 (m), 1042 (m), 755 (m), 695 (m) cm^{-1}. MS (EI, 70 eV): m/z (%) = 490 (9) [M, $C_{29}H_{38}N_4O_3]^+$, 361 (36) $[C_{21}H_{21}N_4O_2]^+$, 335 (100) $[C_{19}H_{19}N_4O_2]^+$, 306 (3) $[C_{17}H_{14}N_4O_2]^+$, 279 (14) $[C_{15}H_{11}N_4O_2]^+$, 242 (13) $[C_{12}H_{10}N_4O_2]^+$, 216 (5) $[C_{11}H_8N_2O_3]^+$, 186 (11) $[C_{10}H_6N_2O_2]^+$, 160 (9) $[C_9H_6NO_2]^+$, 130 (2) $[C_9H_6O]^+$, 99 (4) $[C_8H_3]^+$, 55 (3) $[C_4H_7]^+$. $C_{29}H_{38}N_4O_3 \cdot 1/2H_2O$ (499.65): calcd. C 69.71, H 7.87, N 11.21; found C 69.31, H 7.03, N 11.10.

8-(3-Butylureido)-4-isobutoxy-quinoline-2-carboxylic Acid Phenylamide (1c): A solution of 4-isobutoxy-8-aminoquinoline-2-car-

boxylic acid phenylamide (4b; 0.3 g, 0.89 mmol, 1.0 equiv.) and *n*-butyl isocyanate (0.133 g, 1.335 mmol, 1.5 equiv.) in dichloromethane (30 mL) was heated at reflux for 1 d. After cooling to room temperature, the solvent was removed in vacuo. After column chromatography (silica gel, CH_2Cl_2), 1c was obtained as a yellow solid. Yield: 0.29 g (0.69 mmol, 75%). M.p. 210 °C. ^{1}H NMR (300 MHz, $CDCl_3$): δ = 9.93 (s, NH), 8.83 (s, NH), 8.53 (dd, J = 1.0, 7.2 Hz, 2 H), 7.72 (dd, J = 1.0, 7.4 Hz, 2 H), 7.64 (s, NH), 7.43 (t, J = 8.0 Hz, 1 H), 7.24 (t, J = 7.2 Hz, 2 H), 7.07 (d, J = 8.0 Hz, 1 H), 5.57 (s, NH), 3.94 (d, J = 6.5 Hz, 2 H), 3.20 (m, 2 H), 2.23 (m, 1 H), 1.41 (m, 2 H), 1.21 (m, 2 H), 1.10 (d, J = 6.5 Hz, 6 H), 0.83 (t, J = 7.4 Hz, 3 H) ppm. IR (KBr): $\tilde{\nu}$ = 3681 (s), 3441 (vs), 2961 (s), 2360 (vs), 1687 (m), 1650 (m), 1532 (s), 1458 (w), 1388 (w), 1322 (w), 1043 (m), 754 (m), 668 (m) cm^{-1}. MS (EI, 70 eV): *m/z* (%) = 434 (15) [M, $C_{25}H_{30}N_4O_3$]$^+$, 361 (39) [$C_{21}H_{21}N_4O_2$]$^+$, 335 (100) [$C_{19}H_{19}N_4O_2$]$^+$, 306 (5) [$C_{17}H_{14}N_4O_2$]$^+$, 279 (23) [$C_{15}H_{11}N_4O_2$]$^+$, 242 (19) [$C_{12}H_{10}N_4O_2$]$^+$, 216 (7) [$C_{11}H_8N_2O_3$]$^+$, 187 (5) [$C_{10}H_7N_2O_2$]$^+$, 160 (17) [$C_9H_6NO_2$]$^+$, 130 (3) [C_9H_6O]$^+$, 104 (1) [C_8H_8]$^+$, 57 (2) [C_4H_9]$^+$. $C_{25}H_{30}N_4O_3 \cdot 1/2H_2O$ (443.54): calcd. C 67.70, H 7.04, N 12.63; found C 67.45, H 6.95, N 12.53. X-ray quality crystals were obtained from acetonitrile: Crystal data ($C_{25}H_{30}N_4O_3$)(CH_3CN): FW = 475.58, plate, 0.60 × 0.15 × 0.03 mm^3, monoclinic, space group P 2$_1$/n, a = 15.454(3) Å, b = 8.2659(17) Å, c = 21.183(4) Å, β = 105.44(3)°, V = 2608.2(9) Å^3, Z = 4, $D_{calcd.}$ = 1.211 g cm^{-3}, F(000) = 1016, Mo-K_α radiation, λ = 0.71073 Å, μ = 0.081 mm^{-1}, T = 173(2) K, $2\theta_{max}$ = 55.0°, 6723 reflections collected, 2641 unique (R_{int} = 0.0650), 1020 with $I_o > 2\sigma(I_o)$. Solved by using SHELXS[21] and refined with SHELX-97, full-matrix least-squares on F^2, 317 parameters, 0 restraints, GoF = 1.070, R_1 = 0.2447, wR_2 = 0.3109 (all reflections), 0.29 < $\Delta\rho$ < –0.28 e Å^{-3}.

4-Isobutoxy-8-(3-phenylureido)quinoline-2-carboxylic Acid Hexylamide (1d): A solution of 8-amino-4-isobutoxyquinoline-2-carboxylic acid hexylamide (4a; 0.22 g, 0.59 mmol, 1.0 equiv.) and phenyl isocyanate (0.11 g, 0.89 mmol, 1.5 equiv.) in chloroform (30 mL) was heated at reflux for 3 h. After cooling to room temperature, the solvent was removed in vacuo. After column chromatography (silica gel, CH_2Cl_2), 1d was obtained as a yellow solid. Yield: 0.15 g (0.32 mmol, 56%). M.p. 153 °C. ^{1}H NMR (300 MHz, $CDCl_3$): δ = 9.83 (s, NH), 8.76 (d, J = 7.2 Hz, 1 H), 8.35 (s, NH), 7.81 (d, J = 7.7 Hz, 1 H), 7.76 (s, 1 H), 7.54 (t, J = 8.03 Hz, 1 H), 7.35 (d, J = 7.7 Hz, 2 H), 7.15 (t, J = 7.67 Hz, 2 H), 6.96 (t, J = 7.15 Hz, 1 H), 3.94 (d, J = 6.43 Hz, 2 H), 2.22 (m, 1 H), 1.35 (m, 3 H), 1.07 (d, J = 6.70 Hz, 6 H), 0.73 (m, 4 H), 0.51 (m, 6 H) ppm. ^{13}C NMR (100 MHz, $CDCl_3$): δ = 165.0, 163.7, 163.4 (2 C), 137.4, 136.3, 131.6, 128.8 (2 C), 128.2, 121.9, 113.9, 100.2, 98.6, 75.2, 40.4 (2 C), 31.3, 30.5, 29.2, 28.1, 26.7, 22.3, 19.1 (2 C), 14.2, 13.7 ppm. IR (KBr): $\tilde{\nu}$ = 3328 (m), 2958 (m), 2929 (m), 2869 (m), 1642 (m), 1602 (m), 1531 (vs), 1499 (m), 1440 (m), 1418 (m), 1315 (s), 1269 (w), 1198 (m), 1072 (m), 1014 (m), 966 (w), 894 (w), 754 (m), 696 (m) cm^{-1}. MS (EI, 70 eV): *m/z* (%) = 462 (7) [M, $C_{27}H_{34}N_4O_3$]$^+$, 370 (100) [$C_{21}H_{30}N_4O_2$]$^+$, 343 (18) [$C_{20}H_{29}N_3O_2$]$^+$, 314 (30) [$C_{19}H_{28}N_3O$]$^+$, 242 (9) [$C_{15}H_{20}N_3$]$^+$, 216 (24) [$C_{12}H_{20}N_2$]$^+$, 185 (14) [$C_{10}H_5N_2O_2$]$^+$, 159 (7) [$C_9H_5NO_2$]$^+$, 100 (5) [C_8H_4]$^+$. $C_{27}H_{34}N_4O_3 \cdot 1/4H_2O$ (467.09): calcd. C 69.43, H 7.44, N 11.99; found C 69.42, H 7.26, N 11.95.

4-Isobutoxy-8-(3-phenylureido)quinoline-2-carboxylic Acid Phenylamide (1e): A solution of 4-isobutoxy-8-aminoquinoline-2-carboxylic acid phenylamide (4b; 0.2 g, 0.6 mmol, 1.0 equiv.) and phenyl isocyanate (0.1 g, 0.9 mmol, 1.5 equiv.) in dichloromethane (30 mL) was heated at reflux for 1 d. After cooling to room temperature, the solvent was removed in vacuo. After column chromatography (silica gel, CH_2Cl_2), 1e was obtained as a white solid. Yield: 0.21 g, (0.46 mmol, 77%). M.p. 236 °C. ^{1}H NMR (400 MHz, $CDCl_3$): δ = 9.62 (s, NH), 9.18 (s, NH), 8.54 (d, J = 7.9 Hz, 1 H), 8.00 (s, NH), 7.64 (d, J = 8.5 Hz, 4 H), 7.50 (s, 1 H), 7.48 (d, J = 7.9 Hz, 1 H), 7.30 (t, J = 8.5 Hz, 1 H), 7.13 (t, J = 7.8 Hz, 2 H), 7.06 (t, J = 7.8 Hz, 2 H), 6.93 (t, J = 7.4 Hz, 1 H), 6.87 (t, J = 7.4 Hz, 1 H), 3.83 (d, J = 6.4 Hz, 2 H), 2.18 (m, 1 H), 1.06 (d, J = 6.4 Hz, 6 H) ppm.^{13}C NMR (100 MHz, $CDCl_3$): δ = 163.0, 162.8 (2 C), 153.3, 148.8, 137.8, 137.4.136.8, 134.8, 128.9 (2 C), 128.5, 127.4, 124.5, 123.9, 121.7, 121.0, 120.7, 116.8, 114.4, 98.6, 75, 28.1, 19.1 (2 C) ppm. IR (KBr): $\tilde{\nu}$ = 3909 (w), 3851 (m), 3737 (vs), 3448 (s), 2940 (w), 2856 (w), 2361 (vs), 1843 (w), 1649 (s), 1542 (vs), 1315 (w), 667 (vs) cm^{-1}. MS (EI, 70 eV): *m/z* (%) = 454 (1) [M, $C_{27}H_{26}N_4O_3$]$^+$, 362 (64) [$C_{21}H_{20}N_3O_3$]$^+$, 363 (15) [$C_{21}H_{21}N_3O_3$]$^+$, 335 (21) [$C_{20}H_{21}N_3O_2$]$^+$, 306(29) [$C_{19}H_{20}N_3O$]$^+$, 278 (7) [$C_{16}H_{12}N_3O_2$]$^+$, 242 (7) [$C_{13}H_{12}N_3O_2$]$^+$, 216 (4) [$C_{11}H_{10}N_3O_2$]$^+$, 186 (21) [$C_{10}H_6N_2O_2$]$^+$, 160 (17) [$C_9H_6NO_2$]$^+$, 130 (6) [C_9H_6O]$^+$, 119 (100) [$C_7H_3O_2$]$^+$, 93 (61) [C_6H_5O]$^+$, 77 (5) [C_6H_5]$^+$, 64 (23) [C_5H_5]$^+$, 51 (10) [C_4H_3]$^+$. $C_{27}H_{26}N_4O_3 \cdot 1/2H_2O$ (463.53): calcd. C 69.96, H 5.87, N 12.08; found C 70.14, H 5.55, N 11.26. X-ray quality crystals were obtained from DMSO: Crystal data ($C_{27}H_{26}N_4O_3$)(C_2H_6SO): FW = 532.65, block, 0.20 × 0.10 × 0.10 mm^3, monoclinic, space group P 2$_1$/n, a = 9.3881(19) Å, b = 11.631(2) Å, c = 13.968(3) Å, α = 109.68(3)°, β = 101.96(3)°, γ = 100.26(3)°, V = 1353.2(5) Å^3, Z = 2, D_c = 1.307 g cm^{-3}, F(000) = 564, Mo-K_α radiation, λ = 0.71073 Å, μ = 0.162 mm^{-1}, T = 173(2) K, $2\theta_{max}$ = 55.0°, 4689 reflections collected, 4689 unique (R_{int} = 0.0710, before merging), 3793 with $I_o > 2\sigma(I_o)$. Solved by using SHELXS[21] and refined with SHELX-97, full-matrix least-squares on F^2, 343 parameters, 0 restraints, GoF = 1.081, R_1 = 0.0769, wR_2 = 0.1251 (all reflections), 0.22 < $\Delta\rho$ < –0.31 e Å^{-3}.

Acknowledgments

Financial support by the DFG, the Fonds der Chemischen Industrie, COST D31, and the Academy of Finland (proj. no. 205729; K. R. and L. R.) is gratefully acknowledged. We thank Prof. E. Weinhold and M. Bahr for their help with the fluorescence spectroscopy.

[1] a) I. Stibor (Ed.), *Topics in Current Chemistry Vol. 255: Anion Sensing*, Springer, Heidelberg, 2005; b) P. D. Beer, P. A. Gale, *Angew. Chem.* 2001, *113*, 502; *Angew. Chem. Int. Ed.* 2001, *40*, 486; c) A. Bianchi, K. Bowman-James, E. Garcia-Espana (Eds.), *Supramolecular Chemistry of Anions*, Wiley-VCH, New York, 1997; d) K. Gloe (Ed.), *Macrocyclic Chemistry*, Springer, Berlin, 2005.

[2] S. M. Rowe, S. Miller, E. J. Sorscher, *New Engl. J. Med.* 2005, *352*, 1992.

[3] K. Bowman-James, *Acc. Chem. Res.* 2005, *38*, 671.

[4] R. Herges, A. Dikmans, U. Jana, F. Köhler, P. G. Jones, I. Dix, T. Fricke, B. König, *Eur. J. Org. Chem.* 2002, 3004.

[5] a) G. Müller, J. Riede, F. P. Schmidtchen, *Angew. Chem.* 1988, *100*, 1574; *Angew. Chem. Int. Ed. Engl.* 1988, *27*, 1516; b) A. Metzger, V. M. Lynch, E. V. Anslyn, *Angew. Chem.* 1997, *109*, 911; *Angew. Chem. Int. Ed. Engl.* 1997, *36*, 862; c) C. Schmuck, *Chem. Commun.* 1999, 843; d) C. Schmuck, *Chem. Eur. J.* 2000, *6*, 709; e) R. Martinez-Manez, F. Sancanon, *Chem. Rev.* 2003, *103*, 4419; f) J. Yoon, S. K. Kim, N. J. Singh, K. S. Kim, *Chem. Soc. Rev.* 2006, *35*, 355.

[6] a) P. J. Gale, J. L. Sessler, V. Kral, V. Lynch, *J. Am. Chem. Soc.* 1996, *118*, 5140; b) F. P. Schmidtchen, *Org. Lett.* 2002, *4*, 431; c) J. L. Sessler, D. E. Gross, W.-S. Cho, V. M. Lynch, F.-P. Schmidtchen, G. W. Bates, M. E. Light, P. A. Gale, *J. Am. Chem. Soc.* 2006, *128*, 12281; d) J. M. Llinares, D. Powell, K.

Bowman-James, *Coord. Chem. Rev.* **2003**, *204*, 57; e) K. Kavallieratos, S. R. de Gala, D. J. Austin, R. H. Crabtree, *J. Am. Chem. Soc.* **1997**, *119*, 2325; f) K. Kavallieratos, C. M. Bertao, R. H. Crabtree, *J. Org. Chem.* **1999**, *64*, 1675; g) P. A. Gale, *Acc. Chem. Res.* **2006**, *39*, 465.

[7] M. Albrecht, Triyanti, M. de Groot, M. Bahr, E. Weinhold, *Synlett* **2005**, 2095.

[8] a) H. Jiang, J.-M. Leger, P. Guionneau, I. Huc, *Org. Lett.* **2004**, *6*, 2985; b) H.-Y. Hu, C.-F. Chen, *Tetrahedron Lett.* **2006**, *47*, 175.

[9] M. Albrecht, K. Witt, E. Wegelius, K. Rissanen, *Tetrahedron* **2000**, *56*, 591.

[10] H. Jiang, J.-M. Leger, C. Dolain, P. Guionneau, I. Huc, *Tetrahedron* **2003**, *59*, 8365.

[11] a) P. Roychowdury, P. N. Das, B. S. Basak, *Acta Crystallogr., Sect. B* **1978**, *34*, 1047; b) T. Banerjee, N. N. Saha, *Acta Crystallogr., Sect. C* **1986**, *42*, 1408; c) M. Albrecht, K. Witt, R. Fröhlich, O. Kataeva, *Tetrahedron* **2002**, *58*, 561.

[12] a) K. A. Connors, *Binding Constants*, Wiley, New York, **1987**; b) C. S. Wilcox in *Frontiers in Supramolecular Chemistry and Photochemistry* (Eds.: H.-J. Schneider, H. Dürr), Wiley-VCH, Weinheim, **1991**, p. 123.

[13] A. Tejeda, A. I. Oliva, L. Simon, M. Grande, M. C. Caballero, J. R. Moran, *Tetrahedron Lett.* **2000**, *41*, 4563.

[14] O. S. Wolfbeis, *Fluorescence Spectroscopy: New Methods and Applications*, Springer, Berlin, **1993**.

[15] M. J. Frisch, G. W. Trucks, H. B. Schlegel, G. E. Scuseria, M. A. Robb, J. R. Cheeseman, J. A. Montgomery Jr, T. Vreven, K. N. Kudin, J. C. Burant, J. M. Millam, S. S. Iyengar, J. Tomasi, V. Barone, B. Mennucci, M. Cossi, G. Scalmani, N. Rega, G. A. Petersson, H. Nakatsuji, M. Hada, M. Ehara, K. Toyota, R. Fukuda, J. Hasegawa, M. Ishida, T. Nakajima, Y. Honda, O. Kitao, H. Nakai, M. Klene, X. Li, J. E. Knox, H. P. Hratchian, J. B. Cross, V. Bakken, C. Adamo, J. Jaramillo, R. Gomperts, R. E. Stratmann, O. Yazyev, A. J. Austin, R. Cammi, C. Pomelli, J. W. Ochterski, P. Y. Ayala, K. Morokuma, G. A. Voth, P. Salvador, J. J. Dannenberg, V. G. Zakrzewski, S. Dapprich, A. D. Daniels, M. C. Strain, O. Farkas, D. K. Malick, A. D. Rabuck, K. Raghavachari, J. B. Foresman, J. V. Ortiz, Q. Cui, A. G. Baboul, S. Clifford, J. Cioslowski, B. B. Stefanov, G. Liu, A. Liashenko, P. Piskorz, I. Komaromi, R. L. Martin, D. J. Fox, T. Keith, M. A. Al-Laham, C. Y. Peng, A. Nanayakkara, M. Challacombe, P. M. W. Gill, B. Johnson, W. Chen, M. W. Wong, C. Gonzalez, J. A. Pople, *Gaussian 03*, Revision D.02, Gaussian, Inc., Wallingford, CT, **2004**.

[16] S. F. Boys, F. Bernardi, *Mol. Phys.* **1970**, *19*, 553.

[17] A. E. Reed, L. A. Curtiss, F. Weinhold, *Chem. Rev.* **1988**, *88*, 899.

[18] E. D. Glendening, A. E. Reed, J. E. Carpenter, F. Weinhold, *NBO 3.0 Program Manual*, Theoretical Chemistry Institute and Department of Chemistry, University of Wisconsin, Madison, Wisconsin.

[19] V. Amendola, M. Bonizzoni, D. Esteban-Gomez, L. Fabbrizzi, M. Licchelli, F. Sancenon, A. Taglietti, *Coord. Chem. Rev.* **2006**, *250*, 1451.

[20] M. Hassani, W. Cai, D. C. Holley, J. P. Lineswala, B. R. Maharjan, G. R. Ebrahimian, H. Seradj, M. G. Stocksdale, F. Mohammadi, C. C. Marvin, J. M. Gerdes, H. D. Beall, M. Behforouz, *J. Med. Chem.* **2005**, *48*, 7733.

[21] G. M. Sheldrick, *SHELXTL 6*, Bruker AXS Inc., Madison, Wisconsin, USA.

Received: February 13, 2007
Published Online: April 17, 2007

